Title
Synthetic Studies toward Indole Alkaloids and Catalytic Asymmetric Staudinger–Aza-Wittig Reaction via Desymmetrization

Author
Cai, Lingchao

Publication Date
2017

Peer reviewed|Thesis/dissertation

UNIVERSITY OF CALIFORNIA

Los Angeles

Synthetic Studies toward Indole Alkaloids

and

Catalytic Asymmetric Staudinger–Aza-Wittig Reaction *via* Desymmetrization

A dissertation submitted in partial satisfaction of the

requirements for the degree Doctor of Philosophy

in Chemistry

by

Lingchao Cai

2017

ABSTRACT OF THE DISSERTATION

Synthetic Studies toward Indole Alkaloids

and

Catalytic Asymmetric Staudinger–Aza-Wittig Reaction *via* Desymmetrization

by

Lingchao Cai

Doctor of Philosophy in Chemistry

University of California, Los Angeles, 2017

Professor Ohyun Kwon, Chair

In Chapter 1, we developed a catalytic asymmetric total synthesis of (–)-actinophyllic acid, with the key step being a chiral phosphine-catalyzed [3 + 2] annulation between an imine and an allenoate to form a pyrroline intermediate in 99% yield and 94% ee. The synthesis also features a CuI-catalyzed coupling between a ketoester and a 2-iodoindole to shape the tetrahydroazocine ring; intramolecular alkylative lactonization; SmI_2-mediated intramolecular pinacol coupling between ketone and lactone subunits to assemble the complex skeleton of (–)-actinophyllic acid; and an unprecedented regioselective dehydroxylation.

In Chapter 2, we applied our phosphine-catalyzed [4 + 2] annulation between an imine and an allenoate toward the synthetic studies on akuammiline indole alkaloids. We successfully constructed indole fused [3.3.1]azabicycles from [4 + 2] annulation precursor *via* Barbier reaction in high yields. We also developed a Lewis acid promoted dehydration to form the key indole–quinonemethide intermediate, which could generate a challenging quaternary carbon by trapping with a carbon nucleophile. By adopting this strategy, we proposed a pathway to finish formal total syntheses of aspidodasycarpine and lonicerine.

In Chapter 3, we have successfully developed the catalytic asymmetric Staudinger–aza-Wittig reaction. Historically, both Staudinger and Wittig reactions need stoichiometric amounts of phosphine, which impede the development of catalytic asymmetric versions of these reactions. In 2006, Marsden and co-workers reported the first asymmetric Staudinger–aza-Wittig reaction with stoichiometric chiral phosphine, which was undesirable considering economic efficiency and environmental concerns. Based on our previous study, we found that the bridged [2.2.1]bicyclic phosphine oxide had higher efficiency than the known phosphine oxides during the reduction cycle in the presence of silane. In this project, after screening various Brønsted acids, we could realize the catalytic asymmetric Staudinger–aza-Wittig reaction at room temperature.

The dissertation of Lingchao Cai approved.

Fuyuhiko Tamanoi

Paula L. Diaconescu

Craig A. Merlic

Ohyun Kwon, Committee Chair

University of California, Los Angeles

2017

To my parents, Mr. Baoguo Cai and Mrs. Caixiang Zhu.

Also, to my wife, Kui Zhang and my son, Jinghuan Cai.

Table of Contents

Chapter 1 Catalytic Asymmetric Total Synthesis of (–)-Actinophyllic Acid 1

Section 1.1 Introduction 2

Section 1.2 Biosynthesis 3

Section 1.3 Previous Syntheses of Actinophyllic Acid 4

Section 1.3.1 Overman's Synthetic Approach to Racemic Actinophyllic Acid 4

Section 1.3.2 Overman's Synthetic Approach to (–)-Actinophyllic Acid 6

Section 1.3.3 Martin's Synthetic Approach to (±)-Actinophyllic Acid 8

Section 1.3.4 Wood's Synthetic Progress Toward (±)-Actinophyllic Acid 9

Section 1.3.5 Taniguchi's Synthesis of the Core of (±)-Actinophyllic Acid 10

Section 1.3.6 Maldonado's Synthetic Approach to the (±)-Actinophyllic Acid 11

Section 1.3.7 Coldham's Synthesis of Azabicyclic Framework of (±)-Actinophyllic Acid 12

Section 1.4 Kwon's Chiral Phosphine-catalyzed Allene/Imine [3 + 2] Annulation 13

Section 1.5 Our Synthetic Strategy 13

Section 1.6 Exploration of the key [3 + 2] Annulation 14

Section 1.7 First Attempt to Form Hexahydrozaocinone Ring through Oxidative Coupling 17

Section 1.8 Further Attempt to Form Hexahydrozaocinone Ring through CuI-Catalyzed Coupling Reaction 18

Section 1.9 Intramolecular Alkylative Lactonization 18

Section 1.10 Azepane Ring Formation through Pinacol Coupling 19

Section 1.11 Complete the Synthesis of Actinophyllic Acid 20

Section 1.12 Conclusion 21

Section 1.13 Experimental procedures 22

Section 1.14 References 35

Chapter 2 Synthetic Study toward Total Synthesis of Akuammiline Indole Alkaloids.....39

Section 2.1 Introduction 40

Section 2.2 Biosynthesis.....42

Section 2.3 Previous Syntheses toward Akuammiline Indole Alkaloids.....44

SECTION 2.3.1 GARG'S SYNTHETIC APPROACH TO (±)-ASPIDOPHYLLINE A 44

SECTION 2.3.2 MA'S SYNTHETIC APPROACH TO (±)-ASPIDOPHYLLINE A 45

SECTION 2.3.3 ZHU'S SYNTHETIC APPROACH TO (±)-ASPIDOPHYLLINE A.....46

SECTION 2.3.4 YANG'S TOTAL SYNTHESIS OF (–)-ASPIDOPHYLLINE A 47

SECTION 2.3.5 GARG'S SECOND GENERATION SYNTHESIS OF (–)-ASPIDOPHYLLINE A 48

SECTION 2.3.6 ZHU'S SYNTHETIC APPROACH TO (±)-STRICTAMINE 50

SECTION 2.3.7 OHNO'S FORMAL TOTAL SYNTHESIS OF (±)-STRICTAMINE.....50

SECTION 2.3.8 GARG'S SYNTHETIC APPROACH TO (±)-PICRININE 51

SECTION 2.3.9 LI'S SYNTHETIC APPROACH TO ASPIDODASYCARPINE AND LONICERINE.....52

Section 2.4 Kwon's Phosphine-catalyzed Allene/Imine [4 + 2] Annulation.....54

Section 2.5 Retrosynthetic Analysis.....56

Section 2.6 Exploration of the key [4 + 2] Annulation 56

Section 2.7 Synthesis of Allylic Chloride.....57

Section 2.8 Synthesis of α-Ketoester.....57

Section 2.9 Developing Barbier Reaction between Allylic Chloride and α-Ketoester 58

Section 2.10 Attempt toward Indole C3 Cyclization.....60

Section 2.11 Constructing Quaternary Carbon from Hydroxyl Ester.....63

Section 2.12 Exploration toward Indole C3 Cyclization with Adjacent Quaternary Carbon..64

Section 2.13 Synthetic Plan toward Formal Total Syntheses of Aspidodasycarpine and Lonicerine 65

Section 2.14 Conclusion 65

Section 2.15 Experimental procedures 66

Section 2.16 References 80

Chapter 3 Catalytic Asymmetric Staudinger–Aza-Wittig Reaction *via* Desymmetrization ... 83

Section 3.1 Introduction 84

Section 3.2 Phosphorus-Mediated Reaction *via* Redox-Neutral Process 86

SECTION 3.2.1 MCKEEVER-ABBAS'S CATALYTIC AZA-WITTIG REACTION WITH ISOCYANATES 86

SECTION 3.2.2 DENTON'S PHOSPHORUS(V)-CATALYZED DICHLORINATION OF EPOXIDES 87

SECTION 3.2.3 DENTON'S PHOSPHORUS(V)-CATALYZED APPEL REACTION 87

SECTION 3.2.4 DENTON'S PHOSPHORUS(V)-CATALYZED SYNTHESIS OF NITRILES FROM OXIMES 88

SECTION 3.2.5 DENTON'S PHOSPHORUS(V)-CATALYZED DEOXYDICHLORINATION REACTION 88

Section 3.3 Phosphorus-Mediated Reaction *via* Redox-Driven Process 88

SECTION 3.3.1 O'BRIEN'S CATALYTIC WITTIG REACTION 88

SECTION 3.3.2 DELFT'S CATALYTIC APPEL REACTION *VIA* IN SITU PHOSPHINE OXIDE REDUCTION 90

SECTION 3.3.3 DELFT'S PHOSPHINE-CATALYZED STAUDINGER REACTION 91

SECTION 3.3.4 ASHFELD'S PHOSPHINE-CATALYZED STAUDINGER LIGATION REACTION 92

SECTION 3.3.5 DING'S PHOSPHINE-CATALYZED AZA-WITTIG REACTION 93

SECTION 3.3.6 VOITUREZ'S CYCLIZATION REACTION OF HUISGEN ZWITTERION WITH *A*-KETOESTERS 93

SECTION 3.3.7 ALDRICH'S PHOSPHINE-CATALYZED MITSUNOBU REACTION 94

SECTION 3.3.8 WERNER'S FIRST MICROWAVE-ASSISTED CATALYTIC WITTIG REACTION 94

SECTION 3.3.9 WERNER'S FIRST BASE-FREE CATALYTIC WITTIG REACTION 95

Section 3.4 Reduction of Phosphine Oxide to Phosphine 96

SECTION 3.4 1 REDUCTION VIA ACTIVATION MODEL 97

SECTION 3.4 2 REDUCTION VIA METAL HYDRIDE 97

SECTION 3.4 3 REDUCTION VIA SILANES 98

SECTION 3.4 4 REDUCTION VIA COMBINATION OF METAL CATALYST AND SILANES 98

Section 3.5 First Asymmetric Aza-Wittig reaction 99

Section 3.6 Reaction Design 100

Section 3.7 Results 103

Section 3.8 Conclusion 108

Section 3.9 Experimental procedures 109

Section 3.10 References 118

LIST OF FIGURES

Chapter 1

Figure 1.1.1 Structure of the Indole Alkaloid Actinophyllic Acid 3

Figure 1.10.1 ORTEP structure of **66** 20

Chapter 2

Figure 2.1.1 Structures of Akuammiline Indole Alkaloids memebers 41

Chapter 3

Figure 3.1.1 Approaches in Organophosphorus Catalysis 86

LIST OF SCHEMES

Chapter 1

Scheme 1.2.1 Proposed Biogenetic Pathway for Actinophyllic Acid 4

Scheme 1.3.1 Overman's Synthetic Approach to Racemic Actinophyllic Acid 6

Scheme 1.3.2 Enantioselective Synthesis of Diacetoxypiperidine 7

Scheme 1.3.3 Second-generation total synthesis of (–)-Actinophyllic Acid 8

Scheme 1.3.4 Martin's Synthetic Approach to (±)-Actinophyllic Acid 9

Scheme 1.3.5 Formation of Cycloheptanone Ring of Actinophyllic Acid 10

Scheme 1.3.6 Construction of indole Nucleus 10

Scheme 1.3.7 Ring-Closing Metathesis and Acyl Radical Annulation 11

Scheme 1.3.8 Synthesis Core of Actinophyllic Acid 11

Scheme 1.3.9 Maldonado's Synthetic Approach to (±)-Actinophyllic Acid 12

Scheme 1.3.10 Key Step in Coldham's Synthesis toward Actinophyllic Acid 12

Scheme 1.4.1 Kwon's Chiral Phosphine-catalyzed Allene/Imine [3 + 2] Annulation 13

Scheme 1.5.1. Retrosynthesis of (–)-Actinophyllic Acid 14

Scheme 1.7.1 Attempted Oxidative Coupling 17

Scheme 1.8.1 CuI-Catalyzed Redox-Neutral Coupling 18

Scheme 1.9.1 Intramolecular Alkylative Lactonization 19

Scheme 1.10.1 Azepane Ring Formation through Pinacol Coupling 20

Scheme 1.11.1 Complete the Syntheses of Actinophyllic Acid 21

Chapter 2

Scheme 2.2.1 Biosynthesis of Geissoschizine toward Other Alkaloid Families 43

Scheme 2.2.2 Proposed Akuammiline Indole Alkaloids Biosynthetic Pathway 44

Scheme 2.3.1 Garg's Synthetic Approach to (±)-Aspidophylline A 45

Scheme 2.3.2 Ma's Synthetic Approach to (±)-Aspidophylline A 46

Scheme 2.3.3 Zhu's Synthetic Approach to (±)-Aspidophylline A 47
Scheme 2.3.4 Yang's Total Synthesis of (–)-Aspidophylline A 48
Scheme 2.3.5 Garg's Second Generation toward (–)-Aspidophylline A 49
Scheme 2.3.6 Garg's Synthetic Pathway toward (+)-Strictamine and (–)-2(*S*)-Cathafoline ...49
Scheme 2.3.7 Zhu's Synthetic Approach to (±)-Strictamine 50
Scheme 2.3.8 Ohno's Formal Total Synthsis of (±)-Strictamine 51
Scheme 2.3.9 Garg's Synthetic Approach to (±)-Picrinine 52
Scheme 2.3.10 Li's Synthetic Approach to Aspidodasycarpine and Lonicerine 53
Scheme 2.4.1 Phosphine-Catalyzed [4 + 2] Annulation 54
Scheme 2.4.2 Phosphine-Catalyzed Enantioselective [4 + 2] Annulation 54
Scheme 2.4.3 Total Synthesis of (±)-Hirsutine 55
Scheme 2.5.1 Retrosyntheic Analysis of Akuammiline Indole Alkaloids 56
Scheme 2.6.1 Exploration of the key [4 + 2] Annulation 57
Scheme 2.7.1 Synthesis of Allylic Chloride 57
Scheme 2.8.1 Synthesis of α-Ketoester 58
Scheme 2.9.1 Barbier Reaction with Secondary Allylic Chloride 60
Scheme 2.10.1 Reduction of Hydroxyl Group 61
Scheme 2.10.2 Testing Tsuji-Trost Reaction for Indole C3 Allylation 61
Scheme 2.10.3 Intramolecular Cyclization with Alkyl Chloride 62
Scheme 2.10.4 Intramolecular Cyclization with Alkyl Iodide 62
Scheme 2.10.5 Other Strategies toward Intramolecular Cyclization 63
Scheme 2.11.1 Quaternary Carbon Formation from Hydroxyl Ester 64
Scheme 2.12.1 Attempted Cyclization with Alkyl Iodide 64
Scheme 2.13.1 Synthetic Plan toward formal total synthesis of Aspidodasycarpine and Lonicerine 65

Chapter 3

Scheme 3.2.1 McKeever-Abbas's Catalytic Aza-Wittig Reaction with Isocyanates.....87

Scheme 3.2.2 Denton's Phosphorus(V)-Catalyzed Dichlorination of Epoxides 87

Scheme 3.2.3 Denton's Phosphorus(V)-Catalyzed Appel Reaction 88

Scheme 3.2.4 Denton's Phosphorus(V)-Catalyzed Synthesis of Nitriles from Oximes.....88

Scheme 3.2.5 Denton's Phosphorus(V)-catalyzed Deoxydichlorination Reaction 88

Scheme 3.3.1 O' Brien's First Catalytic Wittig Reaction and Proposal.....89

Scheme 3.3.2 O' Brien's Room Temperature Catalytic Wittig Reaction.....90

Scheme 3.3.3 Delft's Catalytic Appel Reaction.....91

Scheme 3.3.4 Delft's Phosphine Oxide for Reduction Test.....91

Scheme 3.3.5 Delft's Phosphine-Catalyzed Staudinger Reaction 92

Scheme 3.3.6 Ashfeld's Phosphine-Catalyzed Staudinger Ligation reaction 92

Scheme 3.3.7 Ding's Phosphine-Catalyzed Aza-Wittig Reaction and Vasicinone Synthesis..93

Scheme 3.3.8 Voiturez's Cyclization Reaction of Huisgen Zwitterion with α-Ketoesters 94

Scheme 3.3.9 Aldrich's Catalytic Misunobu Reaction 94

Scheme 3.3.10 Microwave-Assisted Catalytic Wittig Reaction and Asymmetric Wittig Reaction 95

Scheme 3.3.11 Werner's First Base-Free Catalytic Wittig Reaction 96

Scheme 3.5.1 Chiral Phosphorus(III) Catalysts and First Asymmetric Aza-Wittig Reaction100

Scheme 3.6.1 Synthesis of Hydroxyproline-Derived Chiral Phosphine.....101

Scheme 3.6.2 Chiral Phosphine-Catalyzed Enantioselective Allene–Imine [3 + 2] Annulations 101

Scheme 3.6.3 Our Proposal for Asymmetric Staudinger–Aza-Wittig Reaction 103

Scheme 3.7.1 Catalytic Asymmetric Staudinger–Aza-Wittig Reaction for Five-Member Ring Formation.....107

Scheme 3.7.2 Attempted Seven-Membered Ring Formation 108

LIST OF TABLES

Chapter 1

Table 1.6.1. Phosphine-Catalyzed Pyrrolidine Synthesis 16

Chapter 2

Table 2.9.1. Optimization of Intramolecular Barbier Reaction 59

Table 2.9.2. Substrates Screen of Intramolecular Barbier Reaction 60

Chapter 3

Table 3.4.1 Phosphine Oxide Reduction *via* Activation Model.....97

Table 3.4.2 Reduction *via* Metal Hydride.....98

Table 3.4.3 Reduction *via* Silanes.....98

Table 3.4.4 Reduction *via* Combination of Metal Catalyst and Silanes 99

Table 3.7.1 Optimization of Staudinger Aza-Wittig Reaction.....103

Table 3.7.2 Substrates for Aza-Wittig Staudinger Reaction 105

ACKNOWLEDGEMENTS

Chapter 1 contains a version of work published as: Catalytic Asymmetric Total Synthesis of (–)-Actinophyllic Acid. Cai, L.; Zhang, K.; Kwon, O. *J. Am. Chem. Soc.* **2016**, *138*, 3298.

VITA

2008.9–2011.7 **MS in Organic Chemistry**

Department of Chemistry, Nankai University, Tianjin, China

2004.9–2008.6 **BS in Chemistry**

Department of Chemistry, Nankai University, Tianjin, China

Publications

1. Zhang, K.;‡ **Cai, L.;**‡ Yang, Z.; Houk, K. H.; Kwon, O. "Bridged [2.2.1] Bicyclic Phosphine Oxide Designed for Catalytic Staudinger Reduction and γ-Umpolung Addition–Wittig Olefination", Submitted.

2. Zhou, Q.; Zhang, K.; **Cai, L.**; Kwon, O. "Phosphine-Catalyzed Intramolecular Cyclizations of α-Nitroethylallenoates Forming (Z)-Furanone Oximes," *Org. Lett.* **2016**, *18*, 2954. [PDF]

3. Cai, L.; Zhang, K.; Kwon, O. "Catalytic Asymmetric Total Synthesis of (–)-Actinophyllic acid," *J. Am. Chem. Soc.* **2016**, *138*, 3298. [PDF] Highlighted in Org. Chem. On November 21st, 2016: http://www.organic-chemistry.org/Highlights/2016/21November.shtm

4. Zhang, K.; **Cai, L.**; Jiang, X.; Garcia-Garibay, M. A.; Kwon, O. "Phosphine-Mediated Iterative Arene Homologation Using Allenes," *J. Am. Chem. Soc.* **2015**, *137*, 11258. [PDF]

5. Cai, **L.**; Zhang, B.; Wu, G.; Song, H.; He, Z. "Chemoselective Phosphine-catalyzed Cascade Annulations between Two Different Activated Alkenes: Highly Diastereoselective Syntheses of Polysubstituted Cyclohexanes and Cyclopentenes," *Chem. Commun.* **2011**, *47*, 1045. [PDF]

6. Zhang, B.; **Cai**, **L.**; Song, H.; Wang, Z.; He, Z. "A Highly Diastereoselective Tertiary Amine-Catalyzed Cascade Michael–Michael–Henry Reaction between Nitromethane, Activated Alkenes and α,β-Unsaturated Carbonyl Compounds," *Adv. Synth. Catal.* **2010**, *352*, 97. [PDF]

7. Wang, F.; Wang, Y.; **Cai**, **L.**; Miao, Z.; Chen, R. "Progress in the Synthesis of Isobenzopyran

and Isobenzofuran Derivatives," *Chin. J. Org. Chem.* **2008**, *28*, 1523. [PDF]

8. Wang, F.; Wang, Y.; **Cai**, **L.**; Miao, Z.; Chen, R. "Efficient Syntheses of (Thio)phosphonylated Isobenzofurans by Tandem Nucleophilic Addition and Regioselective 5-*exo*-*dig* Addition to Carbon-Carbon Triple Bond: Cooperative Effect to 1,8-Diazabicyclo[5.4.0]undec-7-ene (DBU)," *Adv. Synth Catal.* **2008**, *350*, 2733. [PDF]

Chapter 1

Catalytic Asymmetric Total Synthesis of (–)-Actinophyllic Acid

Section 1.1 Introduction

In a search for therapeutic agents for the treatment of cardiovascular disorders, Quinn, Carroll, and co-workers isolated (–)-actinophyllic acid (**1**) from the leaves of the tree *Alstonia actinophylla* growing in Cape York Peninsula, Far North Queensland, Australia (Scheme 1).[1] (–)-Actinophyllic acid was reported to be a potent inhibitor of the zinc-dependent carboxypeptidase U (CPU), with an IC_{50} of 0.84 μM. CPU was an endogenous inhibitor of fibrinolysis, the breakage of fibrin clots. Consequently, inhibitors of CPU could facilitate fibrinolysis and inhibit the blood clot formation that was a cause of various cardiovascular disorders.[2] There had not, however, been any subsequent biological studies reported, presumably because of the scarcity of the natural product, due to its low isolation yield (0.0072%).[3] Therefore, any efficient de novo syntheses of this potent CPU inhibitor should benefit explorations of its biomedical potential.

The structure of Actinophyllic acid was established by a combination of NMR, IR, and mass spectrometric analysis.[1a] In 2009, Overman and co-workers determined the absolute configuration of Actinophyllic acid by the use of optical rotation, electronic circular dichroism (ECD) and vibrational circular dichroism (VCD).[4] The assigned configuration of actinophllyic acid was consistent with a proposed biosynthetic pathway. Structurally, (–)-actinophyllic acid contained the cage-like scaffold of a 1,2,3,5,6,7,8,10a-octahydro-1,7-methanopyrrolo[1,2-a]azocine, with five contiguous stereogenic centers, one of which was a quaternary carbon, bridged by a tetrahydrofuran lactol. This unprecedented architecture, along with great biomedical potential, had garnered widespread attention from the synthetic community.

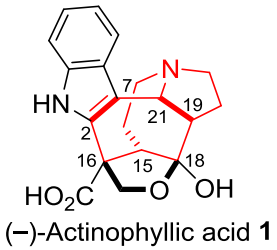

(–)-Actinophyllic acid **1**

Figure 1.1.1 Structure of the Indole Alkaloid Actinophyllic Acid

Section 1.2 Biosynthesis

After elucidation of the structure of actinophyllic acid by Quinn, Carroll, and co-workers, they proposed a plausible biogenetic pathway for actinophyllic acid.[1a] As with all monoterpene indole alkaloids isolated from plants of the family Apocynaceae, the probable biogenetic precursors were tryptamine and (–)-secologanin glucoside. Condensation of tryptamine and (–)-secologanin glucoside formed geissoschizine (2), which underwent rearrangement to deliver precondylocarpine (3), which was isolated from *Vallesia dichrotoma* (Apocynaceae),[5] *via* a stemmadenine iminium cation. Oxidation of the C-20-C-19 double bond at precondylocarpine could yield the epoxide intermediate **i**, which through proton migration produced the allylic alcohol **ii**. Further oxidation of intermediate **ii** could form the epoxide intermediate **iii**. Grob-tpye fragmentation could form iminium cation **iv** followed by ring closure through Mannich cyclization would lead to the keto-alcohol **v**. Oxidation of the alcohol would produce the C-18 carboxylic acid **vi**. Decarboxylation of the α-ketoacid **vi** would give the ketone intermediate **vii**. Re-aromatization of the indole could occur by elimination of C-6 to form the carbocation **viii**. The resulting carbocation could been trapped by enol carbon C-19 to form the five-membered ring **ix**. Hemiacetal formation *via* cyclization of the hydroxyl oxygen 17-OH onto the ketone carbonyl carbon C-20 and hydrolysis of the methyl ester would finally yield actinophyllic acid.

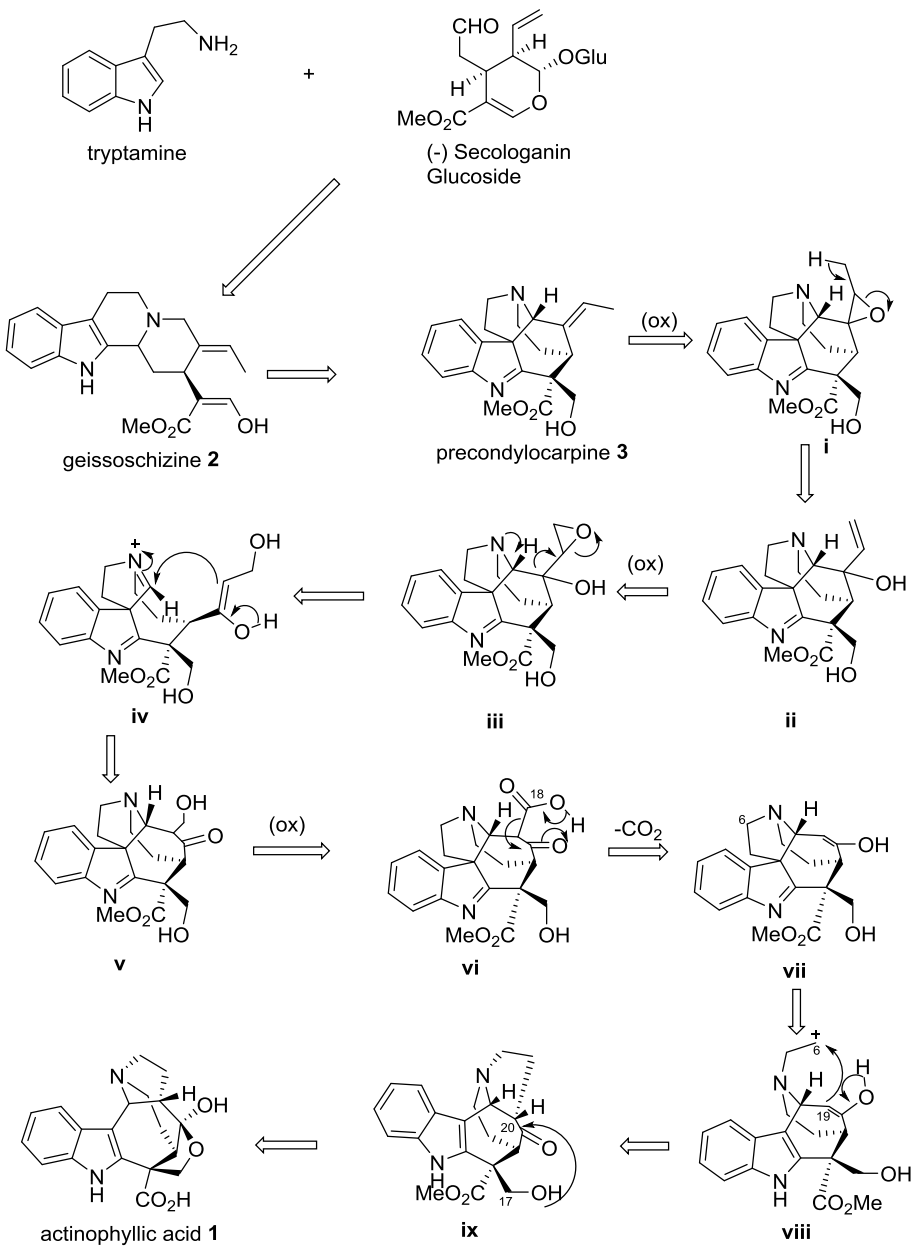

Scheme 1.2.1 Proposed Biogenetic Pathway for Actinophyllic Acid

Section 1.3 Previous Syntheses of Actinophyllic Acid

Section 1.3.1 Overman's Synthetic Approach to Racemic Actinophyllic Acid

In 2008, Overman and co-workers accomplished an elegant total synthesis of (±)-actinophyllic acid through aza–Cope/Mannich cascade strategy.[6a] The synthesis commenced with formation of indole di-*tert*-butyl malonate **5**. Di-*tert*-butyl malonate reacted with 2-

nitrophenylacetyl chloride followed by reduction of nitro group to form indole malonate **5**. Introduction of 3-piperidone at indole C-3 position through nucleophilic displacement with keton-bromide **6** could deliver indole **7**. The key step of their synthesis was the oxidative coupling between malonate and 3-piperidone enolates to construct the keto-bridged hexahydrozaocino [4, 3-b] indole **8** in one step by using $[Fe(DMF)_3Cl_2][FeCl_4]$ as oxidant in 60-63% yield on scale up to 10g. Next, they tried to forge the core structure of actinophyllic acid through aza-Cope-Mannich reaction which was developed by their group. Introduction of allylic alcohol *via* vinyl cerium addition to ketone could form allylic alcohol **9** as a single isomer in nearly quantitative yield. Selective removal of the Boc group from the product, followed by condensation with paraformaldehyde in the presence of a catalytic amount of camphorsulfonic acid could induce the aza-Cope rearrangement and Mannich reaction to deliver diester **10**. Exposure of this crude product to neat trifluoroacetic acid (TFA) gave amino acid trifluoroacetate salt **11**. Esterification of **11**, could provide methyl ester **12**. They could directly transform allylic alcohol **9** to pentacyclic ester **16** in a one-pot process by initially exposing **9** to TFA at room temperature, which cleaved the Boc and tert-butyl esters and promoted decarboxylation. Then switching the solvent to acetonitrile, exposure of the resulting amino acid trifluoroacetate salt to paraformaldehyde could promote aza-Cope-Mannich transformation to the carboxylic acid, which was esterified to provide **12** as a 1:1 mixture of ester epimers. Finally, stereoselective aldol reaction with monomeric formaldehyde could install the tetrahydrofuran ring, followed by acidic hydrolysis to finish the synthesis of (±)-actinophyllic acid.

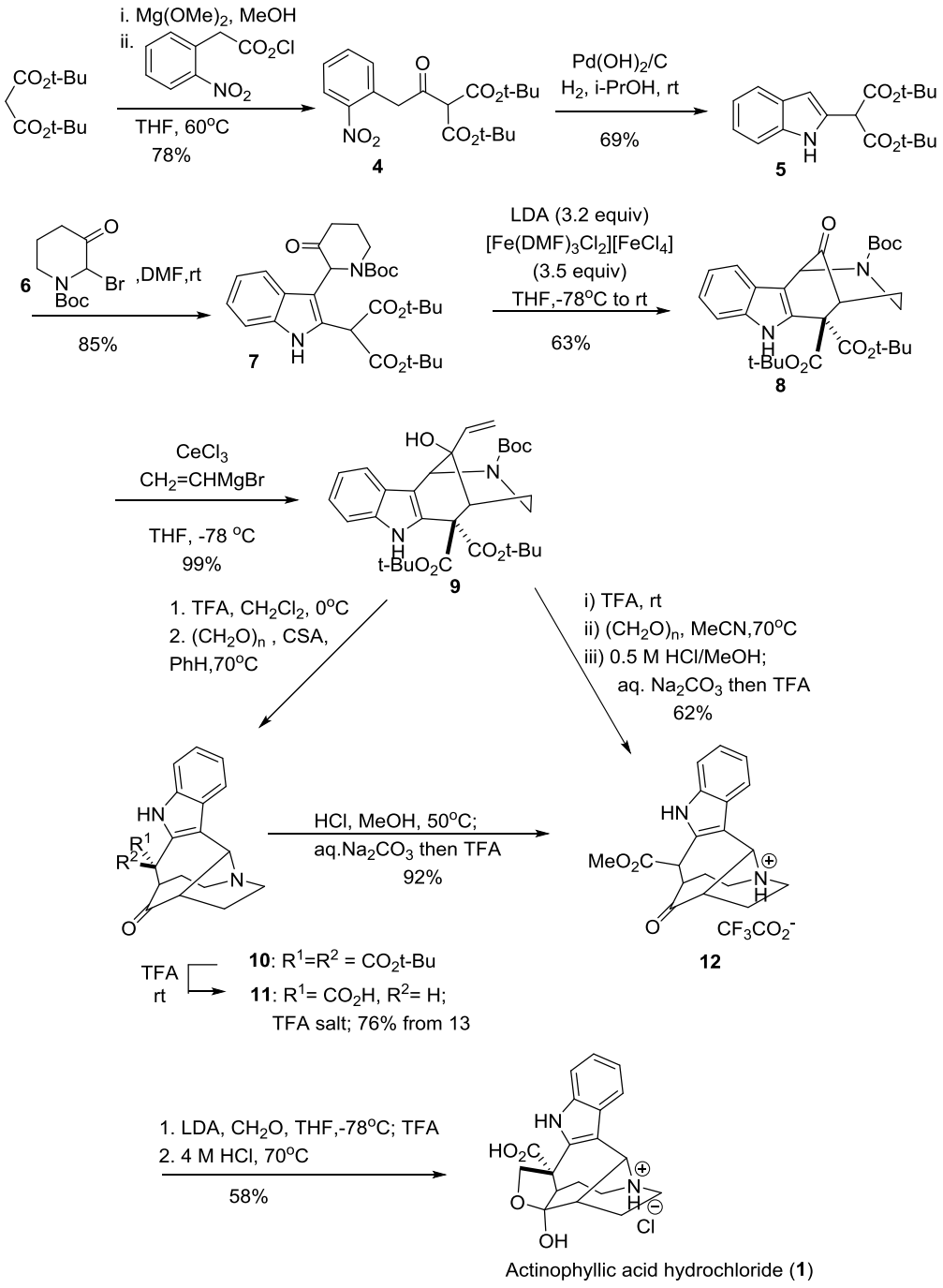

Scheme 1.3.1 Overman's Synthetic Approach to Racemic Actinophyllic Acid

Section 1.3.2 Overman's Synthetic Approach to (–)-Actinophyllic Acid

Two years later, the Overman group published the second generation syntheses of both (±)-actinophyllic acid and (–)-actinophyllic acid with a shorter approach.[6b] Failure with catalytic

enantioselective syntheses of the key intermediate **7** between indole malonate **5** and ketone **6**, they turned to develop a diasteroselective construction of this key intermediate between indole malonate and *N*-Boc piperidine. Scheme **1.3.2** showes the procedure to enantioselectively synthesize *N*-Boc piperidine. Starting from commercially available amino acid **13,** which was converted Weinreb amide, followed by cerium chloride mediated vinylation, they could get enone **14** in 88% yield over the two steps. Then, Noyori asymmetric reduction gave allylic alcohol (*R*)-**15** in 91% ee. Ozonolysis followed by acetylation produced diacetoxypiperidine (3*R*)-**16** in 73% yield from enone **14**.

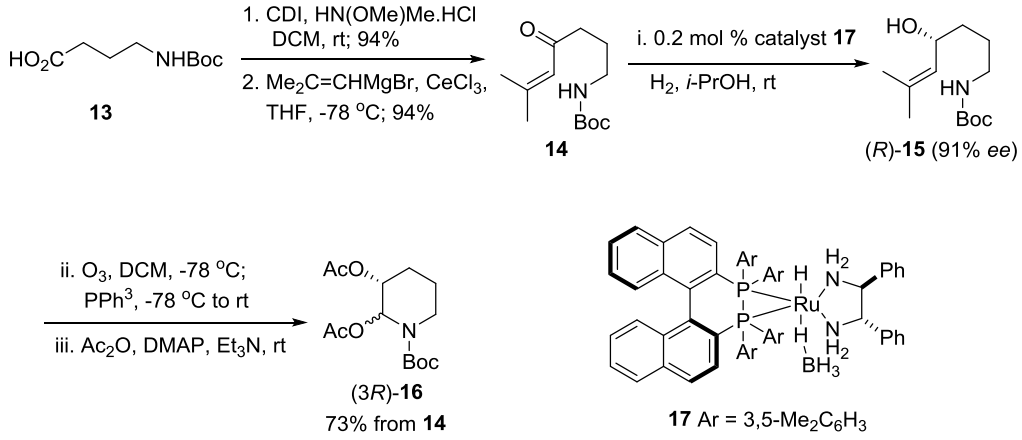

Scheme 1.3.2 Enantioselective Synthesis of Diacetoxypiperidine

Piperidine electrophile (*R*)-**16** reacted with indole malonate **5** in the presence of scandium triflate to give adduct (*2S, 3R*)-**18** in 88% yield (dr = 17:1) on a multigram scale. Deacetylation followed by Swern oxidation delivered indole piperidone (*S*)-**7**, which underwent intramolecular oxidative coupling to furnish ketone (*1S, 5R*)-**8** in 57-59% yield and 91% ee. Vinyl addition to ketone spontaneously formed lactone **20** in 83% yield. Chemoselective Luche reduction of lactone **20** furnished hydroxyl ester (+)-**21** in 86% yield. Then, the Boc and *t*-butyl groups were removed under acidic conditions. The resulting product condensed with paraformaldehyde, which underwent aza-Cope/Mannich reaction to furnish (–)-actinophyllic acid in one pot in a high

efficiency way.

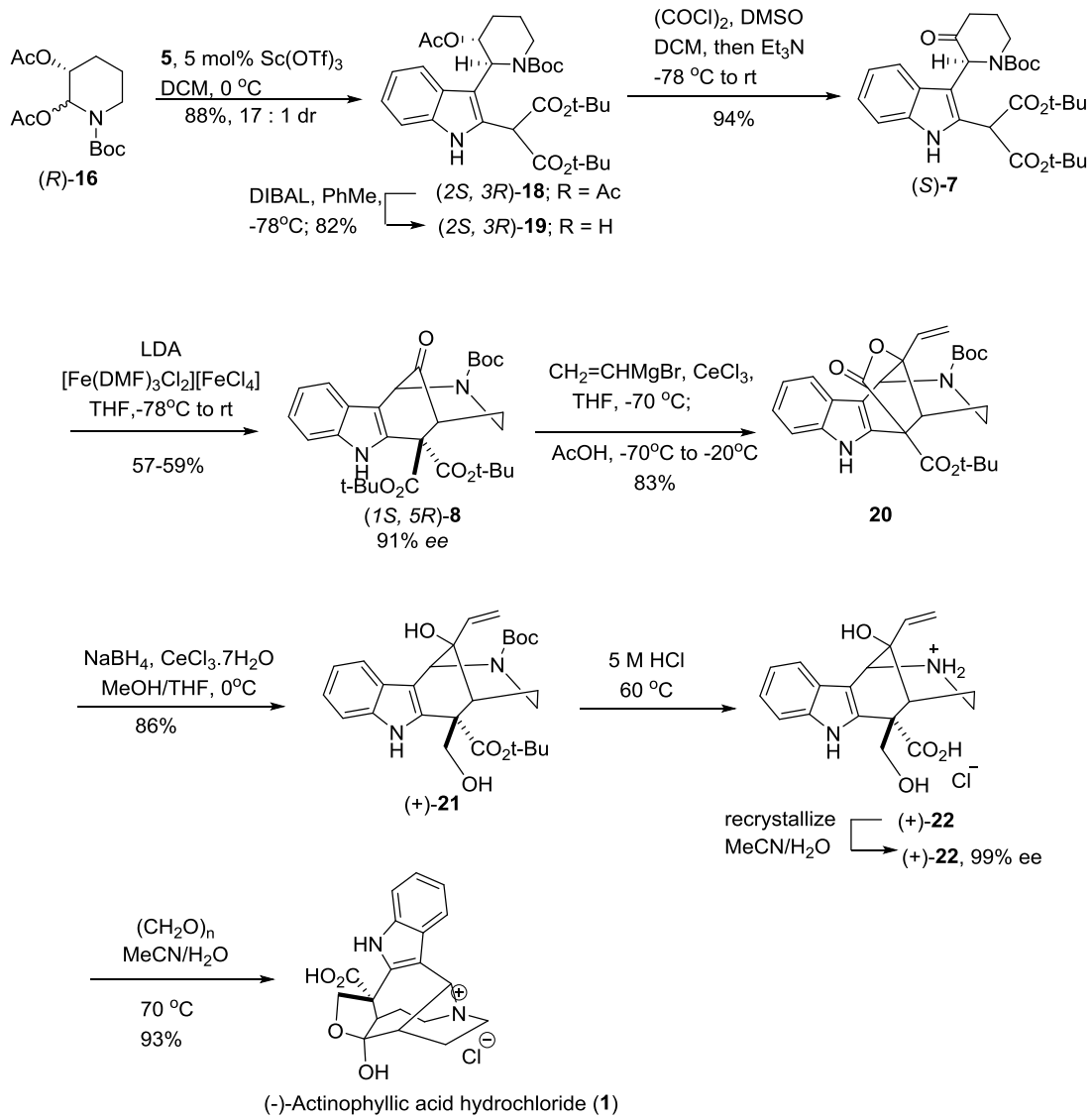

Scheme 1.3.3 Second-generation total synthesis of (–)-Actinophyllic Acid

Section 1.3.3 Martin's Synthetic Approach to (±)-Actinophyllic Acid

In 2013, Martin group completed a total synthesis of (±)-Actinophyllic Acid in only 10 steps from readily available, known compounds **23** and **24**.[7] The synthesis featured a novel cascade of reactions of *N*-stabilized carbocations with π-nucleophiles to create the tetracyclic core of actinophyllic **25** in a single chemical operation. Then protection, deprotection, reductive amination

and alkylation could form the intermediate **26**. Finally, a few more transformations could deliver the racemic actinophyllic acid.

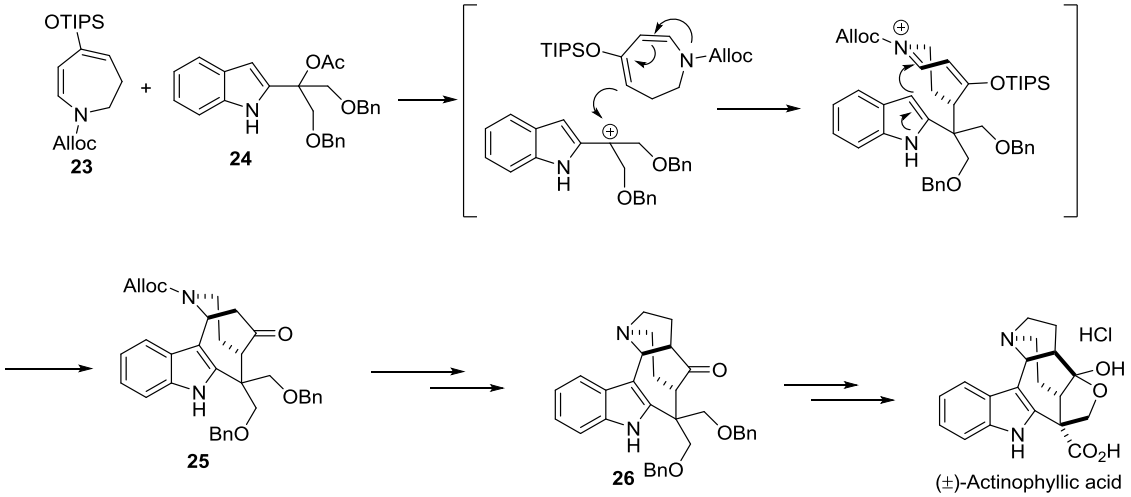

Scheme 1.3.4 Martin's Synthetic Approach to (±)-Actinophyllic Acid

Section 1.3.4 Wood's Synthetic Progress Toward (±)-Actinophyllic Acid

In 2009, Wood and co-workers reported their progress toward the total synthesis of (±)-actinophyllic acid.[8a] One of their key steps involved copper catalyzed cyclopropanation from diazo **27** to cyclopropane **28**. Then under soft enolization conditions, divinylcyclopropane [3.3]-sigmatropic rearrangement could lead to cycloheptanone **29**. Tsuji-Trost allylation could install the quaternary carbon to form allylated *β*-ketoamide **30** as a single diastereoisomer.

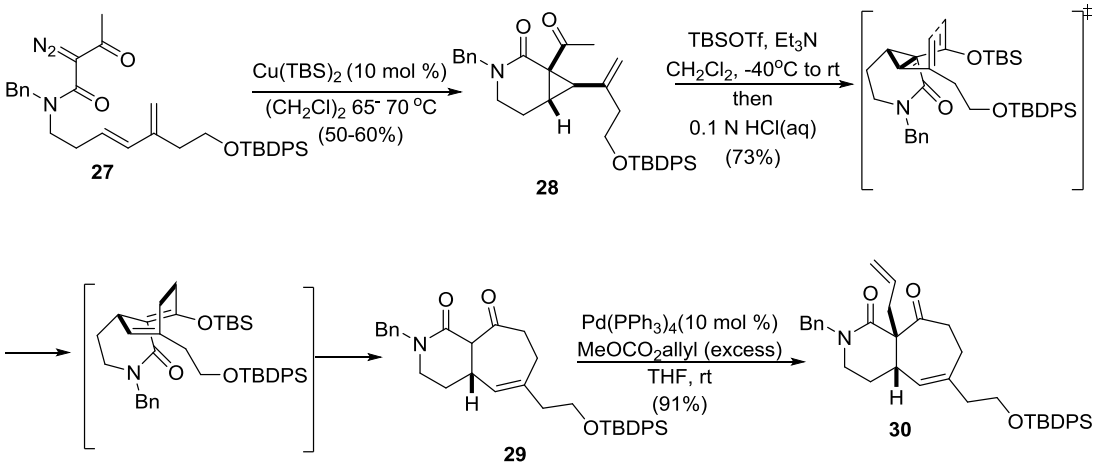

Scheme 1.3.5 Formation of Cycloheptanone Ring of Actinophyllic Acid

Next, they used Fischer indole synthesis to construct indole **32** as a single regioisomer under Lewis acid conditions. Further on, they planned to use indole-quinonemethide method to form pyrrole ring to complete the synthesis of actinophyllic acid **1** under oxidative conditions.

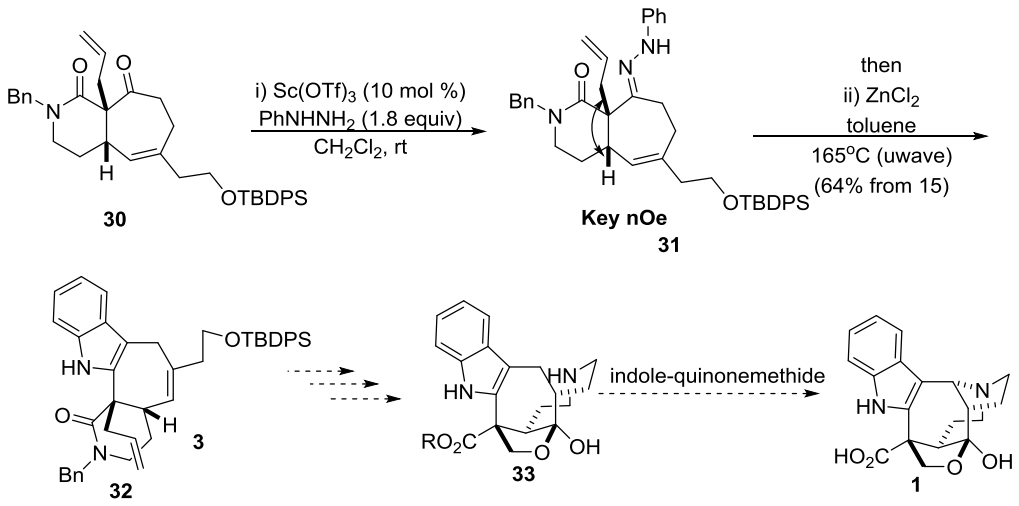

Scheme 1.3.6 Construction of indole Nucleus

Section 1.3.5 Taniguchi's Synthesis of the Core of (±)-Actinophyllic Acid

In 2012, Taniguchi and co-workers reported synthesis of the core of actinophyllic acid using a transannular acyl radical cyclization to obtain a key bicyclo[3.3.2] framework.[8b] They started from commercially available indole **34**, which underwent several transformations to form diene precursor **35**. After ring-closing metathesis, they could obtain eight-membered ring compound **36**, which was transformed to selenoester **37**, setting ready for acyl radical cyclization. Under standard radical condtions (nBu$_3$SnH, ACN, toluene, reflux), they could obtain the desired compound **38** which contained the caged skeleton of actinophyllic acid.

With indole ketone **38** in hand, they tried to form pyrrole ring by using reductive amination followed by alkylation. First, reduction amination formed N–C bond in compound **41**. Then oxidation followed by base induced alkylation could finish the pyrrole ring formation to deliver

their final compound **42**.

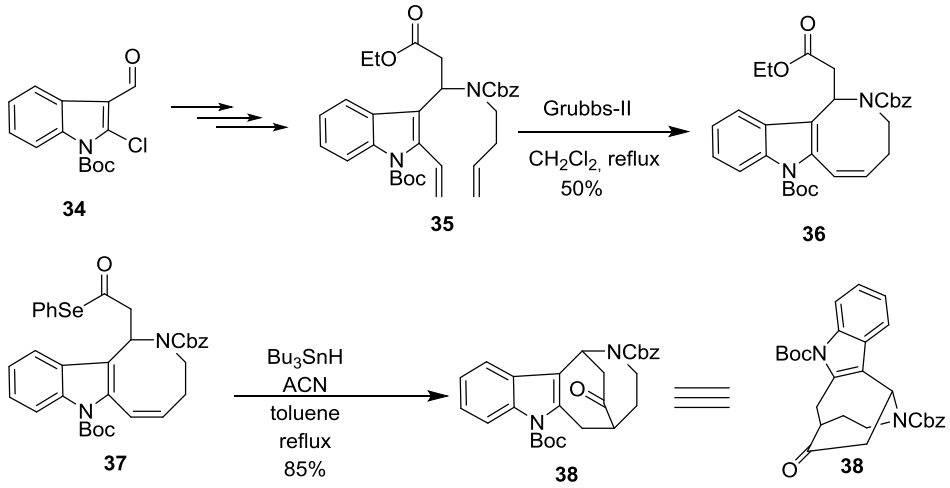

Scheme 1.3.7 Ring-Closing Metathesis and Acyl Radical Annulation

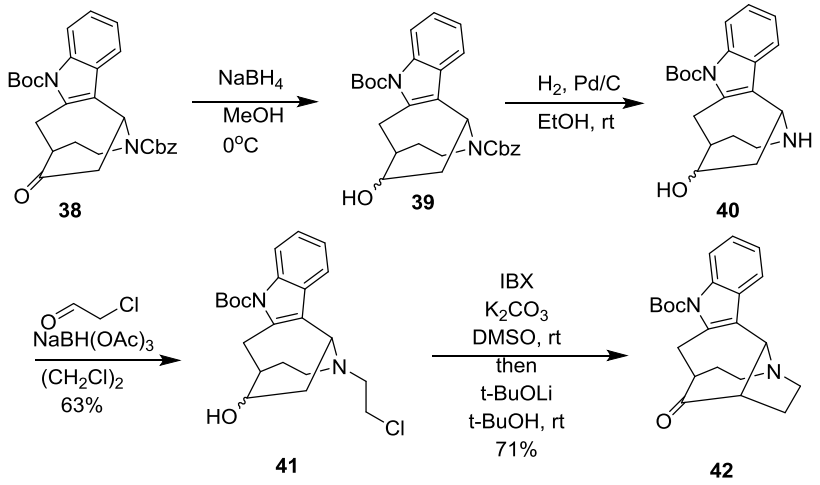

Scheme 1.3.8 Synthesis Core of Actinophyllic Acid

Section 1.3.6 Maldonado's Synthetic Approach to the (±)-Actinophyllic Acid

In 2013, Maldonado's group reported methodology to form 1-azabicyclo[4.2.1]nonane ring system present in actinophyllic acid.[8c] The method involved acid induced intramolecular cyclization of the azafulvene **45**, which was formed between indol-3-carbaldehyde **44** and azocan-5-one **43**, into ketone **46** in efficient way. Unfortunately, X-ray analyses of the compound showed 'wrong' stereochemistry (highlighted in red) from actinophyllic acid.

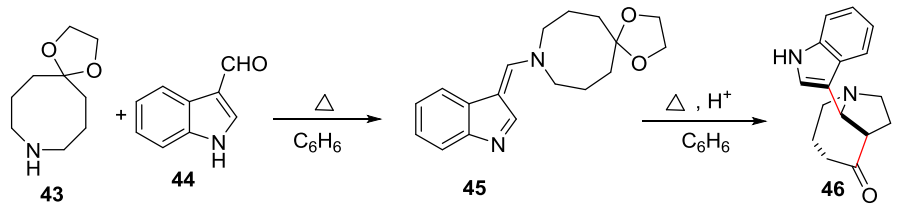

Scheme 1.3.9 Maldonado's Synthetic Approach to (±)-Actinophyllic Acid

Section 1.3.7 Coldham's Synthesis of Azabicyclic Framework of (±)-Actinophyllic Acid

One year later, in 2014, Coldham and co-workers reported synthesis of an azabicyclic framework of actinophyllic acid which adopted very similar strategy as Maldonado's group.[8d] Under Lewis acid conditions, indole aldehyde **47** was condensed with azocinone **48**, which underwent intramolecular Mannich reaction to form the 1-azabicyclo[4.2.1]nonan-5-one core framework in a single diastereoisomer. They faced the same problem as Maldonado's group had. The X-ray analyses showed the product they isolated had the undesired stereochemistry in comparison with the natural product.

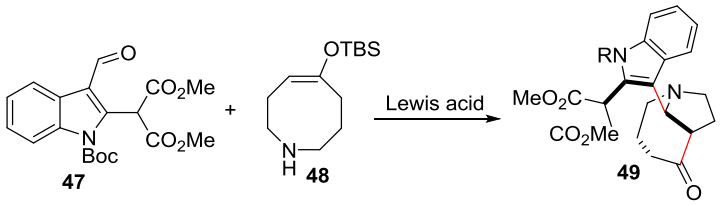

Scheme 1.3.10 Key Step in Coldham's Synthesis toward Actinophyllic Acid

Section 1.4 Kwon's Chiral Phosphine-catalyzed Allene/Imine [3 + 2] Annulation

In 1995, the Lu group first reported phosphine catalyzed allene/alkenes [3 + 2] annulation to form cyclopentenes.[9] Later several groups reported catalytic asymmetric allene/imines and allene/alkenes [3 + 2] annulations.[10] Recently, our group developed two chiral phosphines, which were prepared from naturally occurring *trans*-4-hydroxy-$_L$-proline, and functioned as pseudoenantiomers, providing the [3 + 2] annulation products with opposite absolute configurations (shown in scheme 1.4.1).[11]

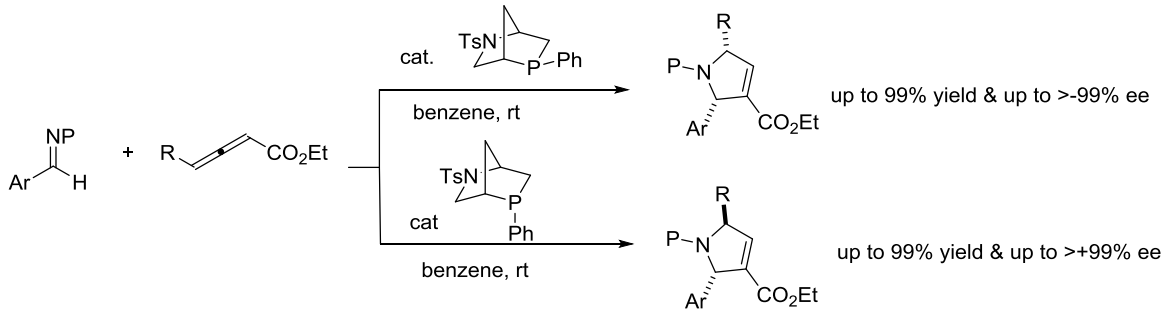

Scheme 1.4.1 Kwon's Chiral Phosphine-catalyzed Allene/Imine [3 + 2] Annulation

In our synthetic strategy toward actinophyllic acid, we planned to adopt chiral phosphine-catalyzed allene/imine [3 + 2] annulation to form the enantiomerically enriched pyrroline.

Section 1.5 Our Synthetic Strategy

We originally envisioned that (–)-actinophyllic acid could be obtained from the diester **50** through Overman's decarboxylation, hydroxymethylation, and lactol formation sequence (Scheme 1.5.1). We targeted forming the C15–C16 bond in **50** through oxidative coupling between the malonate and ketone units of intermediate **51**. The 1-azabicyclo[4.2.1]nonan-5-one scaffold (in green) of compound **51** was to be fashioned from pyrroline **52** *via* azepinone ring formation. The pyrroline **52**, in turn, could be assembled through a well-established phosphine-catalyzed [3 + 2] annulation between an indole imine and an electron-deficient allene.[9] While reduction of the pyrroline **52** to the 2,3-*cis*-substituted pyrrolidine was readily accomplished, formation of the

bridged 1-azabicyclo[4.2.1]nonan-5-one system (in green) proved difficult—due to epimerization at C19, even under mild conditions.[12] To circumvent these obstacles, we devised an alternative route in which the hexahydroazocine ring would be built first (from **57** to **56**). Diastereoselective hydrogenation of the pyrroline should, then, bring the carbonyl groups at C15 and C18 in close proximity to form the azepane ring through pinacol coupling (from **54** to **53**). The two carbonyl groups would be brought even closer, we surmised, after intramolecular alkylative lactonization (from **55** to **54**). The azocinone ring in compound **56** should be accessible through coupling between the indole C2 atom and the C16 atom of the *β*-ketoester in **57**, which should be readily preparable from intermediate **52**.

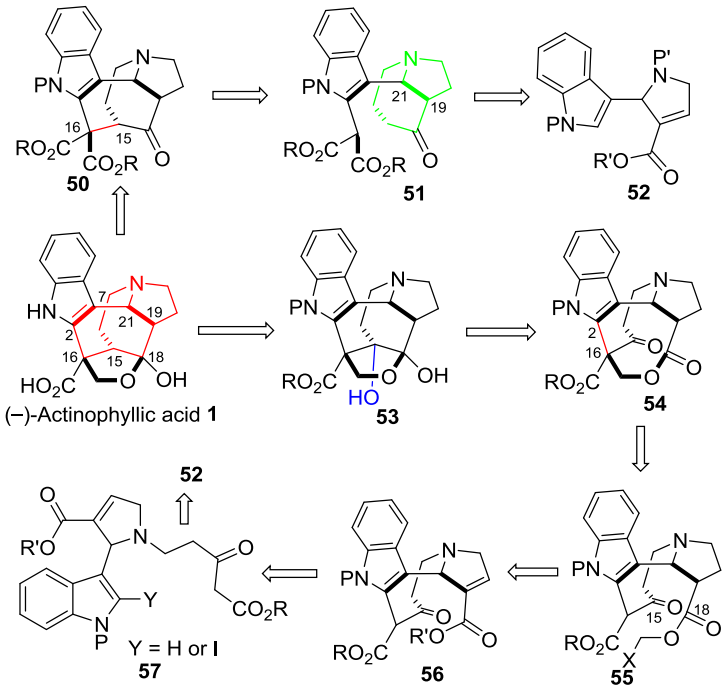

Scheme 1.5.1. Retrosynthesis of (–)-Actinophyllic Acid

Section 1.6 Exploration of the key [3 + 2] Annulation

Our synthetic campaign commenced with an exploration of the key [3 + 2] annulation between benzyl allenoate and the *N*-(*o*-nitrobenzenesulfonyl) (*o*-nosyl) imine **58**, which could be synthesized according to the known procedure from indole 3-carbaldehyde.[13] Initially, when using

PPh_3, the desired racemic pyrroline was obtained in 99% yield after 6 h (Table 1.6.1, entry 1). When we applied 20 mol% of exo-phenyl Kwon [2.2.1] bicyclic phosphine **C** to the annulation, the desired product was formed in 95% yield and 10% ee after 6 h at room temperature in DCM (entry 3). Switching to *endo*-phosphine **A** could improve yield to 99% and ee to 67% (entry 4). Surveying different solvents, chloroform and benzene gave us good enantioselectivity with ee's 75% and 76%, respectively (entries 6 and 10). To avoid solvent freezing at below 5 ^{o}C, chloroform was preferred. Then, different *endo*-phosphines **B**, **D**, **E** and **F** were applied to the annulation reaction.[14] We found electron richer endo-*para*-methoxyphenyl Kwon [2 .2 .1] bicyclic phosphine **B** could improve enantioselectivity up to 83% ee at room temperature in chloroform (entries 11 and 12). Lowering the reaction temperature to 0 ^{o}C could further imporve the ee to 91% within 5 h (entry 13). Further lowering the reaction temperature, however, did not improve enantioselectivity further (entries 14 and 15). From a mechanistic perspective, we suspected that hydrogen bonding would facilitate the proton transfer steps[15] and rigidify the transition state assembly[16] thereby improving the enantioselectivity. Among a variety of hydrogen bond donors tested, we found that phenol and derivatives accelerated the reaction and improved the enantioselectivity. A variety of additives were screened and we found acetic acid, water and sulfamide inhibited the reaction, however, phenol and deriviatives could accelerate reaction, which could complete the reaction in 2 h (entries 16–19). Both electron rich and deficient phenol were effective for the annulation reaction except 2,4-dinitrophenol (entries 19–27). Electron deficient phenol decreased enantioselectivity to 85% ee (entry 20). Finally, we found either *r*-binol or *s*-binol could improve the enantioselectivity to 94% ee without decreasing the yield in 2 h (entries 25 and 26).

Table 1.6.1. Phosphine-Catalyzed Pyrrolidine Synthesis

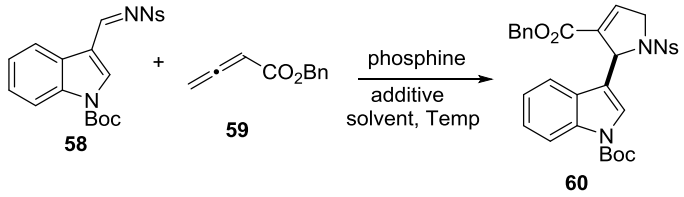

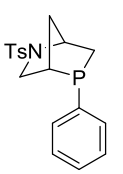

phosphine **A**
Aldrich # L512398

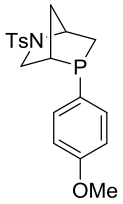

phosphine **B**
Aldrich # L512478

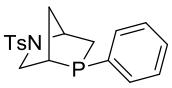

phosphine **C**
Aldrich # L512389

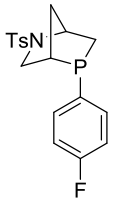

phosphine **D**
Aldrich # L512451

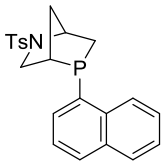

phosphine **E**
Aldrich # L512486

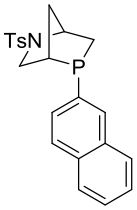

phosphine **F**
Aldrich # L512494

	cat.	solvent	temp	additive	time (h)	yield (%)[b]	ee (%)[c]
1	PPh_3	DCM	rt		6	99	
2	PPh_3	$CHCl_3$	rt		6	99	
3	**C**	DCM	rt		6	95	10
4	**A**	DCM	rt		5	99	67
5	**A**	THF	rt		5	92	55
6	**A**	$CHCl_3$	rt		5	97	75
7	**A**	CH_3CN	rt		5	87	58
8	**A**	toluene	rt		6	94	72
9	**A**	dioxane	rt		6	82	55
10	**A**	benzene	rt		5	99	76
11	**B**	$CHCl_3$	rt		5	99	83
12	**D**	$CHCl_3$	rt		5	97	74
13	**E**	$CHCl_3$	rt		5	98	79
14	**F**	$CHCl_3$	rt		5	99	78
13	**B**	$CHCl_3$	0 °C		5	99	91
14	**B**	$CHCl_3$	–20 °C		12	95	91
15	**B**	$CHCl_3$	–40 °C		24	94	91
16	**B**	$CHCl_3$	0 °C	acetic acid		NR	
17	**B**	$CHCl_3$	0 °C	H_2O		NR[d]	
18	**B**	$CHCl_3$	0 °C	*o*-$NsNH_2$		NR[d]	
19	**B**	$CHCl_3$	0 °C	phenol	2	99	91
20	**B**	$CHCl_3$	0 °C	4-fluorophenol	2	92	85

21	**B**	$CHCl_3$	0 °C	2-aminophenol	2	97	92
22	**B**	$CHCl_3$	0 °C	2,4-diphenylphenol	2	98	91
23	**B**	$CHCl_3$	0 °C	2,4-dinitrophenol		NR	
24	**B**	$CHCl_3$	0 °C	2-amino-5-chlorophenol	2	99	91
25	**B**	$CHCl_3$	0 °C	*S*-Binol	2	99	94
26	**B**	$CHCl_3$	0 °C	*R*-Binol	2	99	94
27	**B**	$CHCl_3$	0 °C	biphenol	2	99	91

[a] Unless otherwise noted, reactions were conducted using 0.1 mmol of imine, 0.12 mmol of allenote, 20 mol% catalyst and 20 mol% of additive. [b] Isolated yield after silica gel flash column chromatography. [c] Determined by HPLC. [d] Slow reaction without completion.

Section 1.7 First Attempt to Form Hexahydrozaocinone Ring through Oxidative Coupling

With the [3 + 2] annulation product in hand, we attempted to form the hexahydroazocinone ring through oxidative coupling between the ketoester and the C2 atom of indole.[17] Quick access to the ketoester **62** was secured in 92% yield through deprotection of the *o*-nosyl group, performed with sodium benzenethiolate in MeCN at room temperature, followed by reaction with ethyl 3-oxopent-4-enoate (Scheme **13**).[18] We examined a list of oxidants, including Fe^{3+}, Cu^{2+}, Mn^{3+}, Co^{2+}, Ag^{+}, and I_2, to facilitate the oxidative coupling of the substrates **62´** and **62´´**, but obtained no fruitful results.

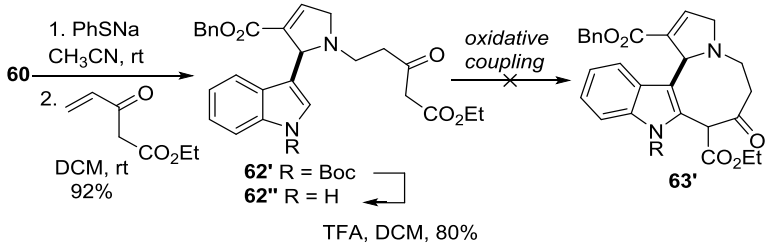

Scheme 1.7.1 Attempted Oxidative Coupling

Section 1.8 Further Attempt to Form Hexahydrozaocinone Ring through CuI-Catalyzed Coupling Reaction

Instead of using an oxidative coupling approach, we anticipated that a redox-neutral coupling reaction between iodole 2-iodide and ketoester subunits might give the desired cyclization product **63** ´.[19] Following the procedure used for the synthesis of **62** ´, the iodoketoester **62** was obtained in 80% yield over two steps (Scheme **1.8.1**). Having efficient access to the necessary iodoketoester **62**, several transition metal catalysts were probed. Pleasingly, subjecting the iodoketoester **62** to CuI in DMSO at room temperature yielded (82%) the desired cyclization product **63**, which existed exclusively in its enol form. One recrystallization increased the ee to 99%.[20] As far as we know, this CuI-catalyzed coupling is the first between a 2-iodoindole and a ketoester to generate a tetrahydroazocine cycle.[19d]

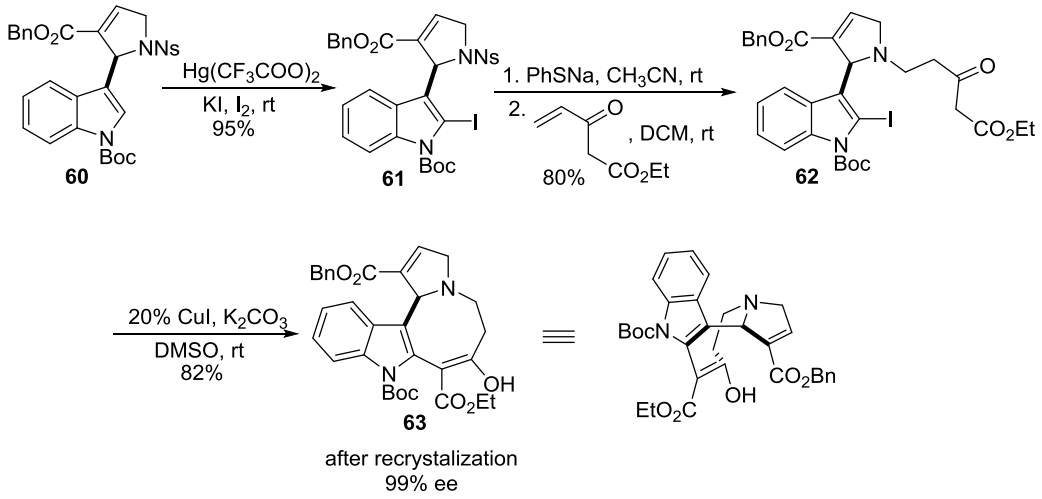

Scheme 1.8.1 CuI-Catalyzed Redox-Neutral Coupling

Section 1.9 Intramolecular Alkylative Lactonization

To our delight, a high pressure of H_2 gas over Pd/C formed the *cis* hydrogenation product along with deprotection of the benzyl group in one pot. Exchanging the solvent to DMF and treating the resulting carboxylic acid with chloroiodomethane and K_2CO_3 readily manufactured

the chloromethyl ester **64** in 78% yield for the two steps. After significant experimentation, we found that 40 equivalents of NaI in DMF with K_2CO_3 as base furnished the lactone **65** in 35–48% yield Although modestly yielding, this alkylative lactonization framed another challenging eight-membered tetrahydrooxocine ring of (–)-actinophyllic acid and set the stage for the final azepane ring, and concomitant tetrahydrofuran ring, formation through intramolecular ketone–lactone pinacol coupling. The pinacol coupling strategy departed significantly from the lactol formation approach adopted by Overman and Martin.

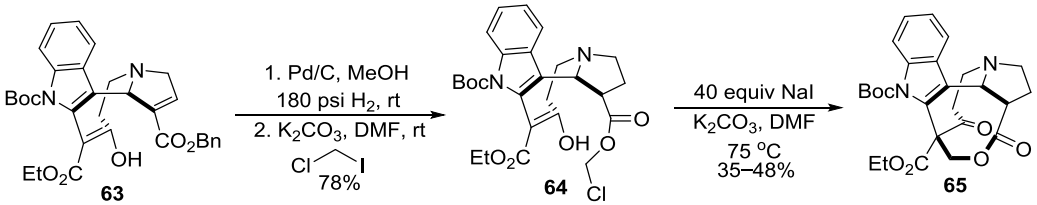

Scheme 1.9.1 Intramolecular Alkylative Lactonization

Section 1.10 Azepane Ring Formation through Pinacol Coupling

Continuing with the synthetic venture, we evaluated the effects of several single-electron-transfer reagents, including Ti^{3+}, Li, Na, and Sm^{2+}, on the pinacol coupling.[21] Only SmI_2 combined with 10 equivalents of *t*-BuOH provided the desired coupling product **66**, in quantitative yield; its structure was confirmed through X-ray crystallographic analysis. Interestingly, without *t*-BuOH, the major product we isolated is diol **66'**, which was formed *via* Pinacol coupling followed by Pinacol rearrangement. The structure of **66'** was confirmed by ^{1}HNMR, ^{13}CNMR and 2D NMR. At this stage, the complete heavy atom arrangement of (–)-actinophyllic acid was in place.

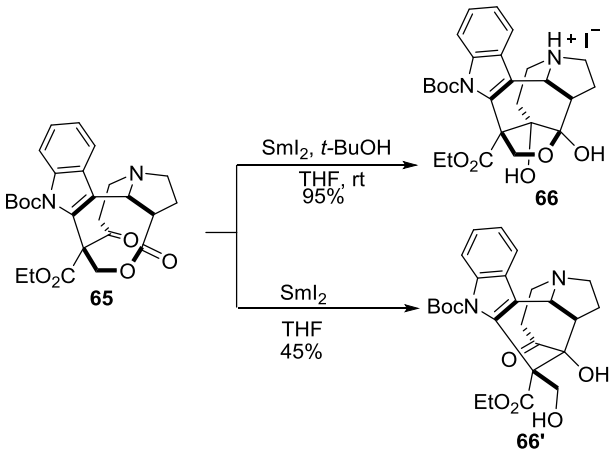

Scheme 1.10.1 Azepane Ring Formation through Pinacol Coupling

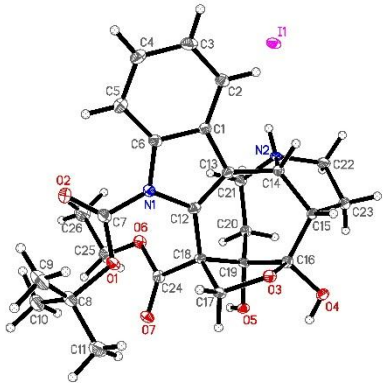

Figure 1.10.1 ORTEP structure of **66**

Section 1.11 Complete the Syntheses of Actinophyllic Acid

After Pinacol coupling, what remained was regioselective removal of the hindered C15 hydroxyl group from compound **66**. To this end, we turned our attention to radical dehydroxylation.[22] The idea was that the thiocarbonate **67**, when treated with a tributyltin radical, would undergo homolytic cleavage of the tertiary carbon–oxygen bond preferably, due to electronic differentiation (the rigid multicyclic framework of actinophyllic acid would not allow the necessary stereoelectronic alignment of the lone pair of electrons on the tetrahydrofuran oxygen with the ensuing α-radical). The dihydroxy compound **66** was reacted with thiophosgene

in the presence of DMAP at –15 ℃, transforming into the thionocarbonate **67** in 72% yield. The standard conditions of *n*-Bu_3SnH and AIBN at 90 ℃ in toluene worked efficiently to furnish the desired lactol product. Finally, global deprotection, through the effect of aqueous HCl under microwave heating at 100 ℃ for 30 min, furnished (–)-actinophyllic acid hydrochloride in 90% yield over two steps $\{[\alpha]_{589}^{22.8}$ –175.8 °(*c* 1.0, MeOH)}. The spectral data of our synthetic sample matched those reported in the literature.[6]

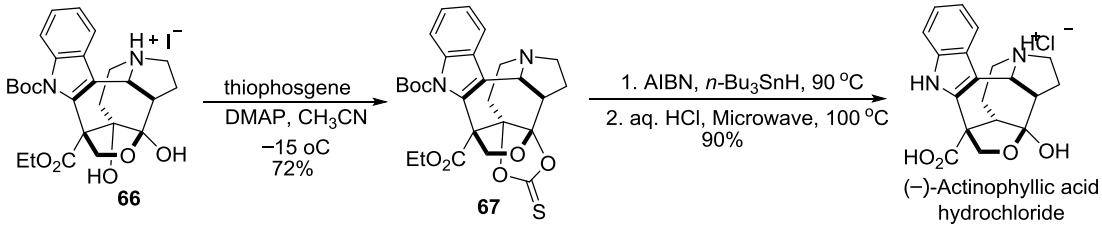

Scheme 1.11.1 Complete the Syntheses of Actinophyllic Acid

Section 1.12 Conclusion

In conclusion, we successfully completed a catalytic asymmetric total synthesis of (–)-actinophyllic acid in 13 steps from a known aldehyde in 12.4% yield. Our synthesis exhibited several salient features: (i) chiral phosphine-catalyzed [3 + 2] annulation between an allenoate and an indole imine; (ii) CuI-catalyzed coupling between a 2-iodoindole and a ketoester to assemble a hexahydro-1*H*-azocino[4,3-b]indole system; (iii) intramolecular alkylative lactonization to form a tetrahydrooxocine ring; (iv) highly efficient pinacol coupling between a ketone and a lactone to form the caged scaffold of (–)-actinophyllic acid; and (v) regioselective removal of a tertiary alcohol by taking advantage of a vicinal hemiketal. Our strategy not only circumvented the difficulties typically associated with forming the correct stereochemistry around the pyrrolidine ring but also resulted in the first enantioselective total synthesis of (–)-actinophyllic acid in which the asymmetric synthesis employed the same starting materials as the racemic synthesis.[6]

Section 1.13 Experimental procedures

General Information

All reactions were performed in dry solvents under an Ar atmosphere and anhydrous conditions. DCM, THF, and MeCN were freshly distilled over CaH_2 prior to use. All other reagents were used as received from commercial sources. Reactions were monitored through thin layer chromatography (TLC) on 0.25-mm SiliCycle silica gel plates and visualized under UV light. Flash column chromatography (FCC) was performed using SiliCycle Silica-P Flash silica gel (60-Å pore size, 40–63 μm). IR spectra were recorded using a Jasco FT-IR 4100 spectrometer. NMR spectra were recorded using Bruker Avance-500 instruments, calibrated to $CD(H)Cl_3$ as the internal reference (7.26 and 77.0 ppm for ^1H and ^{13}C NMR spectra, respectively) unless otherwise noted. ^1H NMR spectral data are reported in terms of chemical shift (δ, ppm), multiplicity, coupling constant (Hz), and integration. ^{13}C NMR spectral data are reported in terms of chemical shift (δ, ppm). The following abbreviations indicate the multiplicities: s, singlet; d, doublet; t, triplet; q, quartet; m, multiplet. High resolution mass spectra were recorded using a Waters LCT Premier XE time-of-flight instrument controlled by MassLynx 4.1 software. Samples were infused using direct loop injection from a Waters Acquity UPLC into the multi-mode ionization source. The lock mass standard for accurate mass determination was leucine enkephalin (Sigma L9133). X-ray crystallographic data were collected using a Bruker SMART CCD-based diffractometer equipped with a low-temperature apparatus operated at 100 K. Optical rotations were recorded using a Rudolph Autopol IV automatic polarimeter. Enantiomeric excess was measured through chiral HPLC using a Shimadzu CBM Lite system and a REGIS (*R*, *R*)-DACH DNB analytical (diameter: 4.5 mm) chiral column, with CH_2Cl_2/hexanes as the eluent and CHIRALCEL AD-H analytical (diameter: 4.6 mm) chiral column, with *i*PrOH/hexanes as the eluent.

General procedure for the [3 + 2] annulation

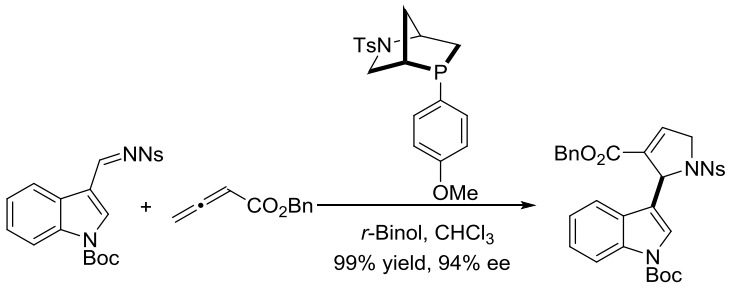

Pyrroline 60. A flame-dried round-bottom flask was charged with the imine **58** (8.58 g, 20 mmol), chiral phosphine (1.50 g, 4 mmol, 0.2 equiv) and *r*-binol (1.14 g, 4 mmol, 0.2 equiv) in a glove box. The flask was capped with a rubber septum, transferred out of the glove box, and placed under a positive pressure of Ar. The solid mixture was dissolved in chloroform (250 mL), followed by the addition of the allenoate (4.18 g, 24 mmol, 1.2 equiv). The mixture was stirred at 0 ^{o}C until the starting imine **58** was consumed (as determined by TLC in benzene). The crude reaction product was loaded directly onto a column of SiO_2 and purified through flash column chromatography (20% EA/Hexanes) to yield compound **60** as a yellow oil (12.06 g, 99%, 94% ee as determined by HPLC). ^{1}H NMR (500 MHz, $CDCl_3$) δ 7.92 (d, *J* = 7.8 Hz, 1H), 7.46 (s, 1H), 7.30 (d, *J* = 8.0 Hz, 2H), 7.24–7.21 (m, 5H), 7.15 (td, *J* = 7.8, 1.1 Hz, 1H), 7.06–7.04 (m, 2H), 7.01–6.98 (m, 2H), 6.89 (td, *J* = 7.3, 1.0 Hz, 1H), 6.18 (app t, *J* = 1.9 Hz, 1H), 5.09 (d, *J* = 12.5 Hz, 1H), 4.94 (d, *J* = 12.5 Hz, 1H), 4.90 (ddd, *J* = 17.4, 6.0, 2.1 Hz, 1H), 4.84 (dt, *J* = 17.4, 2.6 Hz, 1H), 1.66 (s, 9H); ^{13}C NMR (125 MHz, $CDCl_3$): δ 161.5, 149.1, 146.9, 136.4, 135.1, 133.6, 132.9, 132.7, 130.3, 130.2, 128.4, 128.2, 127.9, 127.8, 125.9, 124.5, 123.2, 122.6, 119.2, 117.1, 114.9, 84.0, 66.6, 61.8, 55.6, 28.2; IR (ATR) 3029, 2974, 2926, 1745, 1714, 1541, 1454, 1363, 1231, 1165, 1136, 1073, 795, 731, 655 cm^{-1}; HRMS–ESI (m/z) $[M + H]^+$ calcd $C_{31}H_{29}N_3O_9SH$, 620.1702, found 620.1707; $[\alpha]_{589}^{22.8}$ +166.2 °(C = 1.0, CH_2Cl_2).

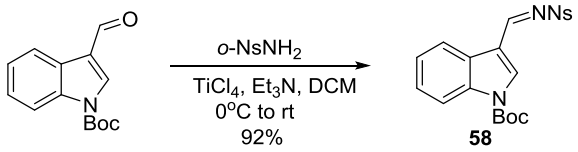

***N*-Nosyl-imine 58.** N-Boc indole-3-aldehyde[1] (4.76 g, 19.4 mmol) and 2-Nitrobenzenesulfonamide (3.96 g, 19.6 mmol, 1.01 equiv) were suspended in freshly distilled DCM (194 mL). The mixture was placed under a positive pressure of Ar and then freshly distilled triethylamine (8.12 mL, 58.2 mmol, 3 equiv) was introduced via syringe. The heterogeneous mixture was cooled to 0 ℃ and then 1 M $TiCl_4$ in DCM (9.71 mL, 9.71 mmol, 0.5 equiv) was added via syringe pump over 1 h. The mixture was then stirred until the starting material was consumed (as determined by TLC; the mixture was slowly warmed to room temperature over the course of the reaction). The mixture was diluted with toluene (200 mL) and filtered through a plug of Celite, eluting with toluene. The solution was concentrated (to ca. 200 mL) and filtered again through Celite, eluting with toluene. The solvent was evaporated and the residue recrystallized (EtOAc/pentanes) to give the imine. Mp: 150–152 ℃; ^{1}H NMR (500 MHz, $CDCl_3$): δ 9.17 (s, 1H), 8.425 (d, *J* = 7.8 Hz, 1H), 8.39 (s, 1H), 8.29 (d, *J* = 7.8 Hz, 1H), 8.17 (d, *J* = 8.3 Hz, 1H), 7.78 (td, *J* = 7.4, 1.4 Hz, 1H), 7.76–7.75 (m, 2H), 7.42 (td, *J* = 7.4, 1.4 Hz, 1H), 7.36 (td, *J* = 7.4, 1.4 Hz, 1H), 1.69 (s, 9H); ^{13}C NMR (125 MHz, CDCl3): δ 166.7, 148.2, 139.2, 136.4, 134.2, 132.5, 131.8, 126.6, 126.1, 124.9, 124.7, 122.9, 116.3, 115.3, 86.3, 28.1; IR (ATR): 3132, 1545, 1365, 1289, 1211, 941, 834, 522 cm^{-1}; HRMS–ESI (m/z) $[M + H]^+$ cald $C_{20}H_{19}N_3O_7SH$, 446.1022, found 446.1025.

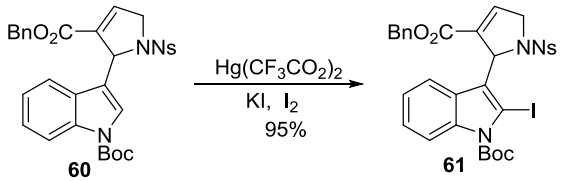

2-Iodoindole 61. To a solution of pyrroline **60** (12.06 g, 20 mmol) in dry dichloromethane

(400 mL) was added mercury (II) trifluoroacetate (9.38 g, 22 mmol, 1.1 equiv). The bright red solution was stirred for 45 minutes, washed with 50 mL of a saturated aqueous solution of potassium iodide, after separation, dried over Na_2SO_4, filtered and then treated with iodine (6.10 g, 24 mmol, 1.2 equiv). The resulting purple solution was stirred overnight and filtered to remove the bright orange precipitate. The filtrate was next successively washed with a saturated aqueous solution of sodium thiosulfate solution and brine, dried over Na_2SO_4, filtered and concentrated. The residue was then purified by flash chromatography over silica gel (20% EA/Hexanes) to yield **61** as yellow foam (13.85 g, 95%).^{1}H NMR (500 MHz, $CDCl_3$) δ 7.74 (s, 1H), 7.51 (s, 1H), 7.24–7.17 (m, 4H), 7.16–7.12 (m, 2H), 7.04-6.99 (m, 5H), 6.87 (s, 1H), 6.32 (s, 1H), 5.11–5.01 (m, 2H), 4.94–4.86 (m, 2H), 1.73 (s, 9H); ^{13}C NMR (125 MHz, $CDCl_3$): δ 161.3, 148.9, 146.5, 138.1, 137.1, 135.1, 133.1, 132.7, 132.6, 130.7, 130.2, 128.4, 128.3, 128.2, 127.9, 126.6, 125.9, 124.4, 123.3, 118.2, 114.7, 85.7, 66.6, 65.3, 55.9, 28.2; IR (ATR) 3002, 2982, 2968, 2879, 1738, 1714, 1542, 1347, 1136, 1075, 743 cm^{-1}; HRMS–ESI (m/z) $[M + H]^+$ calcd $C_{31}H_{28}IN_3O_9SH$, 746.0669, found 746.0673; $[\alpha]_{589}^{23.2}$ +136.9 °(C = 1.0, CH_2Cl_2).

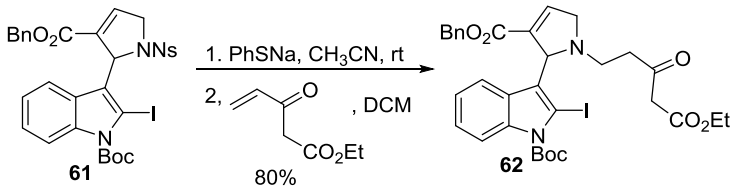

Ketoester 62. Sodium thiophenoxide (1.11 g, 7.5 mmol, 1.5 equiv) was added in one portion to a solution of the 2-iodoindole **61** (3.65 g, 5 mmol) in acetonitrile. The heterogeneous mixture was stirred at room temperature (as determined by TLC). The reaction was quenched by adding water and ethyl acetate. The aqueous phase was extracted five times with ethyl acetate. The combined organic phases were washed once with water then once with a saturated sodium bicarbonate. The organic phase was washed with brine and dried over Na_2SO_4. After filtration and

concentration in *vacuo*, the resulting yellow oil was then purified by flash chromatography over silica gel to give second imine which was used directly for the next step after concentration.

Ethyl 3-oxopent-4-enoate (1 M in DCM, 5 ml, 1 equiv) was add to the solution of second imine in DCM. The resulting reaction mixture was stirred for 30 min (as determined by TLC). After concentration in *vacuo*, the crude material was purified through flash column chromatography (30%–50% EA/Hexanes) to yield compound **62** as yellow foam (2.74 g, 80% over two steps). Major ketone form: ^{1}H NMR (500 MHz, $CDCl_3$) δ 8.04 (d, *J* = 8.6 Hz, 1H), 7.52 (d, *J* = 8.6 Hz, 1H), 7.22–7.16 (m, 4H), 7.10 (t, *J* = 8.1 Hz, 1H), 7.03 (q, *J* = 2.0 Hz, 1H), 6.96–6.93 (m, 2H), 5.14 (td, *J* = 5.7, 2.4 Hz, 1H), 5.05 (d, *J* = 12.6 Hz, 1H), 4.84 (d, *J* = 12.6 Hz, 1H), 4.17 (ddd, *J* = 16.5, 5.7, 2.5 Hz, 1H), 4.06 (q, *J* = 7.2, 2H), 3.57 (ddd, *J* = 16.5, 6.5, 2.1 Hz, 1H), 3.10–2.99 (m, 3H), 2.94–2.87 (m, 1H), 2.61–2.50 (m, 2H), 1.73 (s, 9H), 1.18 (t, *J* = 7.2 Hz, 3H); ^{13}C NMR (125 MHz, $CDCl_3$): δ 202.2, 167.1, 162.7, 149.2, 140.6, 138.7, 135.4, 128.3, 127.9, 127.8, 124.2, 122.3, 115.4, 85.1, 66.0, 61.1, 58.6, 48.5, 47.6, 42.2, 28.3, 14.0; IR (ATR) 2978, 2932, 2879, 1734, 1715, 1444, 1305, 1244, 1151, 1095, 1012 cm^{-1}; HRMS–ESI (m/z) $[M + H]^+$ calcd $C_{32}H_{35}IN_2O_7H$, 687.1567, found 687.1564; $[\alpha]_{589}^{23.5}$ +89.3 °(C = 1.0, CH_2Cl_2).

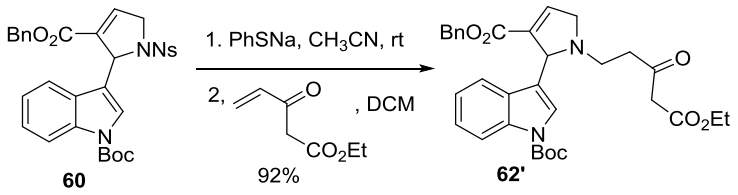

Ketoester 62'. Following the same procedure for ketoester **62**, compound **62'** could be obtain in 92% yield for two steps from compound **60**. Major ketone form: ^{1}H NMR (500 MHz, $CDCl_3$) δ 8.12 (s, 1H), 7.56 (d, *J* = 8.4 Hz, 1H), 7.49 (s, 1H), 7.27 (t, *J* = 8.0 Hz, 1H), 7.23-7.19 (m, 2H), 7.14 (t, *J* = 8.1 Hz, 1H), 6.99–6.96 (m, 3H), 5.05 (d, *J* = 13.2 Hz, 1H), 4.95 (t, *J* = 2.6 Hz, 1H), 4.87 (d, *J* = 12.6 Hz, 1H), 4.11-4,05 (m, 3H), 3.55 (dd, *J* = 16.5, 6.5 Hz, 1H), 3.17 (d, *J* =

15.6 Hz, 1H), 3.12 (d, *J* = 15.6 Hz, 1H), 3.04–2.99 (m, 1H), 2.87–2.82 (m, 1H), 2.65–2.61 (m, 1H), 2.58–2.53 (m, 1H), 1.66 (s, 9H), 1.18 (t, *J* = 7.2 Hz, 3H); ^{13}C NMR (125 MHz, $CDCl_3$): δ 202.1, 167.1, 162.9, 149.6, 139.9, 136.0, 135.5, 129.4, 128.3, 127.9, 127.7, 124.8, 124.3, 122.4, 120.3, 119.8, 115.3, 83.6, 66.0, 65.7, 61.2, 58.3, 48.7, 47.4, 42.3, 28.2, 14.0; IR (ATR) 3020, 2943, 2869, 1744, 1720, 1535, 1367, 1211, 1209, 1099, 1010 cm^{-1}; HRMS–ESI (m/z) $[M + H]^+$ calcd $C_{32}H_{36}N_2O_7H$, 561.2600, found 561.2601;

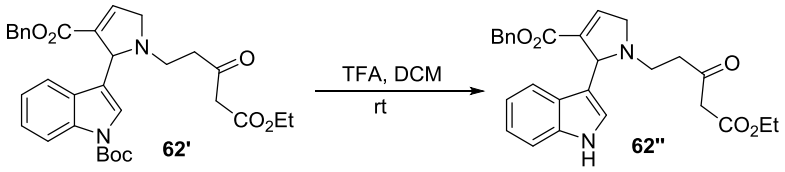

Ketoester 62". TFA (5 mL) was added to a solution of ketoester **62'** (560 mg, 1 mmol) in 20 mL DCM. The reaction mixture were stirred at room temperature for 30 min (as determined by ESI-MS). The reaction was quenched by saturated Na_2CO_3 and DCM. The aqueous phase was extracted with DCM; The organic phase was washed with brine and dried over Na_2SO_4. After filtration and concentration in *vacuo*, the resulting yellow oil was then purified by flash chromatography (80%–100% EA/Hexanes) over silica gel to colorless oil (368 mg, 80%). Major ketone form: ^{1}H NMR (500 MHz, $CDCl_3$) δ 8.17 (s, 1H), 7.62 (d, *J* = 8.4 Hz, 1H), 7.32 (d, *J* = 8.2 Hz, 1H), 7.23–7.14 (m, 4H), 7.08–7.02 (m, 2H), 6.99–6.98 (m, 2H), 6.94 (s, *J* = 2.1 Hz, 1H), 5.10 (t, *J* = 2.6 Hz, 1H), 5.04 (d, *J* = 13.2 Hz, 1H), 4.88 (d, *J* = 12.6 Hz, 1H), 4.11–4,02 (m, 3H), 3.61 (dd, *J* = 16.5, 6.5 Hz, 1H), 3.12 (d, *J* = 15.6 Hz, 2H), 2.98–2.94 (m, 1H), 2.88–2.84 (m, 1H), 2.65–2.56 (m, 2H), 1.19 (t, *J* = 7.2 Hz, 3H); ^{13}C NMR (125 MHz, $CDCl_3$): δ 202.3, 167.2, 163.2, 138.9, 136.8, 136.6, 135.8, 128.3, 127.8, 127.6, 126.7, 123.8, 121.9, 119.9, 119.6, 111.2, 65.8, 65.5, 61.2, 58.3, 48.7, 47.3, 42.3, 14.0; IR (ATR) 3210, 3010, 2968, 2870, 1730, 1715, 1638, 1487, 1321, 1111, 1079 cm^{-1}; HRMS–ESI (m/z) $[M + H]^+$ calcd $C_{32}H_{36}N_2O_7H$, 461.2076, found 461.2081;

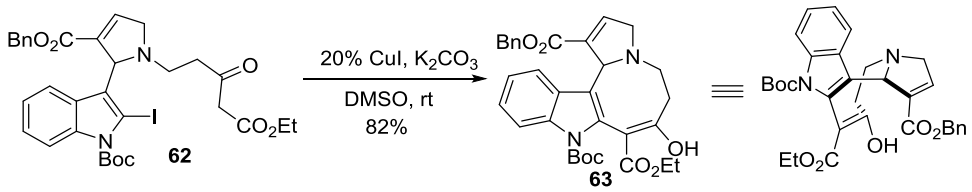

Enol 63. A flame-dried round-bottom flask was charged with ketoester (6.86 g, 10 mmol), and potassium carbonate (2.76 g, 20 mmol, 2 equiv), evacuated and backfilled with argon. DMSO (250 mL) and CuI (380 mg, 2 mmol, 0.2 equiv), were added under argon. The reaction mixture was stirred at the room temperature until the conversion was completed detected by TLC. The mixture was partitioned between ethyl acetate and saturated NH_4Cl. The aqueous phase was extracted five times with EtOAc; the combined organic phases was washed with brine, dried over Na_2SO_4 and concentrated in *vacuo*. The residue was recrystallization from methanol to yield colorless solid (4.57 g, 82%). MP: 148–150 ^oC ^1H NMR (500 MHz, $CDCl_3$) δ 12.77 (s, 1H), 8.14 (d, *J* = 8.4 Hz, 1H), 7.58 (d, *J* = 8.4 Hz, 1H), 7.22 (td, *J* = 7.5, 1.0 Hz, 1H), 7.17–7.15 (m, 1H), 7.13–7.10 (m, 2H), 7.09–7.06 (m, 2H), 6.75 (d, *J* = 7.5 Hz, 2H), 5.05 (d, *J* = 12.8 Hz, 1H), 4.81 (d, *J* = 12.8 Hz, 1H), 4.62 (td, *J* = 6.0, 2.2 Hz, 1H), 4.25 (ddd, *J* = 17.0, 6.0, 2.8 Hz, 1H), 4.07 (qd, *J* = 7.2, 1.0 Hz, 2H), 3.60 (ddd, *J* = 17.0, 6.0, 2.0 Hz, 1H), 3.21 (dd, *J* = 12.0, 7.6 Hz, 1H), 2.74 (t, *J* = 11.5 Hz, 1H), 2.50 (dd, *J* = 13.0, 7.6 Hz, 1H), 2.31 (t, *J* = 12.6 Hz, 1H), 1.60 (s, 9H), 1.02 (t, *J* = 7.2 Hz, 3H); ^{13}C NMR (125 MHz, $CDCl_3$): δ 173.7, 172.2, 163.3, 150.2, 140.0, 136.8, 135.7, 135.5, 131.5, 128.2, 127.7, 127.5, 127.4, 124.2, 122.8, 121.1, 119.3, 115.6, 97.7, 83.3, 65.9, 64.7, 61.1, 60.8, 50.2, 34.7, 28.2, 14.1; IR (ATR) 2971, 2932, 2796, 1739, 1728, 1645, 1454, 1365, 1317, 1228, 1184, 1006 cm^{-1}; HRMS–ESI (m/z) $[M + H]^+$ calcd $C_{32}H_{34}N_2O_7H$, 559.2444, found 559.2448; $[\alpha]_{589}^{23.8}$ -13.89 °(C = 1.0, CH_2Cl_2).

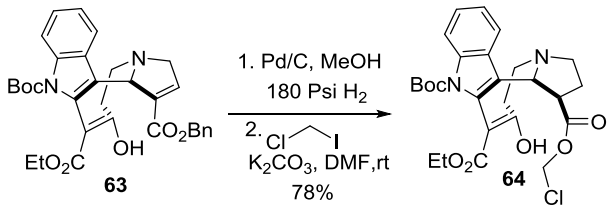

Chloromethyl ester 64. The enol **63** (5.58 g, 10 mmol) and 10% Pd/C (11.16 g, 200% *wt*) were added to a metal high-pressure reaction vessel equipped with a stirrer bar and then methanol (200 mL) was added to form a solution. The reaction vessel was sealed and purged three times with H_2 gas (pressurized to 50 psi, followed by release of the H_2 gas). The vessel was then pressurized to 200 psi with H_2 gas and stirred for 2 days. The mixture was filtered through a pad of Celite and washed with 50 mL methanol. After concentration *in vacuo*, the crude reaction product carboxylic acid was directly used for the next step without further purification.

Chloroiodomethane (3.52 g, 20 mmol, 1 equiv) and potassium carbonate (2.76 g, 20 mmol, 2 equiv) were added to a solution of the carboxylic acid described in the preceding paragraph in 100 mL of dry DMF. The reaction mixture was stirred at room temperature until the conversion was completed detected by TLC. The mixture was partitioned between ethyl acetate and saturated NH_4Cl. The aqueous phase was extracted five times with EtOAc; the combined organic phases was washed with brine, dried over Na_2SO_4 and concentrated in *vacuo*. The crude material was purified through flash column chromatography (30%–50% EA/Hexanes) to yield compound **64** as yellow foam (4.04 g, 78% over two steps). ^{1}H NMR (500 MHz, $CDCl_3$) δ 12.86 (s, 1H), 8.09 (d, *J* = 8.4 Hz, 1H), 7.46 (d, *J* = 8.4 Hz, 1H), 7.29 (td, *J* = 7.5, 1.0 Hz, 1H), 7.26–7.20 (m, 1H), 5.15 (d, *J* = 6.1 Hz, 1H), 4.46 (d, *J* = 6.1 Hz, 1H), 4,34–4.18 (m, 2H), 4.03 (d, *J* = 8.2 Hz, 1H), 3.56 (td, *J* = 9.0, 6.0 Hz, 1H), 3.29 (td, *J* = 9.0, 6.0 Hz, 1H), 3.24 (d, *J* = 8.2 Hz, 1H), 2.85 (td, *J* = 9.0, 6.0 Hz, 1H), 2.47 (dd, *J* = 18.0, 8.6 Hz, 1H), 2.36 (dd, *J* = 12.0, 7.6 Hz, 1H), 2.27–2.23 (m, 2H), 2.20–1.97 (m, 1H), 1.55 (s, 9H), 1.28 (t, *J* = 7.2 Hz, 3H); ^{13}C NMR (125 MHz, $CDCl_3$): δ 173.6, 171.7,

171.3, 150.2, 135.9, 129.9, 128.6, 124.3, 122.4, 118.4, 117.0, 115.1, 98.8, 83.5, 68.3, 65.9, 61.1, 60.8, 56.2, 50.1, 48.9, 32.3, 28.0, 25.1, 14.1; IR (ATR) 2980, 2932, 2806, 1746, 1742, 1725, 1647, 1615, 1459, 1369, 1352, 1120, 1066, 712 cm^{-1}; HRMS–ESI (m/z) $[M + H]^+$ calcd $C_{26}H_{31}ClN_2O_7H$, 519.1898, found 519.1821; $[\alpha]_{589}^{23.9}$ +93.78 °(C = 1.0, CH_2Cl_2).

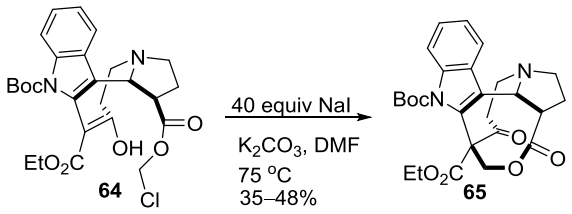

Lactone 65. Sodium iodide (1.8 g, 12 mmol, 40 equiv) and potassium carbonate (165 mg, 1.2 mmol, 4 equiv) were added to a solution of the chloromethylester (155 mg, 0.3 mmol) in 40 mL of dry DMF. The reaction mixture was stirred at 75ºC until the conversion was completed detected by TLC. The mixture was partitioned between ethyl acetate and saturated NH_4Cl. The aqueous phase was extracted five times with EtOAc; the combined organic phases was washed with brine, dried over Na_2SO_4 and concentrated in *vacuo*. The crude material was purified through flash column chromatography (30%–50% EA/Hexanes) to yield **65** as yellow foam (69 mg, 40%). ^1H NMR (500 MHz, $CDCl_3$) δ 7.93 (d, *J* = 8.4 Hz, 1H), 7.55 (d, *J* = 8.4 Hz, 1H), 7.34 (t, *J* = 7.5 Hz, 1H), 7.26–7.24 (m, 1H), 5.29–5.25 (m, 2H), 4.39 (d, *J* = 6.1 Hz, 1H), 4,19–4.10 (m, 2H), 3.37–3.23 (m, 3H), 3.15 (td, *J* = 7.0, 2.0 Hz, 1H), 2.87 (td, *J* = 9.0, 3.0 Hz, 1H), 2.70 (dd, *J* = 18.0, 8.6 Hz, 1H), 2.32–2.28 (m, 1H), 2.22–2.17 (m, 1H), 2.04–1.97 (m, 1H), 1.65 (s, 9H), 1.24 (t, *J* = 7.2 Hz, 3H); ^{13}C NMR (125 MHz, $CDCl_3$): δ 199.7, 175.7, 165.5, 151.2, 136.2, 133.1, 128.4, 125.4, 122.7, 121.4, 118.1, 114.8, 85.3, 69.3, 68.0, 63.1, 61.8, 55.5, 53.5, 47.1, 37.5, 28.2, 24.7, 13.7; IR (ATR) 2981, 2854, 2826, 1741, 1720, 1710, 1450, 1354, 1302, 1253, 1153, 1125, 1030, 710 cm^{-1}; HRMS–ESI (m/z) $[M + H]^+$ calcd $C_{26}H_{30}N_2O_7H$, 483.2131, found 483.2128; $[\alpha]_{589}^{22.8}$ +122.2 °(C

= 1.0, CH_2Cl_2).

Single crystals suitable for X-ray diffraction were prepared through slow evaporation of methanol solution of **65**. An ORTEP image of **65** is provided below.

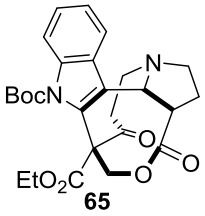

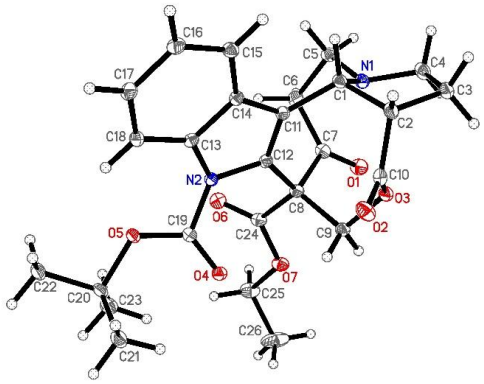

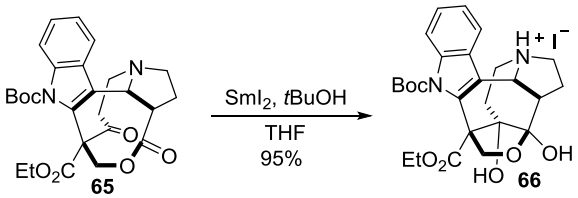

Hemiketal 66. A flame-dried round-bottom flask was charged with the lactone **65** (48 mg, 0.1 mmol) in a glove box. The flask was capped with a rubber septum, transferred out of the glove box, and placed under a positive pressure of Ar. The solid mixture was dissolved in 0.5 mL THF, followed by the addition of *t*-butanol (74 mg, 1 mmol, 10 equiv). The reaction mixture was slowly added fresh 0.4 M SmI_2 in THF (0.75 mL, 0.3 mmol, 3 equiv), stir at room temperature until the lactone was consumed (as determined by TLC). The mixture was partitioned between DCM and 1M HCl aqueous solution. The aqueous phase was extracted five times with DCM; the combined

organic phases was dried over Na_2SO_4 and concentrated in *vacuo*. The crude reaction product was loaded directly onto a short column of SiO_2 and purified through flash column chromatography (10% Methanol/DCM) to yield compound **66** as yellow foam (58mg, 95%). If the reaction quenched by saturated NH_4Cl, the iodide salt **66** will slowly converted to tertiary amine which, after flash column chromatography (10% Methanol/DCM), could also been used for the next step. ^{1}H NMR (500 MHz, $CDCl_3$) δ 8.11 (d, *J* = 8.4 Hz, 1H), 7.93 (d, *J* = 8.4 Hz, 1H), 7.36 (t, *J* = 7.5 Hz, 2H), 5.33 (d, *J* = 7.1 Hz, 1H), 4.79 (d, *J* = 8.6 Hz, 1H), 4.59 (s, 1H), 4,37–4.24 (m, 1H), 4,22–4.17 (m, 2H), 3.99 (d, *J* = 8.6 Hz, 1H), 3.41 (t, *J* = 8.6 Hz, 1H), 3.36–3.28 (m, 2H), 3.12 (d, *J* = 7.0 Hz, 1H), 2.79–2.75 (m, 1H), 2.55–2.51 (m, 1H), 2.38 (td, *J* = 16.0, 3.0 Hz, 1H), 2.03 (d, *J* = 16.0 Hz, 1H), 1.69 (s, 9H), 1.28 (t, *J* = 7.2 Hz, 3H); ^{13}C NMR (125 MHz, $CDCl_3$): δ 169.4, 151.1, 137.1, 134.9, 128.3, 126.7, 126.6, 123.9, 120.5, 115.2, 109.8, 105.8, 86.6, 81.6, 74.5, 62.9, 62.7, 59.5, 50.3, 45.9, 29.7, 28.1, 24.6, 14.4; IR (ATR) 3408, 3394, 2980, 2864, 1778, 1768, 1498, 1332, 1263, 1147, 1041 cm^{-1}; HRMS–ESI (m/z) $[M + H]^+$ calcd $C_{26}H_{33}N_2O_7$, 485.2288, found 485.2280; $[\alpha]_{589}^{22.8}$ -65.6 °(C = 1.0, CH_2Cl_2).

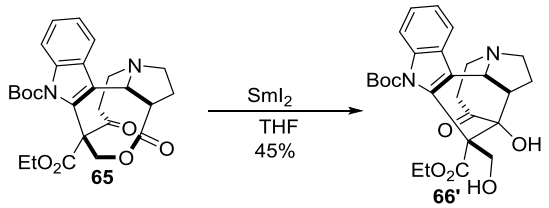

By using less than 10 equivalents of *t*-BuOH or without *t*-BuOH, a side product **66'** was also isolated in 45% yield whose structure was determined based on H and C NMR.[2] ^{1}H NMR (500 MHz, $CDCl_3$) δ 7.97 (d, *J* = 8.6 Hz, 1H), 7.87 (d, *J* = 6.8 Hz, 1H), 7.37–7.31 (m, 2H), 4.61 (d, *J* = 12.0 Hz, 1H), 4.54 (d, *J* = 12.0 Hz, 2H), 4,02–3.99 (m, 2H), 3.44–3.39 (m, 2H), 2.92–2.83 (m, 2H), 2.79–2.74 (m, 1H), 2.70–2.62 (m, 1H), 2.57–2.51 (m, 1H), 2.10–2.06 (m, 2H), 1.67 (s, 9H), 1.51–1.47 (m, 1H), 1.14 (t, *J* = 7.2 Hz, 3H); ^{13}C NMR (125 MHz, $CDCl_3$): δ 211.4, 169.9,

151.2, 136.2, 133.9, 128.3, 127.7, 125.4, 123.6, 119.9, 115.8, 85.4, 85.2, 64.7, 61.3, 59.1, 58.1, 53.7, 45.8, 41.0, 28.1, 26.4, 13.8; IR (ATR) 3408, 3484, 3011, 2964, 2934, 1789, 1778, 1458, 1362, 1213, 1057 cm^{-1}; HRMS–ESI (m/z) $[M + H]^+$ calcd $C_{26}H_{33}N_2O_7$, 485.2288, found 485.2281;

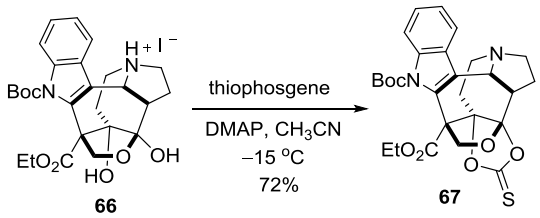

Thiocarbonate 67. Diol **66** (12.2 mg, 0.02 mmol) and DMAP (7.32 mg, 0.06 mmol, 3 equiv) in CH_3CN (1 mL) was cooled –15 ℃. A solution of thiophosgene in CH_3CN (1.0 M, 30 uL, 0.03 mmol) then was added slowly over 5 min. Stirring at –15 ℃ was continued for 20 min (Monitored by ESI-MS); saturated aqueous $NaHCO_3$ (3.0 mL) was added and the mixture was allowed to warm to room temperature. After extraction with CH_2Cl_2 five times, the combined organic phases were dried (Na_2SO_4) and the solvents were removed in *vacuo*. The crude reaction product was loaded directly onto a short column of SiO_2 and purified through flash column chromatography (5% methanol/DCM) to yield compound **67** as yellow foam (8.9 mg, 72%).^{1}H NMR (500 MHz, $CDCl_3$) δ 7.94 (d, *J* = 8.4 Hz, 1H), 7.59 (d, *J* = 8.4 Hz, 1H), 7.35 (t, *J* = 7.5 Hz, 1H), 7.29 (t, *J* = 7.5 Hz, 1H), 4.83 (d, *J* = 9.0 Hz, 1H), 4.72 (d, *J* = 8.0 Hz, 1H), 4.34–4.22 (m, 3H), 3.41 (q, *J* = 10.0 Hz, 1H), 3.21–3.13 (m, 2H), 2.85 (td, *J* = 15.0, 4.0 Hz, 1H), 2.61 (dd, *J* = 15.0, 3.7 Hz, 1H), 2.33–2.26 (m, 1H), 2.21–2.15 (m, 2H), 2.09 (td, *J* = 16.0, 3.0 Hz, 1H), 1.67 (s, 9H), 1.35 (t, *J* = 7.2 Hz, 3H); ^{13}C NMR (125 MHz, $CDCl_3$): δ 188.8, 166.4, 151.2, 134.8, 132.3, 128.6, 125.7, 123.5, 118.5, 117.8, 115.1, 98.9, 85.7, 75.4, 61.9, 61.5, 59.4, 52.1, 47.2, 45.8, 30.6, 28.2, 14.2; IR (ATR) 2979, 2885, 1738, 1456, 1371, 1355, 1319, 1260, 1147, 1084 cm^{-1}; HRMS–ESI (m/z) $[M + H]^+$ calcd $C_{27}H_{30}N_2O_7SH$, 527.1852, found 527.1850; $[\alpha]_{589}^{23.0}$ -149.8 ° (C = 1.0, CH_2Cl_2).

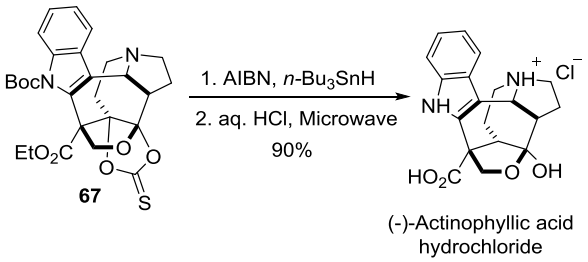

Actinohyllic acid hydrochloride. Thiocarbonate **67** (5.3 mg, 0.01 mmol), *n*Bu_3SnH (5.82 mg, 0.02 mmol, 2 equiv) and catalytic amount of AIBN were dissolved in 2mL dry toluene heated at 90 ℃ for 20 min. (as determined by TLC)). Saturated aqueous $NaHCO_3$ (1.0 mL) was added. After extraction with CH_2Cl_2 five times, the combined organic phases were dried (Na_2SO_4) and the solvents were removed in *vacuo*. The crude product was used directly for the next step without further purification.

The hemiacetal was dissolved in 4 M HCl aqueous solution (1 mL), placed in the microwave reactor at 100 ^oC for 30 min, and cooled to room temperature. The solvent were removed in *vacuo*. The crude product was purified by reverse phase C18 chromatography (0%→10%→20% MeOH in H_2O) to afford (–)-actinophyllic acid hydrochloride as a colorless solid (3.4 mg, 90% over two steps). MP: 242–244 ^oC; ^1H NMR (500 MHz, D_2O) δ 7.64 (d, *J* = 8.0 Hz, 1 H), 7.54 (d, *J* = 8.0 Hz, 1 H), 7.31 (t, *J* = 7.9 Hz, 1 H), 7.24 (t, *J* = 7.9 Hz, 1 H), 5.54 (d, *J* = 7.5 Hz, 1 H), 4.40 (d, *J* = 8.2 Hz, 1 H), 3.79 (d, *J* = 8.2 Hz, 1 H), 3.80–3.74 (m, 1 H), 3.66–3.60 (m, 1 H), 3.30–3.25 (m, 2 H), 3.09–3.05 (m, 2 H), 2.70–2.63 (m, 1 H), 2.61–2.54 (m, 1 H), 2.45–2.40 (m, 1 H), 2.37–2.33 (m, 1 H); ^{13}C NMR (150 MHz, D_2O,) δ 173.3, 137.9, 136.1, 127.2, 123.7, 121.2, 117.8, 112.4, 107.7, 102.4, 74.4, 61.1, 57.8, 54.3, 51.8, 50.2, 46.2, 25.3, 18.6; IR (neat) 3319, 1601, 1482, 1380, 1121, 751 cm^{-1}; HRMS–ESI (m/z) $[M + H]^+$ calcd $C_{27}H_{30}N_2O_7SH$, 527.1852, found 527.1850; $[\alpha]_{589}^{22.8}$ -175.78 °(C = 1.0, MeOH).

Section 1.14 References

(1) (a) Carroll, A. R.; Hyde, E.; Smith, J.; Quinn, R. J.; Guymer, G.; Forster, P. I. *J. Org. Chem.* **2005**, *70*, 1096. Later, Morita and co-workers isolated (+)-actinophyllic methyl ester from *Alstonia pneumatophore* in 0.0009% yield; see: (b) Koyama, K.; Hirasawa, Y.; Hosoya, T.; Hoe, T.; Chan, K.; Morita, H. *Bioorg. Med. Chem.* **2010**, *18*, 4415. In 2005, Luo and co-workers isolated Alstonia scholarine E, which is an ethyl ketal of actinophyllic acid, from *Alstonia scholaris* in 0.000006% yield; see: (c) Qin, X.; Zhao, Y.; Lunga, P.; Yang, X.; Song, C.; Cheng, G.; Liu, L.; Chen, Y.; Liu, Y.; Luo, X. *Tetrahedron* **2015**, *71*, 4372.

(2) (a) Leurs, J.; Nerme, V.; Sim, Y.; Hendriks, D. J. *Thromb. Haemostasis* **2004**, *2*, 416. (b) Polla, M. O.; Tottie, L.; Nordén, C.; Linschoten, M.; Musil, M.; Trumpp-Kallmeyer, S.; Aurkurst, I. R.; Ringom, R.; Holm, K. H.; Neset, S. M.; Sandberg, M.; Thurmond, J.; Yu, P.; Hategan, G.; Anderson, H. *Bioorg. Med. Chem.* **2004**, *12*, 1151. (c) Leurs, J.; Hendriks, D. *Thromb. Haemostasis* **2005**, *94*, 417. (d) *Hemostasis and Thrombosis: Basic Principles and Clinical Practice*, 6th ed.; Marder, V. J., Aird, W. C., Bennett, J. S., Schulman, S., White, G. C., Eds.; Lippincott Williams & Wilkins: Philadelphia, 2013.

(3) The natural actinophyllic acid was isolated as a brown gum, but synthetic (–)-actinophyllic acid hydrochloride is a white solid.

(4) Taniguchi, T.; Martin, C. L.; Monde, K.; Nakanishi, K.; Berova, N.; Overman, L. E. *J. Nat. Prod.* **2009**, *72*, 430.

(5) Misra, N.; Luthra, R.; Singh, K. L.; Kumar, S. In *Comprehensive Natural Product Chemistry*; Barton, D., Nakanishi, K., Editor in Chief; Elsevier: Oxford, UK, **1999**; *Vol. 4*, pp 25-59.

(6) (a) Martin, C. L.; Overman, L. E.; Rohde, J. M. *J. Am. Chem. Soc.* **2008**, *130*, 7568. (b) Martin, C. L.; Overman, L. E.; Rohde, J. M. *J. Am. Chem. Soc.* **2010**, *132*, 4894.

(7) (a) Granger, B. A.; Jewett, I. T.; Butler, J. D.; Hua, B.; Knezevic, C. E.; Parkinson, E. I.; Hergenrother, P. J.; Martin, S. F. *J. Am. Chem. Soc.* **2013**, *135*, 12984. (b) Granger, B. A.; Jewett, I. T.; Butler, J. D.; Martin, S. F. *Tetrahedron* **2014**, *70*, 4094.

(8) (a) Vaswani, R. G.; Day, J. J.; Wood, J. L. *Org. Lett.* **2009**, *11*, 4532. (b) Zaimoku, H.; Taniguchi, T.; Ishibashi, H. *Org. Lett.* **2012**, *14*, 1656. (c) Galicia, I. Z.; Maldonado, L. A. *Tetrahedron Lett.* **2013**, *54*, 2180. (d) Mortinmer, D.; Whiting, M.; Harrity, J. P. A.; Jones, S.; Coldham, I. *Tetrahedron Lett.* **2014**, *55*, 1255. (e) Meketa, M. L. Part One: Total Syntheses Of Ageladine A; Part Two: Studies Directed Towards a Total Synthesis of Actinophyllic Acid. Ph.D. Thesis, Pennsylvania State University, December 2008.

(9) For reports on Lu's original allene–imine [3 + 2] annulation, see: (a) Xu, Z.; Lu, X. *Tetrahedron Lett.* **1997**, *38*, 3461; (b) Xu, Z.; Lu, X. *J. Org. Chem.* **1998**, *63*, 5031.

(10) (a) Scherer, A.; Gladysz, J. A. *Tetrahedron Lett.*, **2006**, *47*, 6335. (b) Jean, L.; Marinetti, A. *Tetrahedron Lett.*, **2006**, *47*, 2141. (c) Fang, Y.-Q.; Jacobsen, E. N. *J. Am. Chem. Soc.*, **2008**, *130*, 5660. (d) Han, X.; Zhong, F.; Wang, Y.; Lu, Y. *Angew. Chem., Int. Ed.*, **2012**, *51*, 767.

(11) (a) Andrews, I. P.; Kwon, O. *Chem. Sci.* **2012**, *3*, 2510. (b) Henry, C. E.; Xu, Q.; Fan, Y. C.; Martin, T. J.; Belding, L.; Dudding, T.; Kwon, O. *J. Am. Chem. Soc.* **2014**, *136*, 11890.

(12) A weak base (e.g., K_2CO_3), a weak acid (e.g., *p*-TSA), or neutral conditions (e.g., $NaBH_3CN$ or PhSNa) could induce the epimerization.

(13) (a) Grehn, L.; Ragnarsson, U. *Angew. Chem. Int. Ed.*, 1984, **23**, 296. (b) Bringmann, G.; Tasler, S.; Endress, H.; Peters, K.; Peters, E.-M. *Synthesis*, 1998, 1501.

(14) All chiral phosphines are commercially available from Sigma–Aldrich.

(15) (a) Xia, Y.; Liang, Y.; Chen, Y.; Mang, M.; Jiao, L.; Huang, F.; Liu, S.; Yu, Z. *J. Am. Chem. Soc.* **2007**, *129*, 3470.

(16) (a) Shi, M.; Chen, L. H. *Chem. Commun.* **2003**, 1310. (b) Han, X.; Zhong, F.; Wang, Y.; Lu, Y. *Angew. Chem. Int. Ed.* **2012**, *51*, 767. (c) Yao, W.; Dou, X.; Lu, Y. *J. Am. Chem. Soc.* **2015**, *137*, 55.

(17) (a) Paquette, L. A.; Bzowej, E. I.; Branan, B. M.; Stanton, K. J. *J. Org. Chem.* **1995**, *60*, 7277. (b) Baran, P. S.; Richter, J. M.; Lin, D. W. *Angew. Chem. Int. Ed.* **2005**, *44*, 609. (c) Magolan, J.; Kerr, M. A. *Org. Lett.* **2006**, *8*, 4561. (d) Richter, J. M.; Whitefield, B. W.; Maimone, T. J.; Lin, D. W.; Castroviejo, M. P.; Baran, P. S. *J. Am. Chem. Soc.* **2007**, *129*, 12857. (e) Chen, P.; Cao, L.; Tian, W.; Wang, X.; Li, C. *Chem. Commun.* **2010**, *46*, 8436. (f) Zi, W.; Xie, W.; Ma, D. *J. Am. Chem. Soc.* **2012**, *134*, 9216. (g) Oisaki, K.; Abe, J.; Kanai, M. *Org. Biomol. Chem.* **2013**, *11*, 4569. (h) Jiang, Q.; Sheng, W.; Tian, M.; Tang, J.; Guo, C. *Eur. J. Org. Chem.* **2013**, 1861. (i) Wang, H.; Guo, L. N.; Duan, X. H. *Chem. Commun.* **2013**, *49*, 10370. (j) Matsubara, T.; Takahashi, K.; Ishihara, J.; Hatakeyama, S. *Angew. Chem. Int. Ed.* **2014**, *53*, 757. For a brief review, see: (k) Csaky, A. G.; Plumet, *J. Chem. Soc. Rev.* **2001**, *30*, 313. (l) Guo, F.; Clift, M. D.; Thomson, R. J. *Eur. J. Org. Chem.* **2012**, 4881.

(18) Barcan, G. A.; Patel, A.; Houk, K. N.; Kwon, O. *Org. Lett.* **2012**, *14*, 5388; in the *Org. Lett.* paper PhSK was generated from KH and thiophenol; this approach worked well for our reactions. PhSNa could be obtained at lower cost by mixing thiophenol and NaOH and drying in a high-vacuum oven.

(19) (a) Hamann, B. C.; Beare, N. A.; Hartwig, J. F. *J. Am. Chem. Soc.* **1997**, *119*, 12382. (b) Hennessy, E. J.; Buchwald, S. L. *Org. Lett.* **2002**, *4*, 269. (c) Xie, X.; Cai, G.; Ma, D. *Org. Lett.* **2005**, *7*, 4693. (d) Coste, A.; Toumi, M.; Wright, K.; Razafimahaleo, V.; Couty, F.; Marrot, J.; Evano, G. *Org. Lett.* **2008**, *10*, 3841. Recent reviews on enolate coupling, see: (e) Culkin, D. A.; Hartwig, J. F. *Acc. Chem. Res.* **2003**, *36*, 234. (f) Johansson, C. C. C.; Colacot, T. J. *Angew. Chem. Int. Ed.* **2010**, *49*, 676. (g) Bellina, F.; Rossi, R. *Chem. Rev.* **2010**, *110*, 1082.

(20) Because we could not identify conditions for the separation of the two enantiomers of compound **14**, we proceeded to compound **15** to determine the enantiomeric excess. See the SI for more details.

(21) (a) Auer, E.; Gossinger, E.; Graupe, M. *Tetrahedron Lett.* **1997**, *38*, 6577. (b) Molander, G. A.; Wolfe, C. N. *J. Org. Chem.* **1998**, *63*, 9031. (c) Yamamoto, Y.; Matsumi, D.; Itoh, K. *Chem. Commun.* **1998**, *34*, 875. (d) Liu, Y.; Zhang, Y. *Tetrahedron Lett.* **2001**, *42*, 5745. (e) Hasegawa, E.; Kentaro, O.; Tanikawa, N.; Nakamura, M.; Iwaya, K.; Hoshi, T.; Suzuki, T. *Tetrahedron Lett.* **2006**, *47*, 7715. (f) Ge, H. M.; Zhang, L. D.; Tan, R. X.; Yao, Z. J. *J. Am. Chem. Soc.* **2012**, *134*, 12323. (g) Frey, G.; Luu, H. T.; Bichovski, P.; Feurer, M.; Streuff, D. *Angew. Chem. Int. Ed.* **2013**, *52*, 7131. (h) Ti Bichovski, P.; Haas, T. M.; Kratzert, D.; Streuff, J. *Chem. Eur. J.* **2015**, 2339. For more recent reviews on SmI_2, see: (i) Edmonds, D. J.; Johnston, D.; Procter, D. J. *Chem. Rev.* **2004**, *104*, 3371. (j) Nicolaou, K. C.; Ellery, S. P.; Chen, J. S. *Angew. Chem. Int. Ed.* **2009**, *48*, 7140.

(22) (a) Emmer, G.; Roth, S. W. *Tetrahedron* **1992**, *48*, 5861. (b) Myers, A. G.; Tom, N. J.; Fraley, M. E.; Cohen, S. B.; Madar, D. J. *J. Am. Chem. Soc.* **1997**, *119*, 6072. (c) Brüggemann, M.; McDonald, A. I.; Overman, L. E.; Rosen, M. D.; Schwink, L.; Scott, J. P. *J. Am. Chem. Soc.* **2003**, *125*, 15284. (d) Nicolaou, K. C.; Sun, Y. P.; Korman, H.; Sarlah, D. *Angew. Chem. Int. Ed.* **2010**, *49*, 5875.

Chapter 2

Synthetic Studies toward Total Synthesis of Akuammiline Indole Alkaloids

Section 2.1 Introduction

Since akuammiline was characterized in 1932, more than 100 akuammiline monoterpenoid indole alkaloids have been discovered from different medicinal plants.[1–2] Initial interest in the akuammilines stemmed from their roles in traditional medicine, where people from southern and southeastern Asia utilized the leaves of native plants to treat various ailments in humans and livestock. Preliminary studies have indicated that these natural products possess a wide range of biological activity, such as the reversal of drug resistance in drug-resistant KB cells by aspidophylline A and the in *vitro* antiinflammatory activity through inhibition of the 5-lipoxygenase enzyme exhibited by picrinine.[3–4] Strictamine has been used in folk medicine for its potent antitumor, antiinflammatory, and antibiosis activities.[5]

Structurally, akuammiline-type indole alkaloid is a highly complex, cage-like molecule that contains: (i) a furoindoline core fused to a densely functionalized cyclohexyl ring and a [3.3.1]azabicycle (aspidophylline A, aspidodasycarpine, and lonicerine); (2) a densely functionalized cyclohexane ring that is part of two conjoined [3.3.1]azabicycles (strictamine, cathafoline, and akuammiline); (iii) a densely functionalized cyclohexane ring that is part of two conjoined [3.3.1]azabicycles and two *N, O*-acetal linkages within its polycyclic skeleton (picrinine and picraline); (iv) adjacent quaternary centers (akuammiline, aspidodasycarpine, and lonicerine); (v) a pyrrolidinoindoline core which arises from a nitrogen migration within the parent akuammiline architecture (corymine and vincorine). This unprecedented architecture, along with great biomedical potential, has garnered widespread attention from the synthetic community. Among these akuammiline family members, the compounds containing the [3.3.1]azabicycle, in our opinion, could be derived from our phosphine-catalyzed [4 + 2] annulation product.

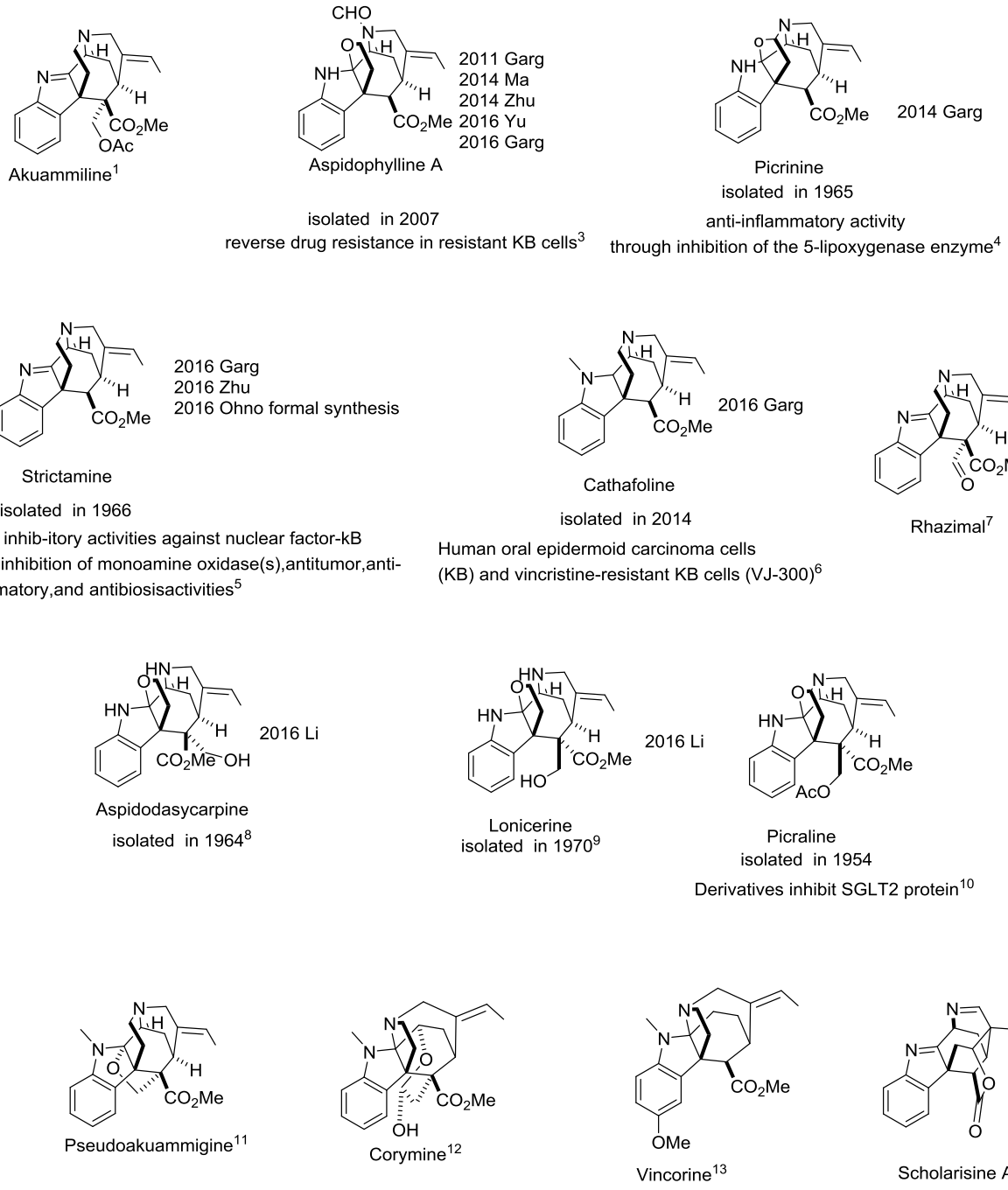

Figure 2.1.1 Structures of Akuammiline Indole Alkaloids Memebers

So far, (±)-Aspidophylline A had been accessed synthetically by Garg's group and the laboratories of Zhu and Ma.[15] In addition, Garg's group has completed the total synthesis of picrinine.[16] More recently, the same group completed enantioselective total syntheses of (−)-aspidophylline A and (+)-strictamine.[17] At the same time, Zhu's group finished the total synthesis

of (±)-strictamine.[18] In 2016, Li's group published an elegant synthetic approach toward the syntheses of aspidodasycarpine and lonicerine.[19]

Section 2.2 Biosynthesis

As with the actinophyllic acid biosynthetic pathway, akuammiline indole alkaloids start with condensation between tryptamine and secologanin to form geissoschizine, which is believed to be the progenitor to many different alkaloid frameworks including the strychnos, marvacurine, and akuammiline through different bond formations.[20] As shown in scheme 2.2.1, forming the bond between C2 and C16 could access strychnos alkaloids. Bond formation between N1 and C16 could reach marvacurine alkaloid. Most importantly, the akuammiline indole alkaloid family member, rhazimal, could be constructed *via* bond formation between C6 and C17. As depicted in Scheme 2.2.2, rhazimal serves as the parent molecule to the other akuammiline indole alkaloids. Rhazimal underwent C17 reduction, N-methylation, and cyclization, which could access akuammigine. Through C17 reduction and acylation, akuammline could be formed, which was further oxidized to more complex picraline. Rhazimal could also go through C16 deformylation to access another akuammiline natural product, strictamine, which could be oxidized to picrinine. Further transformations of picrinine could furnish the other family members: scholarisine A and aspidophylline A.

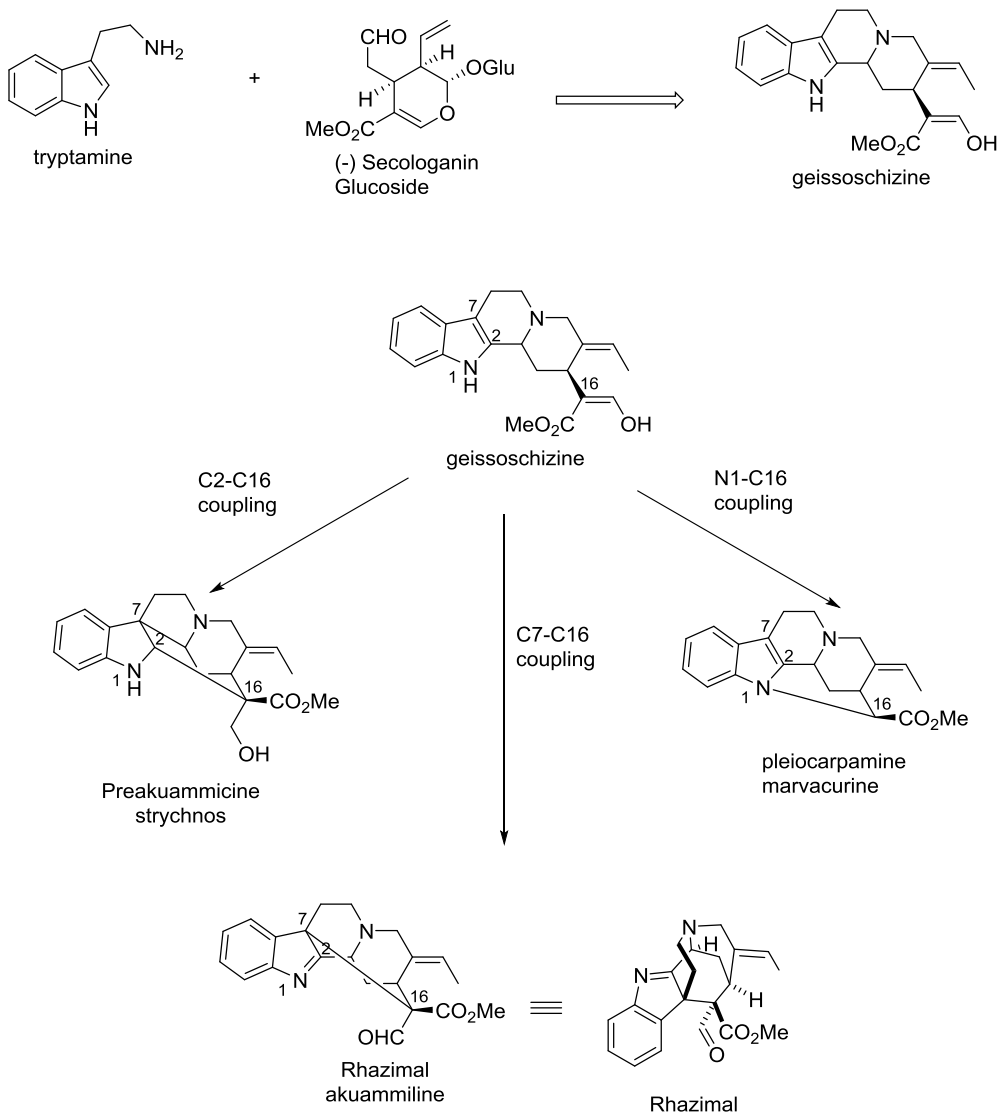

Scheme 2.2.1 Biosynthesis of Geissoschizine toward Other Alkaloid Families

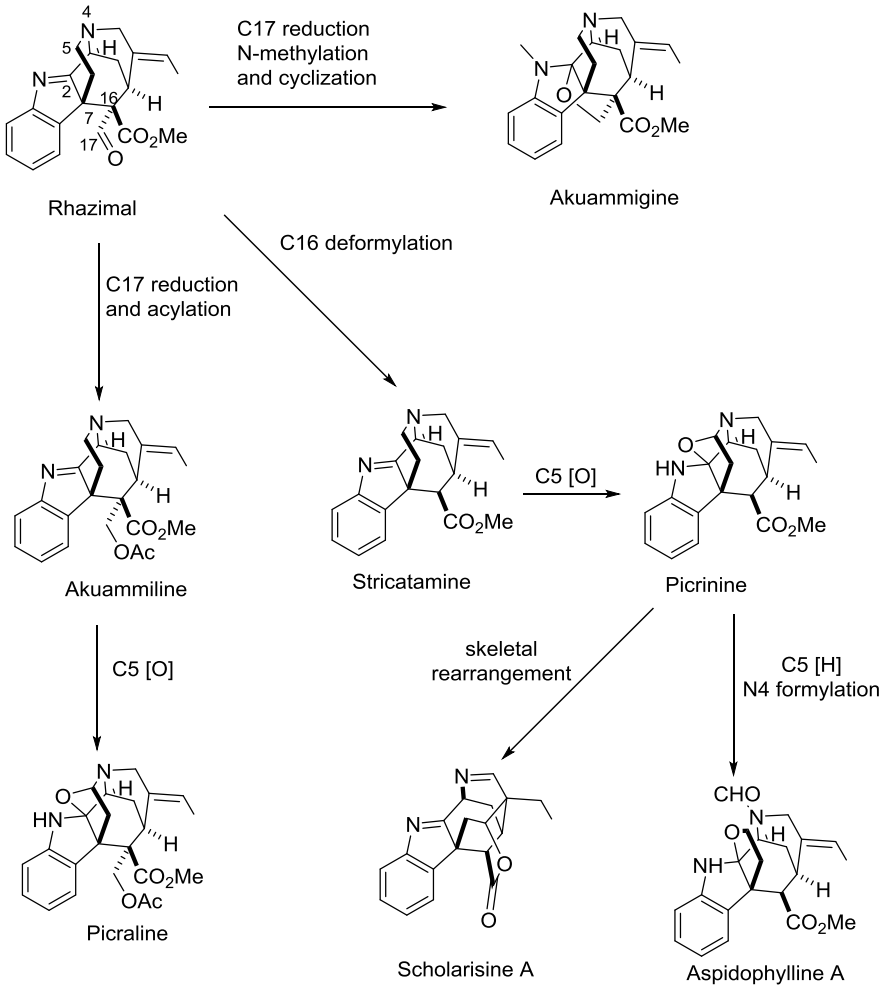

Scheme 2.2.2 Proposed Akuammiline Indole Alkaloids Biosynthetic Pathway

Section 2.3 Previous Syntheses toward Akuammiline Indole Alkaloids

Akuammiline indole alkaloids were isolated over 100 years ago. Synthetic studies were only started by Dolby and co-workers in the 1970s, which brought some attention to the akuammiline indole alkaloids.[21] After 2000, more groups started working on the syntheses of akuammiline natural products.[22]

Section 2.3.1 Garg's Synthetic Approach to (±)-Aspidophylline A

In 2011, Garg's group first reported the total synthesis of (±)-aspidophylline A.[15] Their syntheses featured Heck cyclization between vinyl iodide and *α,β*-unsaturated ester to forge [3.3.1]azabicyclic ring system. They elaborated different derivatives of allyl compounds, which

failed to undergo the interrupted Fischer indolization. Then they built the structurally more rigid lactone **5**, which could undergo Fischer indolization smoothly to deliver desired indolinine **6**. Then methanolysis of lactone gave indoline **7**. Two more steps furnished the final natural product, aspidophylline A.

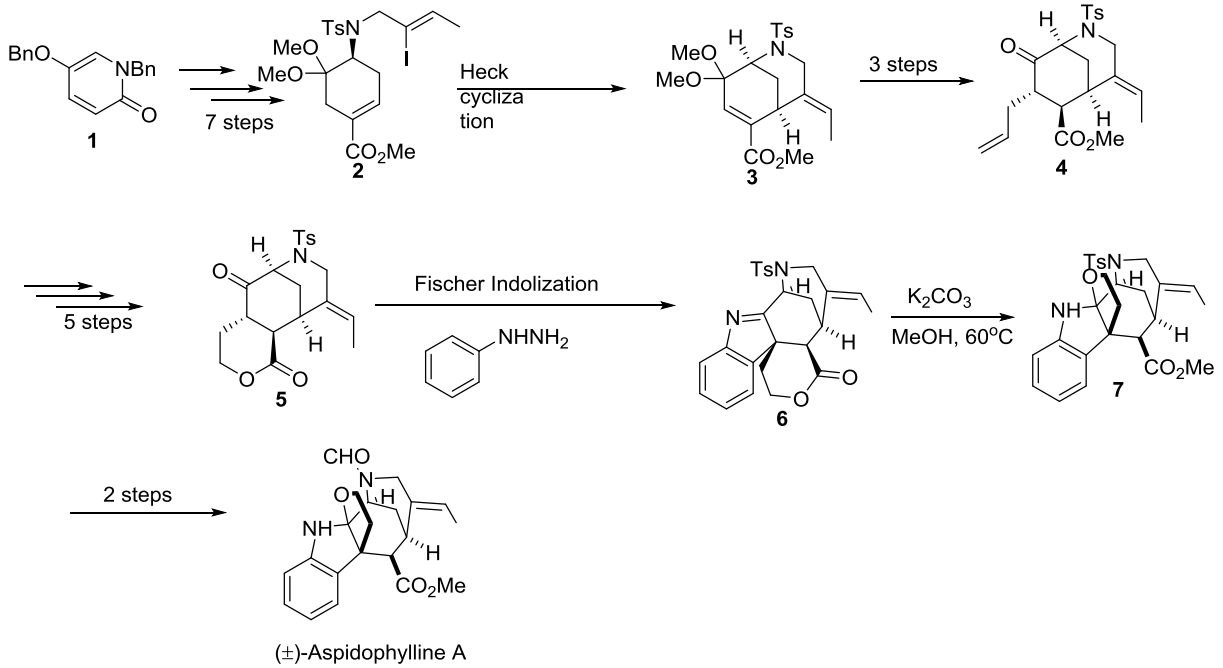

Scheme 2.3.1 Garg's Synthetic Approach to (±)-Aspidophylline A

Section 2.3.2 Ma's Synthetic Approach to (±)-Aspidophylline A

Three years later, Ma's group reported the another total synthesis of (±)-Aspidophylline A.[15] Starting from protected indole **8**, after four-step transformation, a tether at the C2 position of indole was introduced, which prepared for their oxidative coupling to form the quaternary carbon. After extensive screening, they finally found that using iodine as an oxidant with free hydroxyl group could give them the desired cyclization product, although in low yield, which forged the most challenging part of the skeleton. After further transformations, they synthesized vinyl iodide **12**. From there, they adopted a similar strategy to form the [3.3.1]azabicyclic system through a transition metal catalyzed coupling reaction between vinyl iodide and α,β-unsaturated ester. After

removal of the protecting group, they could finally access (±)-aspidophylline A.

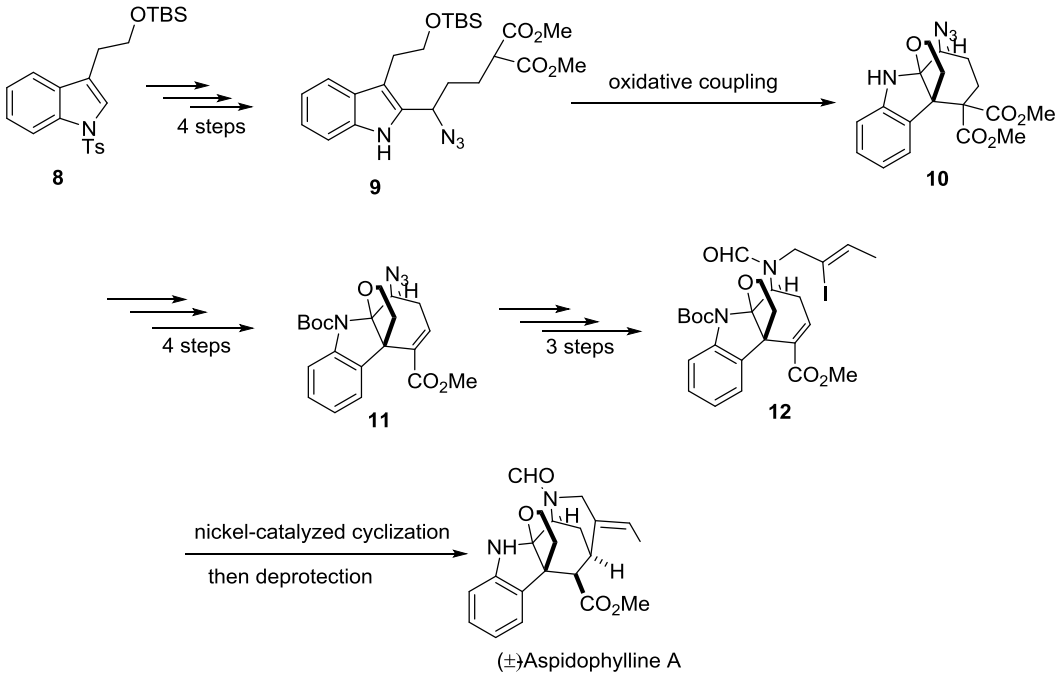

Scheme 2.3.2 Ma's Synthetic Approach to (±)-Aspidophylline A

Section 2.3.3 Zhu's Synthetic Approach to (±)-Aspidophylline A

At the same time, Zhu's group finished the total synthesis of (±)-aspidophylline A.[15] They built a fully functionalized dihydrocarbazole through the desymmetrization of readily available starting material **13**. Oxidative cleavage of the terminal alkene, followed by reduction, could quickly forge the furoindoline motif **15**. After formation of compound **16**, they successfully introduced nitrogen *via* oxidative azadation to form desired product **17**, along with diastereoisomer **18** with a 1:1 mixture. Through a similar bond disconnection, they introduced vinyl iodide to the primary amine to form compound **19**. Different from previous two syntheses, they used an intramolecular Michael addition to finish the skeleton of this natural product.

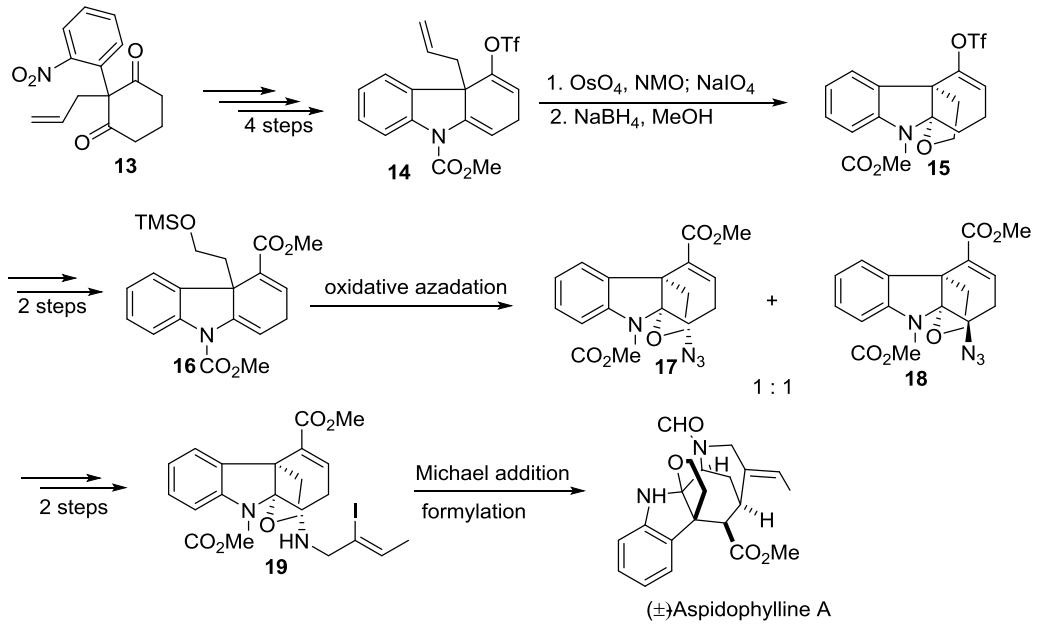

Scheme 2.3.3 Zhu's Synthetic Approach to (±)-Aspidophylline A

Section 2.3.4 Yang's Total Synthesis of (–)-Aspidophylline A

In 2016, Yang reported an enantioselective total synthesis of (–)-Aspidophylline A.[23] Yang's group assigned its absolute configuration as (–)-Aspidophylline A. One of the key steps in their synthesis was a highly enantioselective indole allylation followed by iminium cyclization cascade reaction catalyzed by a combination of Lewis acid and iridium/ligand catalyst. After formation of the furoindoline motif **22**, they used a similar strategy to finish (–)-aspidophylline A: (i) oxidative azadation to introduce nitrogen; and (ii) nickel-catalyzed cyclization reaction to construct [3.3.1]azabicyclic system.

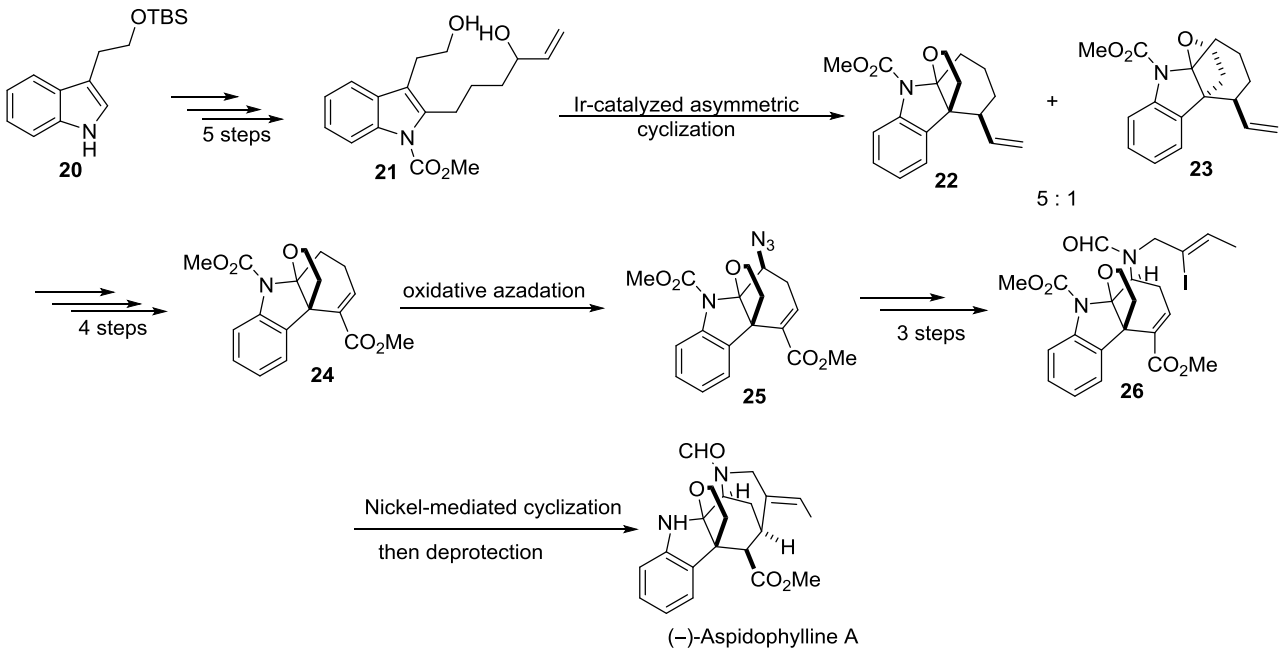

Scheme 2.3.4 Yang's Total Synthesis Toward (–)-Aspidophylline A

Section 2.3.5 Garg's Second Generation Synthesis toward (–)-Aspidophylline A

At the same time as Yang's paper, Garg's group finished their second generation synthesis of (–)-aspidophylline A.[17] In this work, they adopted a Trost desymmetrization reaction to introduce the first chiral center from **27** to **28**. Different from their first generation synthesis, they used a gold-catalyzed ene-yne cyclization to construct [3.3.1]azabicyclic compound **30**, along with 7-endo-dig seven-membered ring product **31**. Interrupted Fischer indolization, methanolysis and deprotection gave them (–)-aspidophylline A. Meanwhile, they used common intermediate **32**, to access other two natural products, (+)-strictamine and (–)-2(*S*)-cathafoline. Starting from compound **32**, several transformations delivered the chloride intermediate **34**. Following the similar sequences: (i) oxidation, deprotection, and alkylation furnished (+)-strictamine; and (ii) reductive amination, deprotection, and alkylation delivered (–)-2(S)-cathafoline.

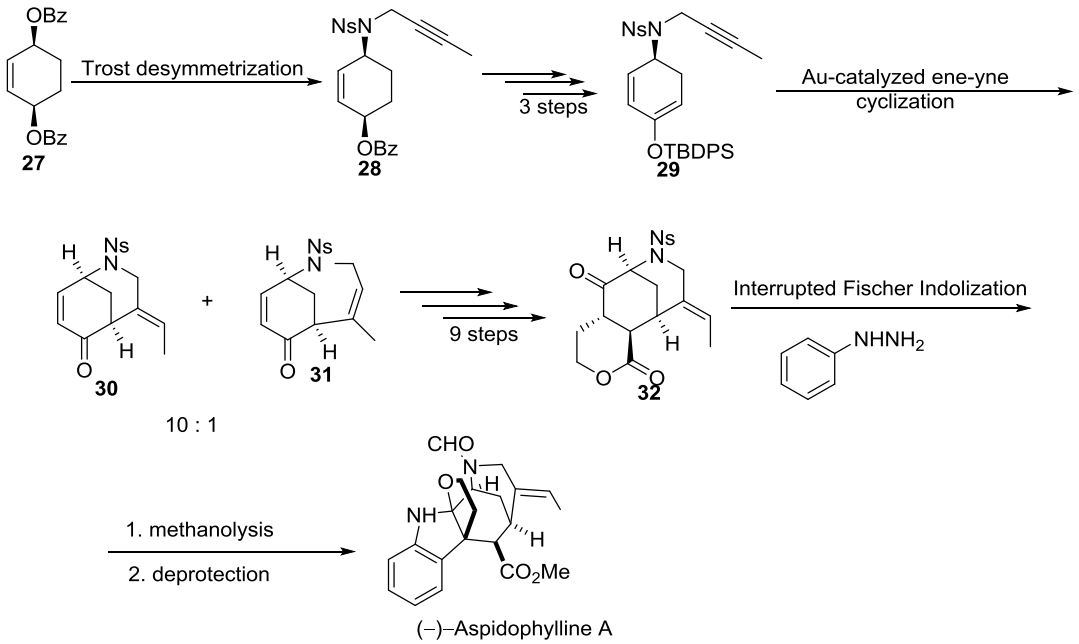

Scheme 2.3.5 Garg's Second Generation toward (–)-Aspidophylline A

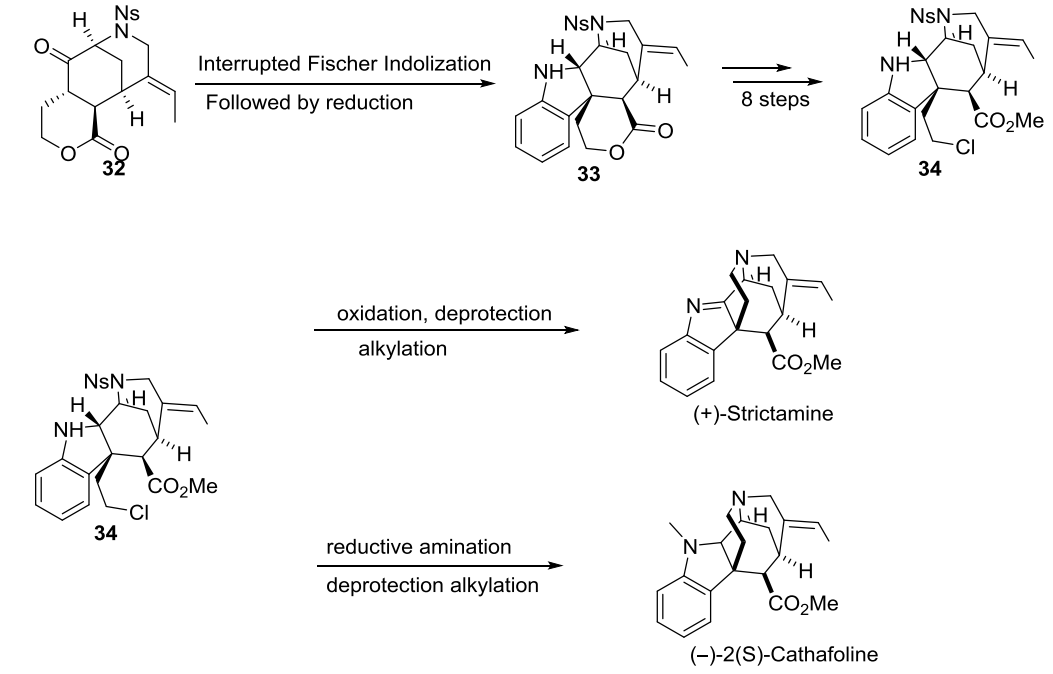

Scheme 2.3.6 Garg's Synthetic Pathway toward (+)-Strictamine and (–)-2(*S*)-Cathafoline

Section 2.3.6 Zhu's Synthetic Approach to the (±)-Strictamine

In 2016, the Zhu group finished the total synthesis of strictamine.[18] Known enol triflate **35**, which underwent a sequence of *α*-bromination of the ketone, and a stereoconvergent intramolecular nucleophilic substitution reaction afforded *N*, *N*-dimethyl tertiary amine **37**. In one single operation, they could build 2-azabicyclo[3.3.1]nonan-9-one skeleton at an early-stage. Subsequently, they formed the indolenine unit at a late stage through reductive imine formation. For the indolenine fused [3.3.1]azabicyclic ring formation, they also used a nickel-catalyzed cyclization between vinyl iodide and *α,β*-unsaturated ester.

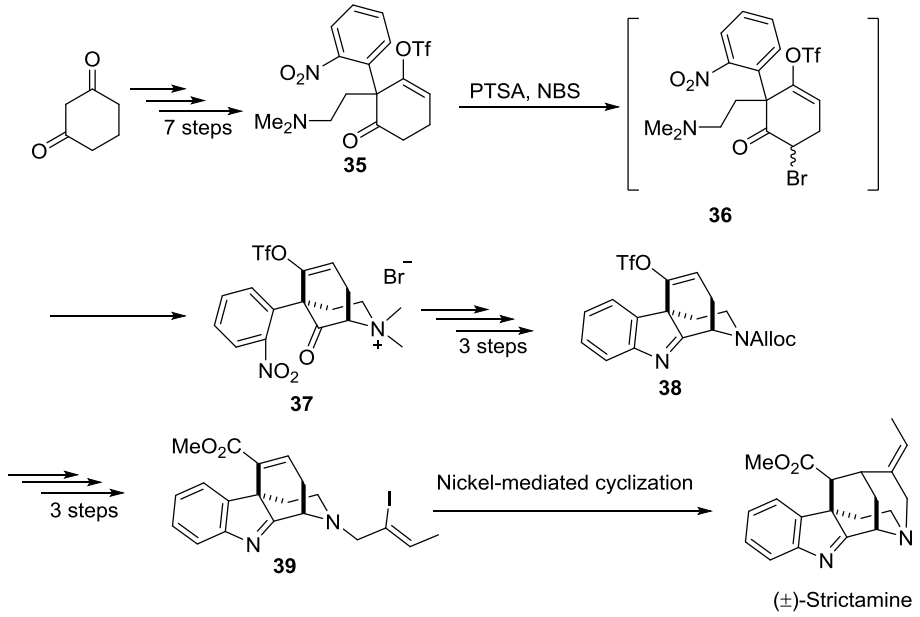

Scheme 2.3.7 Zhu's Synthetic Approach to the (±)-Strictamine

Section 2.3.7 Ohno's Formal Total Synthsis of (±)-Strictamine

Right after Zhu's synthesis of (±)-strictamine, Ohno's group reported a formal total synthesis of (±)-strictamine, following Zhu's nickel-mediated cyclization approach to finish the molecule.[24] In Ohno's synthesis, they utilized a gold-catalyzed cyclization of 1-propargylcarboline **41** to build tetracyclic indolenine **42** quickly. Followed by several transformations, they assembled the common intermediate **39** with Zhu's synthesis, thus finishing the formal synthesis.

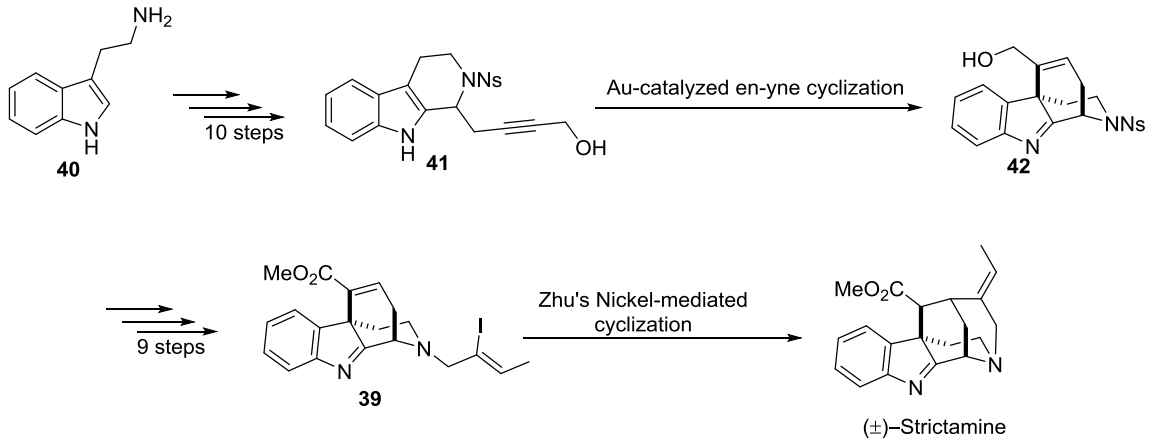

Scheme 2.3.8 Ohno's Formal Total Synthsis of (±)-Strictamine

Section 2.3.8 Garg's Synthetic Approach to (±)-Picrinine

In 2014, Garg's group reported the first total synthesis of the akuammiline alkaloid picrinine.[16] Starting from commercially available ketone **43**, alkylation gave vinyl iodide **44,** which underwent palladium-catalyzed coupling between enolate and vinyl iodide to form aza[3.3.1]bicyclic compound **30**. After formation of cyclopentene **45**, interrupted Fischer indolization gave them desired product **46** smoothly. However, oxidative cleavage of the internal double bond failed to give the desired compound **47**. Before the Fischer indole synthesis, dihydroxylation of the double bond followed by protection gave them the compound **48,** which could undergo interrupted Fischer indolization to give them desired product **49**, the key intermediate to the final natural product.

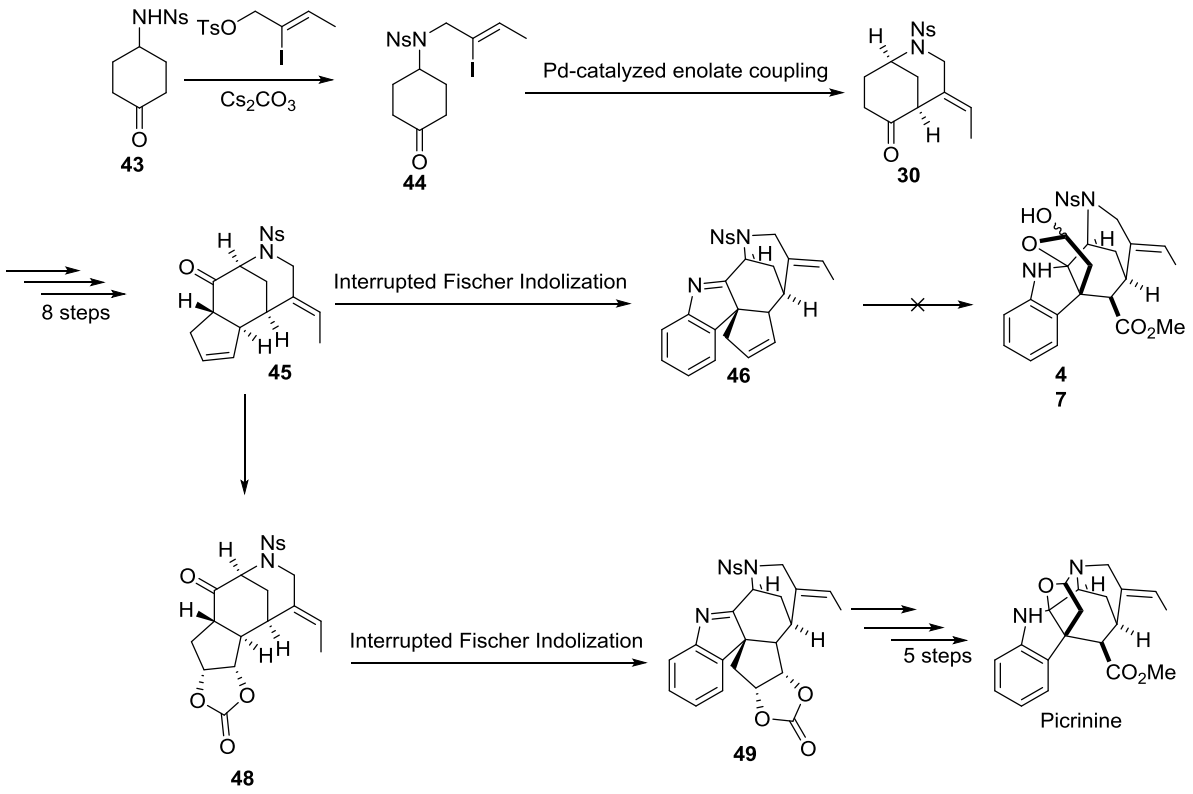

Scheme 2.3.9 Garg's Synthetic Approach to (±)-Picrinine

Section 2.3.9 Li's Synthetic Approach to Aspidodasycarpine and Lonicerine

In 2016, Li's group published the first enantioselective total synthesis of aspidodasycarpine and lonicerine, which bear vicinal quaternary carbons.[19] A Ru-catalyzed asymmetric transfer hydrogenation established the first stereocenter in compound **51** with high yield and enantioselectivity. They adopted a gold-promoted Toste cyclization to assemble the bridged tetracyclic core **53**, at the same time, defining the geometry of the exocyclic olefin. An aldol condensation followed by an intramolecular indole C3 alkylation constructed the adjacent quaternary centers in compound **55** diastereoselectively. Then further transformations could deliver both aspidodasycarpine and lonicerine, which were a pair of epimeric aspidophylline type alkaloids.

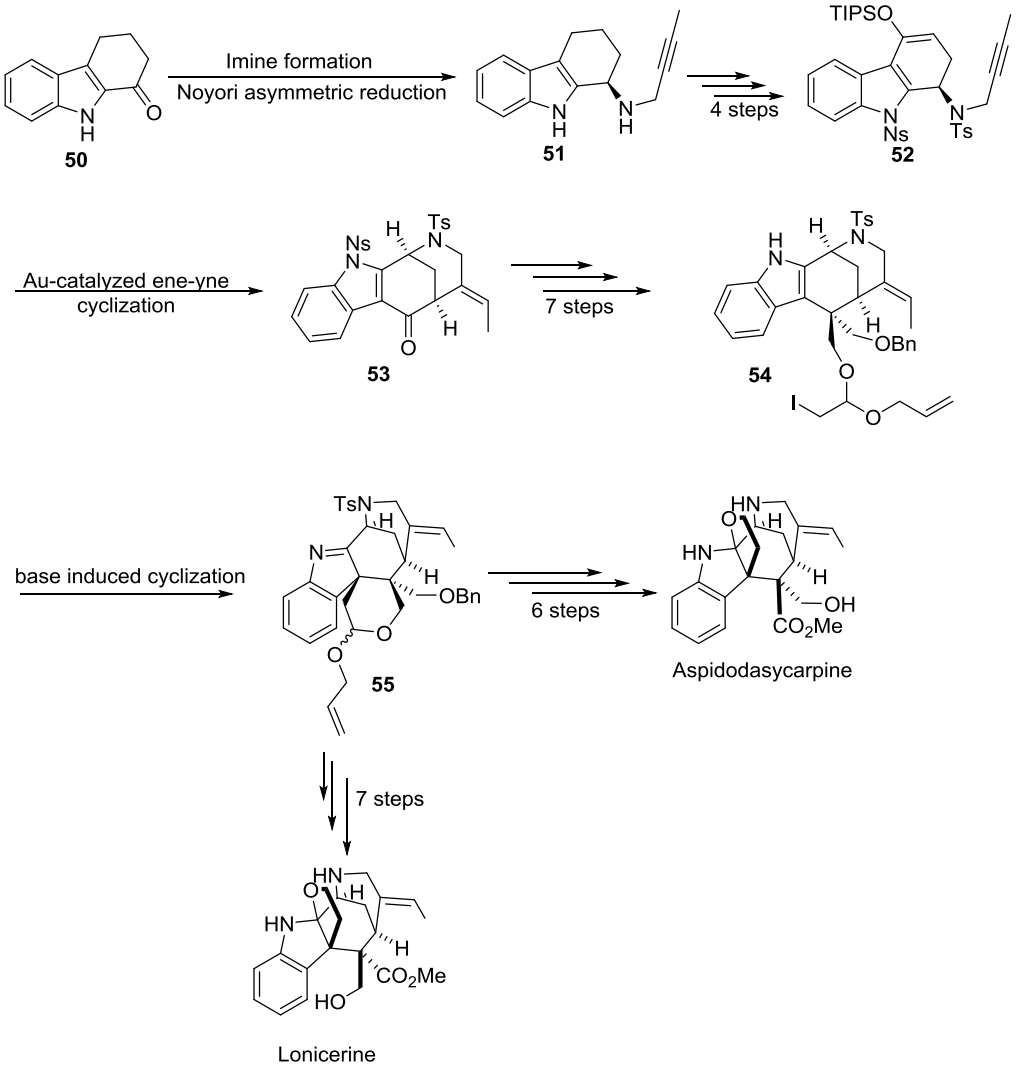

Scheme 2.3.10 Li's Synthetic Approach to Aspidodasycarpine and Lonicerine

Section 2.4 Kwon's Phosphine-Catalyzed Allene/Imine [4 + 2] Annulation

Trivalent phosphines and their derivatives are widely used in organic synthesis. Traditionally, they are applied as stoichiometric reagents in several named reactions, including the Wittig, Staudinger, and Mitsunobu reactions.[25] In modern organic chemistry, organophosphorus compounds are often employed as ligands for transition metal-catalyzed processes.[26] During the past decade, nucleophilic phosphine organocatalysis has attracted much research interest.[27] As a result, a number of highly efficient synthetic reactions, particularly many new annulations to form carbocycles and heterocycles, have been developed. As a class of popular nucleophilic organocatalysts, the superior activity of tertiary phosphines may be primarily attributable to their excellent nucleophilicity as a nucleophile trigger and decent ability as a leaving group in the catalytic process. In 2003, our group developed a tributyl phosphine-catalyzed [4 + 2] annulation reaction between an imine and an allenoate to prepare tetrahydropyridine derivatives. More recently, our group has shown *exo*-phenyl phosphine, which was derived from *trans*-4-hydroxy-L-proline, could promote these type of annulations in high enantiomeric excess.[28] We hoped this methodology could be applied to our akuammiline alkaloid synthesis.

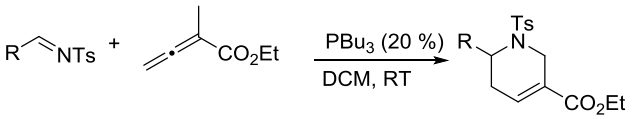

Scheme 2.4.1 Phosphine-Catalyzed [4 + 2] Annulation

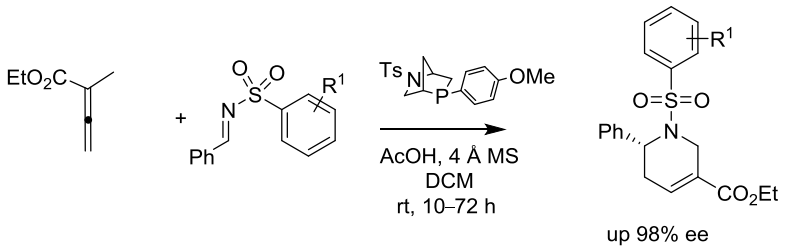

Scheme 2.4.2 Phosphine-Catalyzed Enantioselective [4 + 2] Annulation

In 2012, our group completed the total synthesis of (±)-hirsutine by applying a phosphine-

catalyzed [4 + 2] annulation between indole imine and allenoate.[29] From commercially available indole-2-carboxaldehyde, the phosphine-catalyzed [4 + 2] annulation gave desired product **58**, Then an Appel reaction formed tetracyclic compound **59**. We used malonate as a nucleophile, which underwent Michael addition to the *α,β*-unsaturated ester to form the triester as a single diastereoisomer **60**. Then, regioselective reduction, followed by Wittig reaction could deliver hirsutine in a few steps.

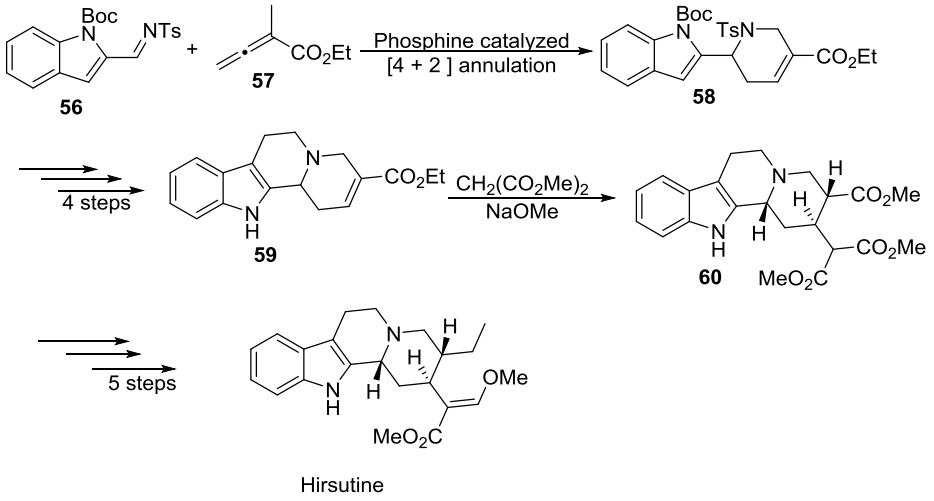

Scheme 2.4.3 Total Synthesis of (±)-Hirsutine

Section 2.5 Retrosynthetic Analysis

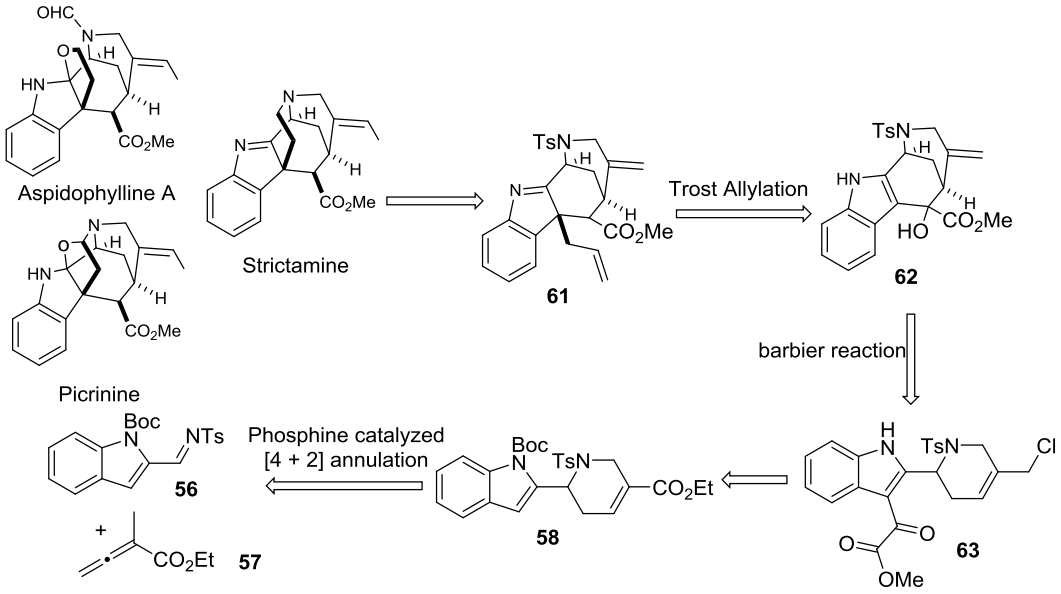

Scheme 2.5.1 Retrosyntheic Analysis of Akuammiline Indole Alkaloids

Our retrosynthetic analysis of akuammiline alkaloids is outlined in Scheme 2.5.1. We planned to build these natural products from the common intermediate **61** through ozonolysis of the allyl tether. The resulting aldehyde could be used to directly construct the skeleton of picrinine. Reductive amination between the aldehyde and secondary amine in piperidine could deliver strictamine. By reducing the resulting aldehyde to an alcohol, we could furnish aspidophylline A. The allyl group in compound **61** could be introduced by Trost allylation from ester **62**, which could be obtained from ketoester **63** *via* Barbier reaction. Ketoester **63**, in turn, could be accessed from the phosphine-catalyzed [4 + 2] annulation between imine **56** and allenoate **57**.

Section 2.6 Exploration of the key [4 + 2] Annulation

Our total synthesis of akuammiline indole alkaloids began with the phosphine-catalyzed [4 + 2] annulation between imine **56** and allenoate **57**. When applying PPh_3 as the catalyst, no annulation product was formed. However, switching to the more nucleophilic phosphine tributylphosphine in DCM at room temperature resulted in a 85% yield of **58**. With this annulation

product in hand, we tried to introduce an α-ketoester on the indole C3 postion.

Section 2.7 Exploration of the key [4 + 2] Annulation

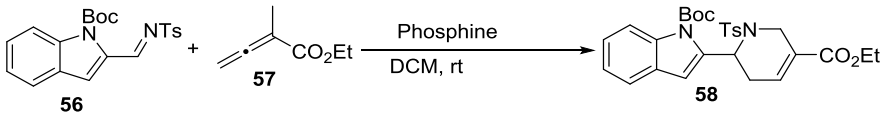

Scheme 2.6.1 Exploration of the key [4 + 2] Annulation

We subjected ester **58** to reflux in toluene with silica gel, which removed the Boc group cleanly in 90% yield. Then DIBAL-H reduction of the α,β-unsaturated ester gave the desired allylic alcohol. After aqueous workup, the crude product was directly subjected to mesylation, which furnished the allylic chloride product **64** in 87% yield over two steps.

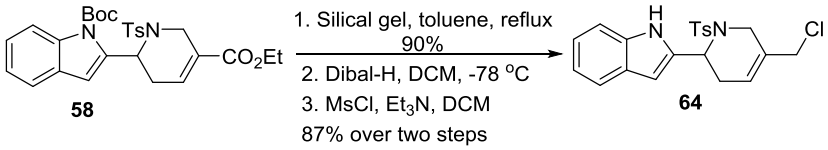

Scheme 2.7.1 Synthesis of Allylic Chloride

Section 2.8 Synthesis of α-Ketoester

With the allylic chloride in hand, we next tried to introduce an α-ketoester to the indole C3 position using oxalyl chloride. The starting material was dissolved in THF, and to the solution was added 2 equiv of oxalyl chloride. After formation of the acyl chloride, the resulting mixture was quenched by different alcohols to provide the desired α-ketoester in high yield. In this step, we introduced different esters, which could be used for the next step by adopting different strategies. For example, for the chloroethyl ester and iodoethyl ester, we hoped that alkylation at the indole C3 position could directly produce the cyclization product; for the phenylthioethyl ester, we anticipated Pummerer rearrangement could deliver the indole C3 cyclization product; for the diethoxyethyl ester, we wanted to form aldehyde, which could undergo nucleophilic addition to

construct the desired skeleton.

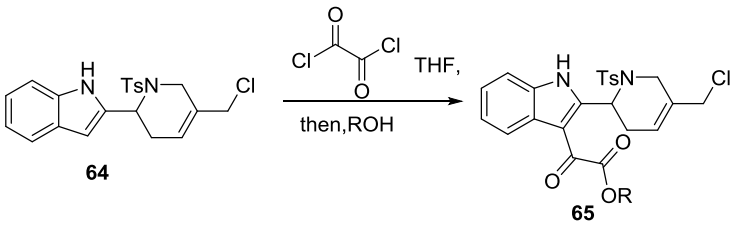

R =
65a Me, 98%
65b $ClCH_2CH_2$, 90%
65c ICH_2CH_2, 85%
65d $(EtO)_2CHCH_2$, 92%
65e $PhSCH_2CH_2$, 87%

Scheme 2.8.1 Synthesis of α-Ketoester

Section 2.9 Developing Barbier Reaction between Allylic Chloride and α-Ketoester

Next, we tried to find a method to develop an intramolecular Barbier reaction between the allylic chloride and α-ketoester. We screened various conditions, which could facilitate this type of reaction. We first used zinc as a reducing reagent, but no reaction occurred (entry 1). The addition of sodium iodide to activate the allylic chloride resulted in decomposition of starting material (entry 2). Raising the temperature did not help the reaction (entry 3). Switching the solvent to a more polar solvent, such as DMF, decomposed the starting material (entry 4). Then we tried other reductants under these four different reaction conditions. Magnesium and indium showed the same results as zinc (entries 5–10). After failing with these metal reductants, we turned to homogeneous reducing reagents. Using SmI_2, which was freshly prepared, did not form the desired product. Then we anticipated to use a palladium-catalyzed allylation reaction. First, palladium (0) underwent nucleophilic displacement of the allylic chloride to form the Trost–Tsuji reaction intermediate. This electrophilic palladium allyl intermediate reacted with reducing reagent, which could either reduce the palladium (II) or undergo transmetallation to form the nuleophilic allylic metal species for the Barbier reaction. Screening combinations of palladium acetate with various

reducing reagents, none of them gave the desired product (entries 12–15). Fortunately, we found that the desired product was formed in quantitative yield when applying tin(II) chloride as reducing agent and sodium iodide as an additive (entry 17). Without sodium iodide, only starting material was recovered (entry 16). The structure of the α-hydroxyester was confirmed through X-ray crystallographic analysis, which showed the ester was the wrong diastereoisomer. We hoped we could reverse the stereochemistry of the ester in the subsequent steps. Our approach to form 2-azabicyclo[3.3.1]nonane ring system through Barbier reaction departed significantly from previous methods for 2-azabicyclo[3.3.1]nonane ring formation.

Table 2.9.1. Optimization of Intramolecular Barbier Reaction

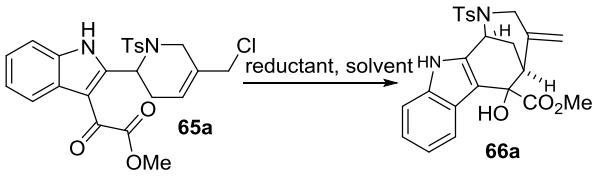

	reductant. /additive	solvent	temp	yield (%)
1	Zn	THF	rt	NR
2	Zn/NaI	THF	rt	decomposed
3	Zn	THF	reflux	NR
4	Zn/NaI	DMF	rt	NR
5	Zn/NaI	DMF	80 °C	decomposed
6	Mg	THF	rt	decomposed
7	Mg/NaI	THF	rt	decomposed
8	In	THF	rt	NR
9	In/NaI	THF	rt	NR
10	In	THF	reflux	NR
11	SmI_2	THF	rt	decomposed
12	$SmI_2/Pd(OAc)_2$	THF	rt	decomposed
13	$Zn/Pd(OAc)_2$	THF	rt	decomposed
14	$SnCl_2/Pd(OAc)_2$	THF	rt	decomposed
15	$(SnCH_3)_2/Pd(OAc)_2$	THF	rt	decomposed
16	$SnCl_2$	THF	rt	NR
17	$SnCl_2$/NaI	THF	rt	99[a]

[a] Isolated yield after silica gel flash column chromatography.

We then applied various α-ketoesters under this optimized condition. All of them gave the Barbier product in high yields.

Table 2.9.2. Substrates Screen of Intramolecular Barbier Reaction

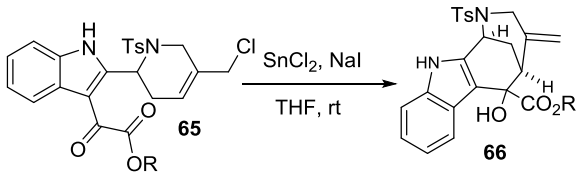

R = Me, $ClCH_2CH_2$, ICH_2CH_2, $(EtO)_2CH_2CH_2$, $PhSCH_2CH_2$,

Substrate	R	Isolated yield (%)
65b	$ClCH_2CH_2$	92
65c	ICH_2CH_2	87
65d	$(EtO)_2CH_2CH_2$	97
65e	$PhSCH_2CH_2$	89

After successfully developing Barbier reaction with substrate **65**, we hoped to extend this method toward secondary allylic chloride **67**, which could set the trisubstituted alkene in one pot. When we applied **67** to the optimized condition, we needed over 100 equiv of $SnCl_2$ to complete the reaction, which also took more than four days. Fortunately, when we raised the reaction temperature to 40 ^oC, the reaction could be finished with 2 equiv of $SnCl_2$ within 24 hours.

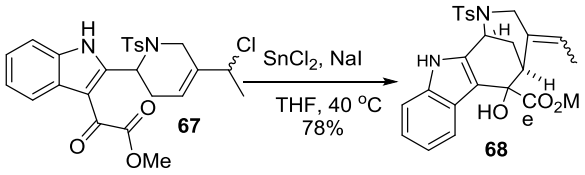

Scheme 2.9.1 Barbier Reaction with Secondary Allylic Chloride

Section 2.10 Attempt toward Indole C3 Cyclization

With the Barbier reaction product in hand, we tried to reduce the extra hydroxyl group, hoping it could invert the ester to the correct position. Subjecting hydroxyl ester **66a** to a reductive condition, we could remove the hydroxyl group in high yield, at the same time, epimerizing the

ester to the correct position.

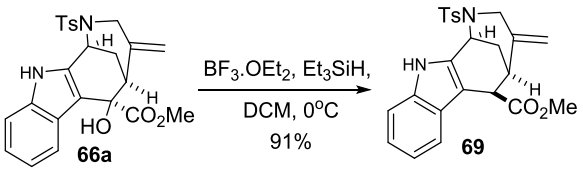

Scheme 2.10.1 Reduction of Hyroxyl Group

After removal of the hydroxyl group, we next tested different ways to introduce the indole C3 quaternary carbon. Based on our previous study, the Tsuji–Trost reaction could introduce the allyl group with alcohol **70** at indole C3 to form quaternary carbon successfully. However, when we applied the same conditions to our tetracyclic compound **69**, it did not give us any desired C-allylation product **72**. Instead, the compound we isolated is was N-allylation product **73** due to steric hindrance at the indole C3 position, as was confirmed by the NMR study.

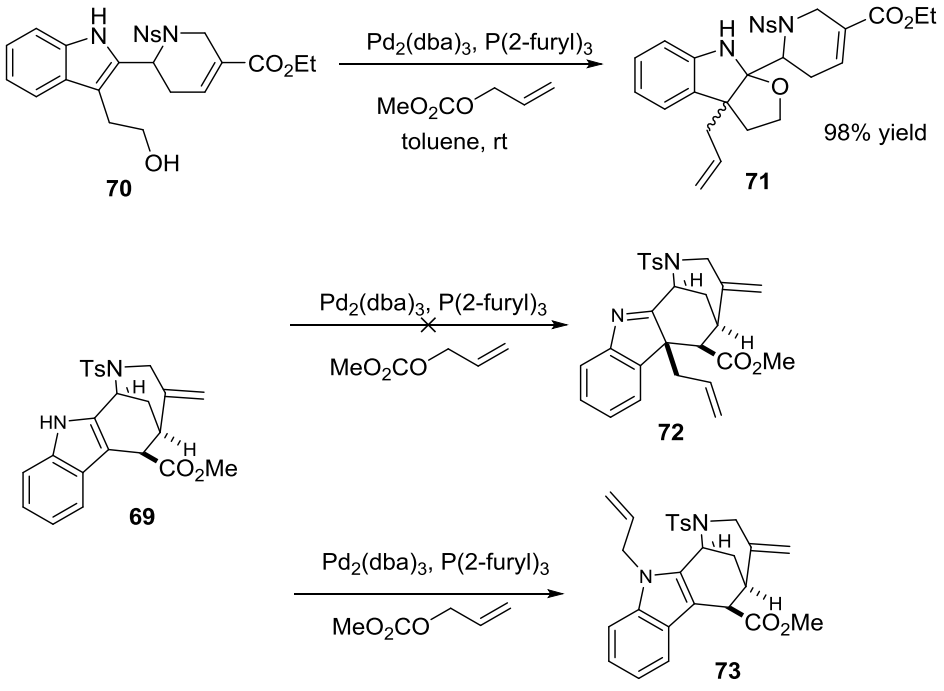

Scheme 2.10.2 Testing Tsuji–Trost Reaction for Indole C3 Allylation

Then, we tried intramolecular alkylation with alkyl chloride **66b**. Following the same procedure, we could remove the hydroxyl group in compound **66b**. In the next step, we tested the

substrate **74** with a variety of inorganic bases. There was no cyclization product observed. Then, we tried to convert chloride to iodide **75**. Even the harsh conditions, (e.g., 100 equiv of NaI in DMF at 100 ^{o}C over a week), mainly led to recovery of starting material **74**.

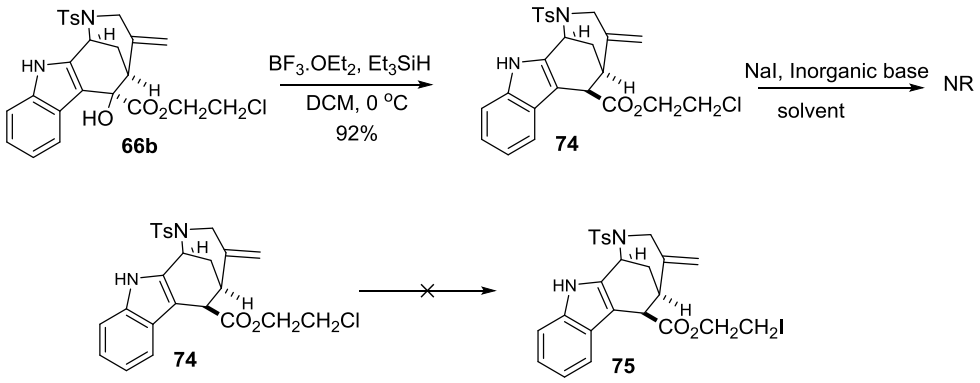

Scheme 2.10.3 Intramolecular Cyclization with Alkyl Chloride

After failure with the Finkelstein reaction to convert chloride to iodide, we directly synthesized the alkyl iodide from Barbier reaction. After removing the hydroxyl group, we used alkyl iodide **75** for the indole C3 cyclization, which was a similar strategy to Li's approach toward aspdodasycarpine. However, we found that compound **75** was labile under basic conditions in DMF, resulting in decomposition of starting material. When we switched the solvent to CH_3CN, we could isolate a compound, which was not our desired indole C3 cyclization product. After NMR analysis, we deduced the structure was lactone **76**.

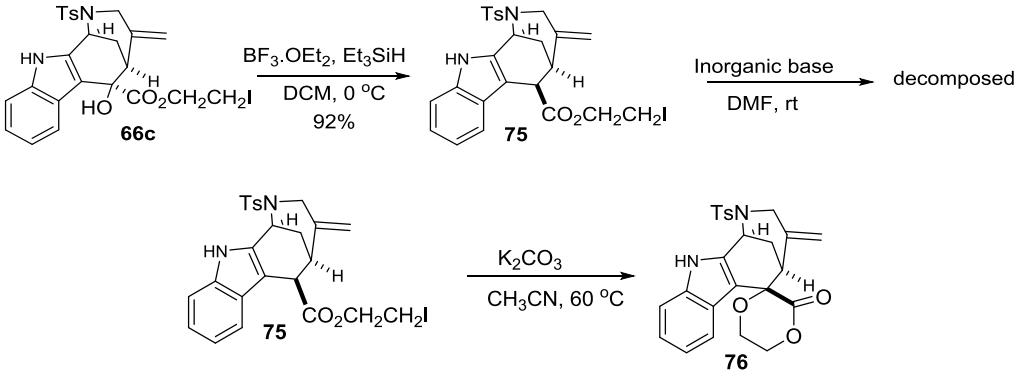

Scheme 2.10.4 Intramolecular Cyclization with Alkyl iodide

We then tested other substrates for the indole C3 cyclization. The diethyl acetal functional group in compound **66d**, under reductive conditions, was reduced to primary alcohol **77**. We also applied hydroxyl ester **66e** for this transformation, which gave the desired product **78** in 85% yield. With phenylthiol ether in hand, we tried different conditions for the Pummerer rearrangement under either acidic or basic conditions. Neither of them gave any desired cyclization product **79**.

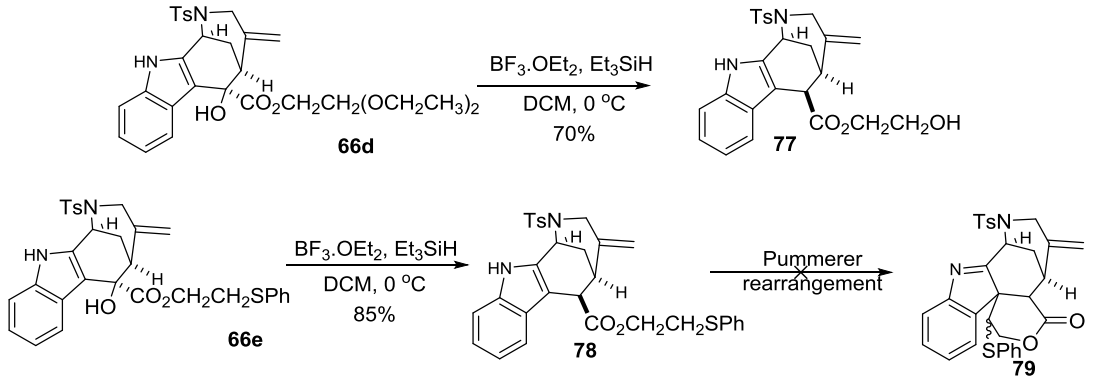

Scheme 2.10.5 Other Strategies toward Intramolecular Cyclization

Section 2.11 Constructing Quaternary Carbon from Hydroxyl Ester

As mentioned earlier, compound **75**, under very mild conditions gave the lactone product **76**, which rendered us assuming the indolyl position was prone to oxidation. At this moment, we hoped to construct the quaternary carbon from the hydroxyl ester, which could remove the proton in indolylic position, preventing oxidation. We used substrate **66a** for quaternary carbon formation. After many attempts, we found subjecting compound **66a** under BF_3 conditions at room temperature, after few minutes, the solution would turn red, which indicated the formation of indole–quinonemethide intermediate **80**. Then fast addition of the zinc reagent could furnish the desired product in 85% yield. The speed of zinc reagent addition was very important. Slow addition of zinc reagent would result in epimerization of **66a**. This method to generate quaternary carbons, so far as we know, is the first example using a combination of BF_3 and zinc reagent.

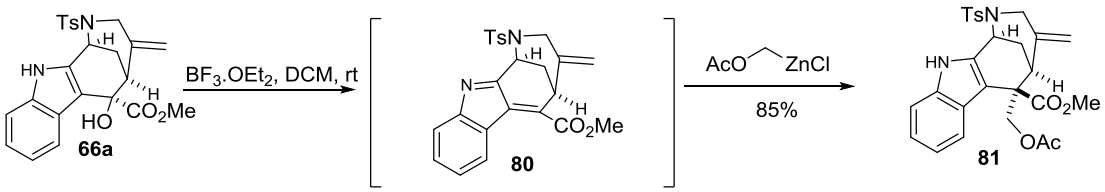

Scheme 2.11.1 Quaternary Carbon Formation from Hydroxyl Ester

Section 2.12 Exploration toward Indole C3 Cyclization with Adjacent Quaternary Carbon

By following the same procedure, we could prepare alkyl iodide **82**, which was ready for the indole C3 cyclization. First, we tried to use DMF as a solvent, using a variety of bases such as, K_2CO_3, Cs_2CO_3, *t*-BuOK, *t*-BuOLi, and NaH, to promote the cyclization reaction at different temperatures. We found even in DMF under relux condition, the compound we isolated was mainly the starting material, which, as we expected, was much more stable than **74**. Then we switched the solvent to DMSO. We found the compound was labile at high temperatures, which resulted in decomposition of the starting material.

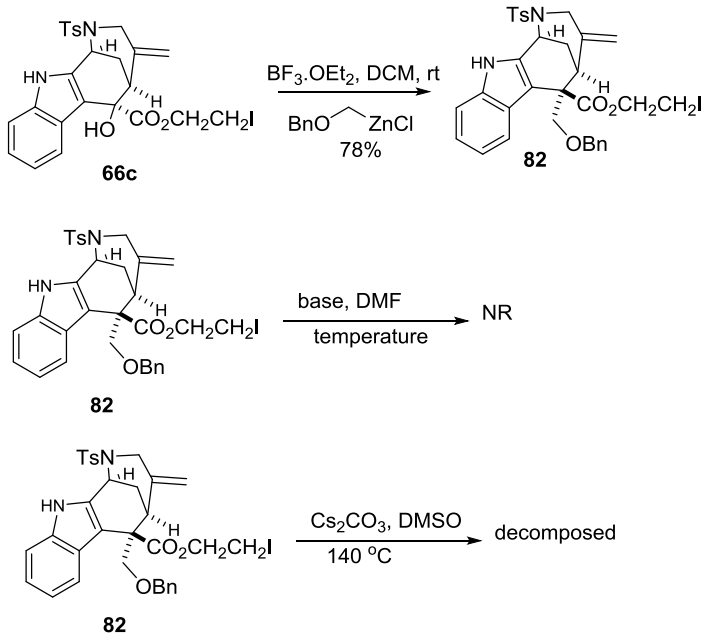

Scheme 2.12.1 Attempt Cyclization with Alkyl Iodide

Section 2.13 Synthetic Plan toward formal total synthesis of Aspidodasycarpine and Lonicerine

As demonstrated earlier, our Barbier reaction worked with secondary allylic chlorides, which gave us hydroxyl ester **68** with trisubstituted alkene. If we subject hydroxyl ester under the indole–quinonemethide formation conditions, the desired indole ester **83** could formed, which under reductive conditions, could deliver primary alcohol **84**, the common intermediate with Li's total synthesis toward aspidodasycarpine and lonicerne (Scheme **2.13.1**).

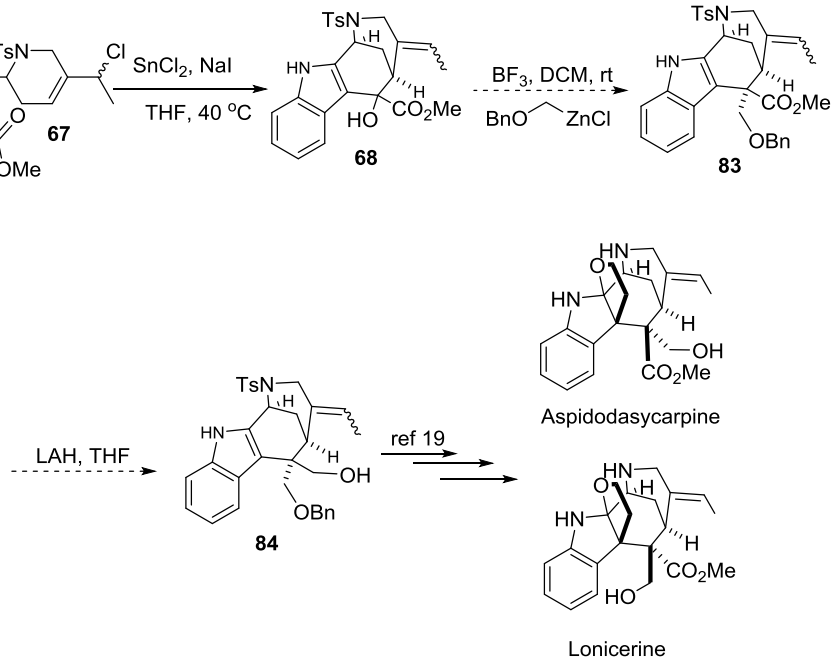

Scheme 2.13.1 Synthetic Plan toward formal total synthesis of Aspidodasycarpine and Lonicerine

Section 2.14 Conclusion

In conclusion, we have successfully constructed indole fused [3.3.1]azabicycles, which are the common structure for the akuammiline indole alkaloids. Through reduction of a hydroxyl ester or the indole–quinonemethide method, we could easily form tertiary or quaternary carbons with a methyl ester, which could accomplish the formal total synthesis of aspidodasycarpine and lonicerine *via* reduction of the methylester. This synthesis exhibits several features: (i) phosphine-

catalyzed [4 + 2] annulation between an α-methylallenoate and an indole imine; (ii) $SnCl_2$-mediated Barbier reaction to quickly access aza[3.3.1]bicyclic ring system; (iii) BF_3 promoted indole-quinonemethide formation followed by nuclophilic addition to form the quaternary carbon in a highly efficient manner.

Section 2.15 Experimental procedures

General Information

All reactions were performed in dry solvents under an Ar atmosphere and anhydrous conditions. DCM, THF, and MeCN were freshly distilled over CaH_2 prior to use. All other reagents were used as received from commercial sources. Reactions were monitored through thin layer chromatography (TLC) on 0.25-mm SiliCycle silica gel plates and visualized under UV light. Flash column chromatography (FCC) was performed using SiliCycle Silica-P Flash silica gel (60-Å pore size, 40–63 μm). NMR spectra were recorded using Bruker Avance-500 instruments, calibrated to $CD(H)Cl_3$ as the internal reference (7.26 and 77.0 ppm for ^1H and ^{13}C NMR spectra, respectively) unless otherwise noted. ^1H NMR spectral data are reported in terms of chemical shift (δ, ppm), multiplicity, coupling constant (Hz), and integration. ^{13}C NMR spectral data are reported in terms of chemical shift (δ, ppm). The following abbreviations indicate the multiplicities: s, singlet; d, doublet; t, triplet; q, quartet; m, multiplet. High resolution mass spectra were recorded using a Waters LCT Premier XE time-of-flight instrument controlled by MassLynx 4.1 software. Samples were infused using direct loop injection from a Waters Acquity UPLC into the multi-mode ionization source. The lock mass standard for accurate mass determination was leucine enkephalin (Sigma L9133). X-ray crystallographic data were collected using a Bruker SMART CCD-based diffractometer equipped with a low-temperature apparatus operated at 100 K. Optical rotations were recorded using a Rudolph Autopol IV automatic polarimeter. Enantiomeric excess

was measured through chiral HPLC using a Shimadzu CBM Lite system and a REGIS (*R,R*)-DACH DNB analytical (diameter: 4.5 mm) chiral column, with CH_2Cl_2/hexanes as the eluent and CHIRALCEL AD-H analytical (diameter: 4.6 mm) chiral column, with *i*PrOH/hexanes as the eluent.

General procedure for the [4 + 2] annulation

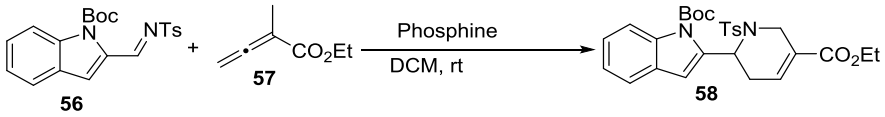

Tetrahydropyridine 58. A flame-dried round-bottom flask was charged with the imine **56** (3.98 g, 10 mmol) and allenoate (1.51 g, 12 mmol, 1.2 equiv) in dichloromethane under argon. Then tributylphosphine (400 mg, 2 mmol, 0.2 equiv) was added to the flask. The mixture was stirred at room temperature until the starting imine **56** was consumed (as determined by TLC). The crude reaction product was loaded directly onto a column of SiO_2 and purified through flash column chromatography (20% EA/Hexanes) to yield compound **58** as a yellow solid (4.45 g, 85% yield). ^{1}H NMR (500 MHz, $CDCl_3$) δ 7.96 (dd, *J* = 8.4, 0.5 Hz, 1H), 7.56 (d, *J* = 8.4 Hz, 2H), 7.29 (d, *J* = 7.6 Hz, 1H), 7.23 (tt, *J* = 8.1, 1.2 Hz, 1H), 7.14 (td, *J* = 7.8, 1.0 Hz, 1H), 7.04 (d, *J* = 8.4 Hz, 2H), 6.95–6,96 (m, 1H), 7.01–6.98 (m, 2H), 6.26 (d, *J* = 6.7 Hz, 1H), 6.16 (s, 1H), 4.43 (d, *J* = 18.3 Hz, 1H), 3.93 (ddd, *J* = 17.6, 6.5, 2.0 Hz, 1H), 2.82 (ddt, *J* = 18.2, 7.1, 1.8 Hz, 1H), 2.64 (dt, *J* = 19.0, 4.4 Hz, 1H), 2.25 (s, 3H), 1.73 (s, 9H); ^{13}C NMR (125 MHz, $CDCl_3$): δ 164.7, 150.2, 143.3, 138.6, 136.2, 136.1, 135.5, 129.3, 128.4, 127.1, 126.7, 124.3, 122.8, 120.4, 115.4, 108.5, 84.8, 60.8, 47.2, 41.1, 30.6, 28.2, 21.3, 14.2; HRMS–ESI (m/z) $[M + H]^+$ cald $C_{28}H_{33}N_2O_6S$, 525.2059, found 525.2056.

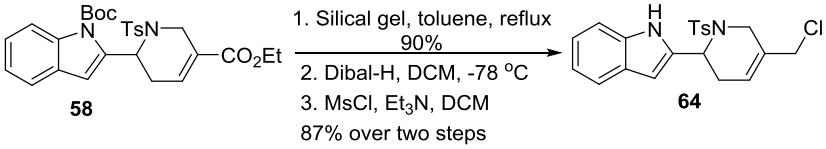

Tetrahydropyridine 64. A mixture of **58** (5.24 g, 10 mmol), and silica gel (10.48 g) in toluene was heated under reflux condition until the starting material was consumed. After cooling to room temperature, the solid was removed by filtration and washed with ethyl acetate. The solution was combined and concentrated in *vacuo*. The crude product was used directly in the next step without further purification.

The crude product from the previous step was dissolved in dichloromethane. DIBAL-H (1.0 M in DCM, 30 mL, 30 mmol, 3 equiv) was added to the solution at -78 ºC. After the starting material was consumed, the reaction was quenched by 5 mL of MeOH, followed by 50 ml of saturated Rochelle salt solution. The mixture was stirred overnight until forming a clear solution. Then the organic layer was separated and concentrated in *vacuo*, which was used directly in next step.

MsCl (1.26 g, 11 mmol, 1.1 equiv) was slowly added to the solution of crude product from previous step and Et_3N (1.21 g, 12 mmol, 1.2 equiv) at 0 ºC. The reaction mixture was stirred overnight. The solution was concentrated in *vacuo*, the resulting solid was recrystallized from EA and DCM solution to give a yellow sold **64** (3.12 g, 78 % yield). ^{1}H NMR (500 MHz, $CDCl_3$) δ 8.61 (s, 1H), 7.76 (d, *J* = 8.3 Hz, 2H), 7.49 (d, *J* = 8.2 Hz, 1H), 7.34 (d, *J* = 8.2 Hz, 1H), 7.29 (d, *J* = 8.2 Hz, 2H), 7.17 (td, *J* = 7.0, 1.1 Hz, 1H), 7.06 (td, *J* = 7.4, 1.0 Hz, 1H), 6.23–6.24 (m, 1H), 5.87 (d, *J* = 1.0 Hz, 1H), 5.32 (d, *J* = 7.0 Hz, 1H), 4.34 (d, *J* = 18.5 Hz, 1H), 3.93 (d, *J* = 12.0 Hz, 1H), 3.85 (d, *J* = 12.0 Hz, 1H), 3.34 (d, *J* = 18.2 Hz, 1H), 2.56 (dd, *J* = 17.3, 5.7 Hz, 1H), 2.43 (s, 3H), 2.31 (dt, *J* = 18.3, 1.4 Hz, 1H); ^{13}C NMR (125 MHz, $CDCl_3$): δ 143.8, 137.1, 136.3, 135.2, 131.0, 129.8, 127.7, 127.0, 123.7, 122.4, 120.4, 119.8, 111.1, 101.3, 47.9, 46.3, 41.3, 26.2, 21.6; HRMS–ESI (m/z) $[M + H]^+$ cald $C_{21}H_{22}ClN_2O_2S$, 401.1091, found 401.1092.

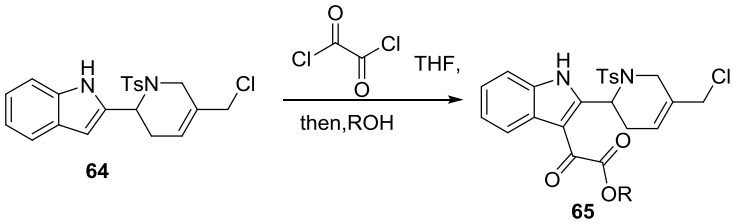

***α*-Ketoester 65.** Oxalyl chloride (0.859 mL, 10 mmol, 2 equiv) was added dropwise to a solution of **64** (2.0 g, 5 mmol) in dry THF (100 mL) at 0 ℃ and then the mixture was stirred at 23 ℃ overnight. The solvent was concentrated in *vacuo* and the residue placed under high vacuum to give a yellow foam. The foam was dissolved in dry THF (100 mL) at 0 ℃, alcohol (10 mmol, 2 equiv) was added via syringe, followed by addition of Et_3N (1.44 mL, 10 mmol, 2 equiv). the mixture was stirred at 23 ℃ for 2 h. The reaction was concentrated in *vacuo* and the residue was purified through FCC to give a yellow foam.

***α*-Ketoester 65a.** (2.38 g, 98% yield) ^{1}H NMR (500 MHz, $CDCl_3$) δ 9.09 (s, 1H), 7.65–7.62 (m, 3H), 7.25–7.19 (m, 3H), 7.15 (d, *J* = 7.8 Hz, 2H), 6.03(t, *J* = 4.8 Hz, 1H), 5.95 (t, *J* = 5.0Hz, 1H), 4.27 (d, *J* = 16.3 Hz, 1H), 4.14 (d, *J* = 16.3 Hz, 1H), 4.11 (q, *J* = 6.8 Hz, 1H), 4.06 (t, *J* = 11.3 Hz, 1H), 4.03 (s, 3H), 2.59(t, *J* = 4.8 Hz, 2H), 2.28 (s, 3H); ^{13}C NMR (125 MHz, $CDCl_3$): δ 181.3, 165.9, 149.7, 144.2, 134.6, 134.3, 132.5, 129.8, 127.2, 126.2, 125.5, 123.7, 123.1, 119.7, 111.8, 108.7, 52.8, 48.3, 46.6, 43.6, 29.6, 21.4, 14.2; HRMS–ESI (m/z) $[M + H]^+$ cald $C_{24}H_{24}ClN_2O_5S$, 487.1094, found 487.1089.

***α*-Ketoester 65b.** (2.40 g, 90% yield) ^{1}H NMR (500 MHz, $CDCl_3$) δ 9.17 (s, 1H), 7.67–7.63 (m, 3H), 7.25–7.19 (m, 3H), 7.16 (d, *J* = 7.8 Hz, 2H), 6.03(t, *J* = 4.8 Hz, 1H), 5.94 (t, *J* = 5.0 Hz, 1H), 4.68 (t, *J* = 5.8 Hz, 2H), 4.27 (d, *J* = 16.3 Hz, 1H), 4.14 (d, *J* = 16.3 Hz, 1H), 4.11 (q, *J* =

6.8 Hz, 1H), 4.06 (t, *J* = 11.3 Hz, 1H), 3.84 (t, *J* = 5.8 Hz, 2H), 2.59(t, *J* = 4.8 Hz, 2H), 2.28 (s, 3H); ^{13}C NMR (125 MHz, $CDCl_3$): δ 180.2, 164.6, 149.7, 143.9, 134.2, 133.9, 132.1, 129.5, 126.8, 125.8, 125.1, 123.5, 122.8, 119.5, 111.5, 108.2, 65.0, 48.1, 46.3, 43.6, 40.5, 29.3, 21.1, 13.8; HRMS–ESI (m/z) $[M + H]^+$ cald $C_{25}H_{25}Cl_2N_2O_5S$, 535.0861, found 535.0859.

***α*-Ketoester 65c.** (2.66 g, 85% yield) ^{1}H NMR (500 MHz, $CDCl_3$) δ 8.91 (s, 1H), 7.70–7.68 (m, 1H), 7.62 (d, *J* = 7.89 Hz, 2H), 7.25–7.20 (m, 3H), 7.15 (d, *J* = 7.8 Hz, 2H), 6.04(dd, *J* = 3.4, 5.8 Hz, 1H), 5.99 (t, *J* = 5.2 Hz, 1H), 4.69 (td, *J* = 1.6, 7.8 Hz, 2H), 4.23 (d, *J* = 16.2 Hz, 1H), 4.16 (d, *J* = 16.5 Hz, 1H), 4.08 (q, *J* = 6.9 Hz, 1H), 3.45 (t, *J* = 7.4 Hz, 2H), 2.63 (t, *J* = 4.8 Hz, 2H), 2.27 (s, 3H); ^{13}C NMR (125 MHz, $CDCl_3$): δ 180.7, 164.6, 149.7, 144.2, 134.5, 134.2, 132.5, 129.8, 127.2, 126.4, 125.4, 123.9, 123.2, 120.0, 111.7, 108.7, 66.0, 48.2, 46.7, 43.5, 29.7, 21.4, -1.4; HRMS–ESI (m/z) $[M + H]^+$ cald $C_{25}H_{25}ClIN_2O_5S$, 627.0218, found 627.0216.

***α*-Ketoester 65d.** (2.70 g, 92% yield) ^{1}H NMR (500 MHz, $CDCl_3$) δ 9.05 (s, 1H), 7.70–7.67 (m, 1H), 7.63 (d, *J* = 8.2 Hz, 2H), 7.24–7.18 (m, 3H), 7.16 (d, *J* = 8.0 Hz, 2H), 6.05(t, *J* = 5.2 Hz, 1H), 5.95 (t, *J* = 5.2 Hz, 1H), 4.85 (t, *J* = 5.6 Hz, 1H), 4.45 (d, *J* = 5.4 Hz, 2H), 4.26 (d, *J* = 16.4 Hz, 1H), 4.14 (d, *J* = 16.4 Hz, 1H), 4.08 (d, *J* = 16.0 Hz, 1H), 4.05 (d, *J* = 11.3 Hz, 1H), 3.77–3.72 (m, 2H), 3.63–3.59 (m, 2H), 2.60 (t, *J* = 4.8 Hz, 2H), 2.27 (s, 3H); ^{13}C NMR (125 MHz, $CDCl_3$): δ 181.0, 165.1, 149.8, 144.2, 134.5, 134.2, 132.4, 129.8, 127.2, 126.3, 125.5, 123.7, 123.1, 119.9, 111.7, 108.6, 99.4, 65.3, 62.8, 48.5, 46.6, 43.6, 29.7, 21.4, 15.3; HRMS–ESI (m/z) $[M + H]^+$ cald $C_{29}H_{34}ClN_2O_7S$, 589.1775, found 589.1770.

***α*-Ketoester 65e.** (2.64 g, 87% yield) ^{1}H NMR (500 MHz, $CDCl_3$) δ 9.02 (s, 1H), 7.66–7.64 (m, 1H), 7.62 (d, *J* = 8.4 Hz, 2H), 7.43–7.41 (m, 2H), 7.31–7.28 (m, 2H), 7.25–7.19 (m, 4H), 7.15 (d, *J* = 8.4 Hz, 2H), 6.03(t, *J* = 4.4 Hz, 1H), 5.96 (t, *J* = 5.00 Hz, 1H), 4.56 (td, *J* = 1.6, 7.8 Hz, 2H), 4.25 (d, *J* = 16.5 Hz, 1H), 4.14 (d, *J* = 16.5 Hz, 1H), 4.07 (q, *J* = 7.1 Hz, 2H), 3.31 (t, *J* = 7.8 Hz, 2H), 2.60 (t, *J* = 4.8 Hz, 2H), 2.27 (s, 3H); ^{13}C NMR (125 MHz, $CDCl_3$): δ 181.0, 165.2,

149.8, 144.2, 134.58, 134.52, 132.4, 130.1, 129.8, 129.2, 127.2, 126.8, 126.3, 125.5, 123.8, 123.1, 119.9, 111.8, 108.6, 64.2, 48.3, 46.6, 43.6, 31.9, 29.7, 21.4; HRMS–ESI (m/z) $[M + H]^+$ cald $C_{31}H_{30}ClN_2O_5S_2$, 609.1285, found 609.1290.

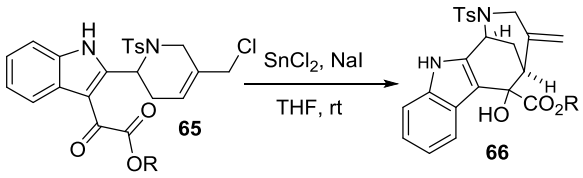

R = Me, $ClCH_2CH_2$, ICH_2CH_2,
$(EtO)_2CH_2CH_2$, $PhSCH_2CH_2$,

Hydroxyester 66. NaI (1.13 g, 7.5 mmol, 1.5 equiv) was added in one potion to 100 mL THF solution of α-Ketoester **65** (5 mmol). The mixture was stirred for a few minutes until the allylic iodide formed. Then $SnCl_2$ (1.42 g, 7.5 mmol, 1.5 equiv) was added to the solution under argon. The reaction mixture was further stirred for 2 h (monitor by TLC). Ethyl acetate and saturated KF solution were added to the reaction mixture. After stirring for 20 min, the organic layer was separated from the aqueous layer, which was extracted by ethyl acetate twice. The combined organic phases were washed with saturated NaCl, dried over Na_2SO_4, and concentrated in *vacuo*. The residue could be used directly for the next step or purified by FCC to give the white solid.

Hydroxyester 66a. (2.26 g, 99% yield) ^{1}H NMR (500 MHz, $CDCl_3$) δ 7.96 (s, 1H), 7.74 (d, *J* = 8.2 Hz, 2H), 7.61 (d, *J* = 8.5 Hz, 1H), 7.31 (d, *J* = 8.1 Hz, 2H), 7.22 (t, *J* = 7.8 Hz, 1H), 7.18 (t, *J* = 8.1 Hz, 1H), 7.09 (t, *J* = 7.6 Hz, 1H), 5.07 (s, 2H), 4.99 (s, 1H), 4.06 (d, *J* = 15.0 Hz, 1H), 3.70 (s, 1H), 3.48 (d, *J* = 15.0 Hz, 1H), 3.39 (s, 1H), 2.96 (t, *J* = 3.1 Hz, 1H), 2.64 (td, *J* = 3.1, 13.3 Hz, 1H), 2.45 (s, 3H), 1.99 (td, *J* = 3.2, 13.5 Hz, 1H); ^{13}C NMR (125 MHz, $CDCl_3$): δ 175.0, 143.8, 139.5, 137.5, 136.1, 129.9, 127.1, 124.3, 123.0, 120.5, 120.0, 116.2, 113.1, 111.4, 73.1, 53.2, 46.6, 45.9, 45.8, 32.5, 21.5, 14.2; HRMS–ESI (m/z) $[M – OH]^+$ cald $C_{24}H_{23}N_2O_4S$,

435.1379, found 435.1381.

Hydroxyester 66b. (2.38 g, 92% yield) ^{1}H NMR (500 MHz, $CDCl_3$) δ 8.10 (s, 1H), 7.74 (d, *J* = 8.2 Hz, 2H), 7.62 (d, *J* = 8.2 Hz, 1H), 7.31 (d, *J* = 8.4 Hz, 2H), 7.24 (d, *J* = 8.1 Hz, 1H), 7.18 (dt, *J* = 1.2, 8.2 Hz, 1H), 7.09 (dt, *J* = 1.2, 7.8 Hz, 1H), 5.08 (s, 2H), 5.00 (s, 1H), 4.45 (ddd, *J* = 4.4, 7.0, 11.8 Hz, 1H), 4.25 (ddd, *J* = 4.3, 7.2, 11.4 Hz, 1H), 4.06 (d, *J* = 15.2 Hz, 1H), 3.61 (ddd, *J* = 4.6, 8.0, 12.1 Hz, 1H), 3.55 (ddd, *J* = 4.5, 7.9, 12.2 Hz, 1H), 3.49 (d, *J* = 14.5 Hz, 1H), 3.35 (s, 1H), 3.00 (t, *J* = 3.1 Hz, 1H), 2.71 (td, *J* = 3.2, 13.2 Hz, 1H), 2.45 (s, 3H), 1.99 (td, *J* = 3.1, 13.4 Hz, 1H); ^{13}C NMR (125 MHz, $CDCl_3$): δ 174.1, 143.8, 139.4, 137.5, 136.1, 131.5, 129.9, 127.1, 124.3, 123.0, 120.4, 120.0, 116.3, 112.8, 111.4, 73.1, 65.4, 60.4, 46.6, 45.9, 45.8, 41.2, 32.4, 21.5, 14.2; HRMS–ESI (m/z) $[M - OH]^+$ cald $C_{25}H_{24}ClN_2O_4S$, 483.1145, found 483.1150.

Hydroxyester 66c. (2.56 g, 87% yield) ^{1}H NMR (500 MHz, $CDCl_3$) δ 8.03 (s, 1H), 7.74 (d, *J* = 8.1 Hz, 2H), 7.62 (d, *J* = 8.4 Hz, 1H), 7.31 (d, *J* = 8.2 Hz, 2H), 7.24 (d, *J* = 8.2 Hz, 1H), 7.19 (dt, *J* = 1.2, 8.0 Hz, 1H), 7.09 (dt, *J* = 1.2, 8.1 Hz, 1H), 5.08 (s, 2H), 5.01 (s, 1H), 4.41 (ddd, *J* = 4.2, 7.1, 11.2 Hz, 1H), 4.30 (ddd, *J* = 4.2, 7.2, 11.7 Hz, 1H), 4.06 (d, *J* = 15.6 Hz, 1H), 3.49 (d, *J* = 14.6 Hz, 1H), 3.33 (s, 1H), 3.22 (ddd, *J* = 4.2, 8.1, 12.2 Hz, 1H), 3.13 (ddd, *J* = 4.4, 8.1, 12.4 Hz, 1H), 3.03 (t, *J* = 3.2 Hz, 1H), 2.73 (td, *J* = 3.4, 13.6 Hz, 1H), 2.45 (s, 3H), 2.01 (td, *J* = 3.2, 13.5 Hz, 1H); ^{13}C NMR (125 MHz, $CDCl_3$): δ 173.8, 143.8, 139.5, 137.5, 136.1, 131.5, 129.9, 127.1, 124.3, 123.1, 120.5, 120.0, 116.3, 112.8, 111.4, 73.1, 66.0, 46.6, 45.9, 45.7, 32.7, 21.5, -0.37; HRMS–ESI (m/z) $[M - OH]^+$ cald $C_{25}H_{24}IN_2O_4S$, 575.0502, found 575.0502.

Hydroxyester 66d. (2.68 g, 97% yield) ^{1}H NMR (500 MHz, $CDCl_3$) δ 8.04 (s, 1H), 7.73 (d, *J* = 8.4 Hz, 2H), 7.61 (d, *J* = 8.1 Hz, 1H), 7.31 (d, *J* = 8.4 Hz, 2H), 7.22 (d, *J* = 8.2 Hz, 1H), 7.16 (dt, *J* = 1.1, 8.3 Hz, 1H), 7.08 (dt, *J* = 1.0, 8.1 Hz, 1H), 5.07 (s, 2H), 4.98 (s, 1H), 4.51 (t, *J* = 5.6 Hz, 1H), 4.15 (dd, *J* = 6.0, 11.4 Hz, 1H), 4.06 (dd, *J* = 6.1, 11.2 Hz, 1H), 4.04 (d, *J* = 13.6 Hz, 1H), 3.35–3.44 (m, 3H), 3.38 (qd, *J* = 7.6, 9.4 Hz, 1H), 3.23 (qd, *J* = 7.4, 9.2 Hz, 1H), 2.95 (t, *J* =

3.0 Hz, 1H), 2.68 (td, *J* = 3.1, 13.4 Hz, 1H), 2.44 (s, 3H), 1.97 (td, *J* = 3.2, 13.6 Hz, 1H), 1.25–1.20 (m, 1H), 1.06 (t, *J* = 7.3 Hz, 3H), 1.00 (t, *J* = 7.4 Hz, 3H); ^{13}C NMR (125 MHz, $CDCl_3$): δ 174.2, 143.8, 139.6, 137.5, 136.1, 131.3, 129.9, 127.1, 124.3, 123.0, 120.4, 120.0, 116.1, 112.9, 111.3, 98.9, 73.1, 65.0, 62.4, 62.2, 46.7, 45.97, 45.92, 32.4, 21.5, 15.1, 15.0, 1.02; HRMS–ESI (m/z) $[M - OH]^+$ cald $C_{29}H_{33}N_2O_6S$, 537.2059, found 537.2058.

Hydroxyester 66e. (2.55 g, 89% yield) ^{1}H NMR (500 MHz, $CDCl_3$) δ 8.01 (s, 1H), 7.74 (d, *J* = 8.4 Hz, 2H), 7.61 (d, *J* = 8.3 Hz, 1H), 7.32 (d, *J* = 8.2 Hz, 2H), 7.24–7.21 (m, 4H), 7.19–7.17 (m, 2H), 7.09 (dt, *J* = 1.1, 8.0 Hz, 1H), 5.07 (s, 1H), 5.04 (t, *J* = 2.8 Hz, 1H), 4.98 (s, 1H), 4.32–4.27 (m, 1H), 4.20–4.15 (m, 1H), 4.05 (d, *J* = 16.1 Hz, 1H), 3.48 (d, *J* = 15.8 Hz, 1H), 3.34 (s, 1H), 3.08–3.02 (m, 1H), 3.00–2.94 (m, 2H), 2.67 (td, *J* = 3.1, 14.4 Hz, 1H), 2.45 (s, 3H), 1.97 (td, *J* = 3.2, 14.4 Hz, 1H); ^{13}C NMR (125 MHz, $CDCl_3$): δ 174.2, 143.8, 139.5, 137.5, 136.1, 134.4, 131.4, 130.1, 129.9, 129.1, 127.1, 126.8, 124.3, 123.0, 120.4, 120.0, 116.2, 113.0, 111.4, 73.1, 64.2, 46.6, 45.9, 45.7, 32.5, 32.3, 21.5; HRMS–ESI (m/z) $[M - OH]^+$ cald $C_{31}H_{29}N_2O_4S_2$, 557.1569, found 557.1560.

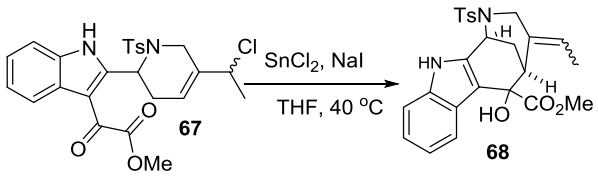

Hydroxyester 68. NaI (1.13 g, 7.5 mmol, 1.5 equiv) and $SnCl_2$ (1.42 g, 7.5 mmol, 1.5 equiv) were added in one portion to 100 mL THF solution of *α*-Ketoester **67** (2.5 g, 5 mmol). The mixture was stirred at 40 °C until starting material was consumed. Then EA and saturated KF solution were added to the reaction mixture. After stirring for 20 min, the organic layer was separated from the aqueous layer, which was extracted by EA twice. The combined organic phase was washed with brine, dried over Na_2SO_4, and concentrated in *vacuo*. The residue could be used directly for the next step or purified by FCC to give the white solid (3.12 g, 78 % yield, *trans:cis*

= 3:1, favor desired product). ^{1}H NMR (500 MHz, $CDCl_3$) δ 8.00 (s, 1.14H), 7.73 (d, *J* = 8.4 Hz, 2.27H), 7.61 (d, *J* = 8.2 Hz, 1.17H), 7.30 (d, *J* = 8.0 Hz, 2.30H), 7.21 (t, *J* = 8.3 Hz, 1.17H), 7.17 (t, *J* = 8.0 Hz, 1.15H), 7.08 (t, *J* = 8.6 Hz, 1.14H), 5.66 (q, *J* = 7.4 Hz, 1.00H), 5.50 (q, *J* = 7.4 Hz, 0.3H), 5.09 (t, *J* = 3.0 Hz, 0.28H), 5.06 (t, *J* = 3.0 Hz, 1H), 4.42 (d, *J* = 14.8 Hz, 0.30H), 3.94 (d, *J* = 14.8 Hz, 1H), 3.72 (s, 3H), 3.69 (s, 0.73H), 3.49 (d, *J* = 14.8 Hz, 1H), 3.36 (t, *J* = 2.6 Hz, 1H), 3.33 (s, 1H), 3.22 (s, 0.25H), 3.19 (d, *J* = 15.1 Hz, 0.25H), 2.83 (t, *J* = 2.8 Hz, 0.27H), 2.61 (td, *J* = 3.2, 14.3 Hz, 1H), 2.58 (td, *J* = 3.2, 14.4 Hz, 0.27H), 2.44 (s, 3.42H), 1.96 (td, *J* = 2.2, 14.5 Hz, 0.27H), 1.90 (td, *J* = 2.8, 14.2 Hz, 1H), 1.68 (d, *J* = 6.5 Hz, 3.00H), 1.64 (d, *J* = 6.6 Hz, 0.84H); ^{13}C NMR (125 MHz, $CDCl_3$): δ 175.1, 174.9, 143.75, 143.71, 137.7, 137.6, 136.1, 136.0, 131.4, 130.2, 130.0, 129.89, 129.84, 127.1, 127.0, 126.0, 125.8, 124.4, 124.3, 122.99, 122.97, 120.4, 120.2, 120.1, 113.5, 113.4, 111.39, 111.37, 73.6, 73.4, 53.2, 53.1, 48.1, 47.1, 46.48, 46.45, 40.7, 38.5, 32.2, 31.9, 29.7, 21.5, 13.12, 13.10; HRMS–ESI (m/z) $[M - OH]^+$ cald $C_{25}H_{25}N_2O_4S$, 449.1535, found 449.1534.

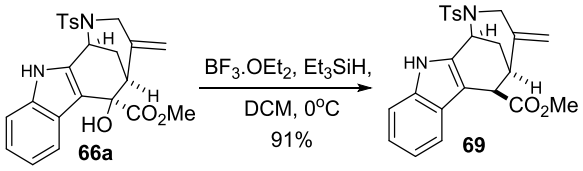

Methyl ester 69. The hydroxyester **66a** (4.52 g, 10 mmol) was dissolved in 50 mL DCM. To the stirred solution were sequentially added BF_3 (2.13 g, 15 mmol, 1.5 equiv) and was Et_3SiH (2.32 g, 20 mmol, 2 equiv) at 0 °C. After starting material was consumed, the reaction was quenched by H_2O. The mixture was extracted with DCM three times and the combined organic phases were washed with brine, dried over Na_2SO_4 and concentrated in *vacuo*. The residue could be used directly for the next step or purified by FCC to give the white solid (3.97 g, 91% yield). ^{1}H NMR (500 MHz, $CDCl_3$) δ 7.87 (s, 1H), 7.74 (d, *J* = 8.3 Hz, 2H), 7.31 (d, *J* = 8.1 Hz, 2H), 7.27 (d, *J* = 7.7 Hz, 1H), 7.23 (t, *J* = 8.0 Hz, 1H), 7.18 (dt, *J* = 1.1, 7.1 Hz, 1H), 7.07 (dt, *J* = 1.2, 8.0

Hz, 1H), 5.07 (t, *J* = 3.0 Hz, 1H), 4.89 (t, *J* = 1.5 Hz, 1H), 4.85 (t, *J* = 1.4 Hz, 1H), 4.16 (d, *J* = 5.9 Hz, 1H), 4.01 (d, *J* = 15.0 Hz, 1H), 3.66 (s, 3H), 3.62 (d, *J* = 13.8 Hz, 1H), 3.32 (q, *J* = 3.6 Hz, 1H), 2.45 (s, 3H), 2.07 (t, *J* = 3.0 Hz, 2H); ^{13}C NMR (125 MHz, $CDCl_3$): δ 172.6, 143.7, 141.4, 137.7, 136.0, 129.9, 129.6, 127.1, 125.7, 122.8, 119.9, 119.3, 113.8, 111.3, 110.0, 51.7, 46.6, 45.8, 45.2, 39.0, 33.0, 21.5; HRMS–ESI (m/z) $[M + H]^+$ cald $C_{24}H_{25}N_2O_4S$, 437.1535, found 437.1536.

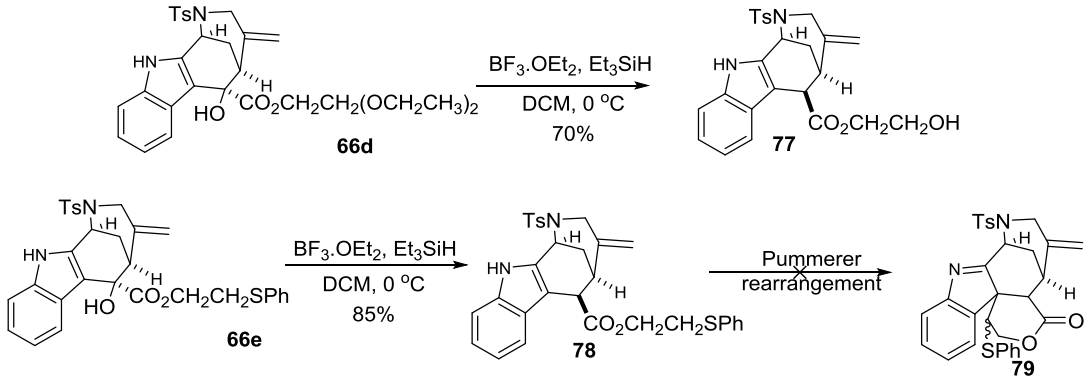

Following the same produce as ester **69**, compound **75** and **76** were prepared.

Compound **75.** ^{1}H NMR (500 MHz, $CDCl_3$) δ 7.99 (s, 1H), 7.75 (d, *J* = 8.8 Hz, 2H), 7.32 (d, *J* = 8.4 Hz, 2H), 7.28 (d, *J* = 8.1 Hz, 1H), 7.26 (d, *J* = 8.5 Hz, 1H), 7.19 (dt, *J* = 1.2, 8.3 Hz, 1H), 7.08 (dt, *J* = 1.1, 8.1 Hz, 1H), 5.08 (t, *J* = 3.4 Hz, 1H), 4.90 (d, *J* = 7.0 Hz, 2H), 4.25 (ddd, *J* = 4.4, 8.1, 12.1 Hz, 1H), 4.19 (d, *J* = 6.0 Hz, 1H), 4.15 (ddd, *J* = 4.3, 8.1, 12.5 Hz, 1H), 4.01 (d, *J* = 15.0 Hz, 1H), 3.75–3.72 (m, 2H), 3.62 (d, *J* = 14.8 Hz, 1H), 3.26 (dt, *J* = 3.4, 6.1 Hz, 1H), 2.45 (s, 3H), 2.09–2.07 (m, 2H); ^{13}C NMR (125 MHz, $CDCl_3$): δ 172.6, 143.7, 141.4, 137.6, 136.0, 129.9, 129.7, 127.1, 125.6, 122.9, 120.0, 118.9, 114.1, 111.5, 109.8, 66.5, 61.1, 46.6, 45.8, 45.2, 39.1, 32.9, 21.5; HRMS–ESI (m/z) $[M + H]^+$ cald $C_{25}H_{27}N_2O_5S$, 467.1641, found 467.1639.

Compound **76.** ^{1}H NMR (500 MHz, $CDCl_3$) δ 7.91 (s, 1H), 7.74 (d, *J* = 8.1 Hz, 2H), 7.34–7.23 (m, 8H), 7.20–7.16 (m, 2H), 7.06 (dt, *J* = 1.3, 8.2 Hz, 1H), 5.06 (t, *J* = 3.1 Hz, 1H), 4.87 (d, *J* = 1.1 Hz, 2H), 4.29 (ddd, *J* = 6.0, 7.2, 11.2 Hz, 1H), 4.20 (ddd, *J* = 6.1, 7.3, 11.5 Hz, 1H), 4.12 (d, *J* = 6.1 Hz, 1H), 4.01 (d, *J* = 15.2 Hz, 1H), 3.62 (d, *J* = 14.3 Hz, 1H), 3.21 (dt, *J* = 3.2, 6.3 Hz,

1H), 3.08 (hept, J = 7.3 Hz, 2H), 2.44 (s, 3H), 2.06 (t, J = 3.2 Hz, 2H); ^{13}C NMR (125 MHz, $CDCl_3$): δ 172.0, 143.7, 141.3, 137.6, 136.0, 135.0, 129.9, 129.64, 129.62, 129.1, 127.1, 126.5, 125.6, 122.8, 119.9, 119.3, 114.2, 111.3, 109.8, 63.1, 46.7, 45.8, 44.9, 39.0, 33.0, 32.2, 21.5; HRMS–ESI (m/z) $[M + H]^+$ cald $C_{31}H_{31}N_2O_4S_2$, 559.1725, found 559.1730.

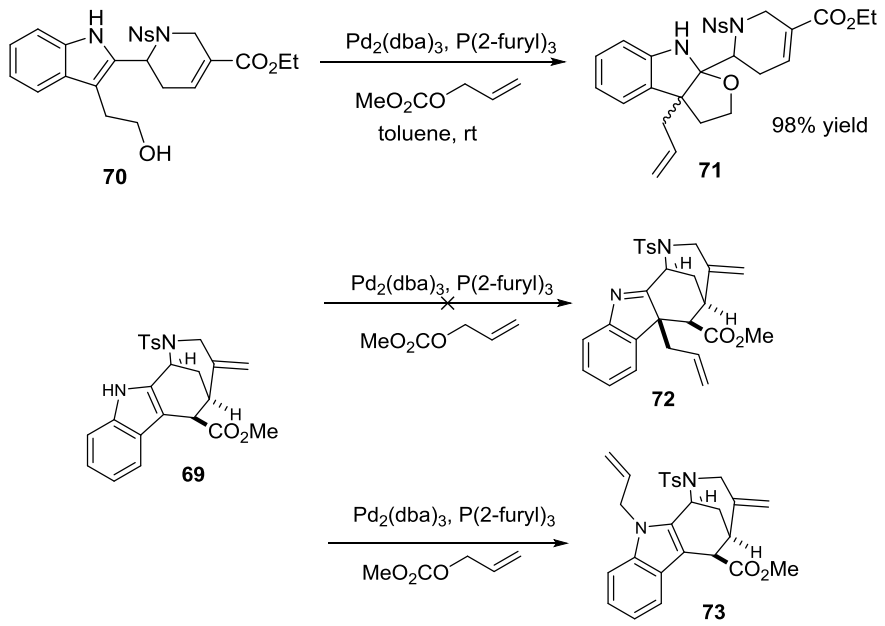

Alcohol **70** was prepared following the procedure reported previously by our group.[28]

Tsuji-Trost Reaction with alcohol 70. A round-bottomed flask flush with argon was charged with $Pd_2(dba)_3$ (91.5 mg, 0.1 mmol) and tri(2-furyl)phosphine (70 mg, 0.3 mmol). Toluene (20 mL) and allyl methyl carbonate (188 μL, 0.80 mmol) were added consecutively and the resulting mixture was stirred at room temperature for 20 min under argon before a solution of indole alcohol **70** (499 mg, 1 mmol) in toluene (20 mL) was added. The mixture was stirred for 24 h at room temperature under argon and then concentrated under reduced pressure. Purification of the crude residue by using flash column chromatography gave allyl product **71** (528 mg, 98% yield). Major product ^{1}H NMR (500 MHz, $CDCl_3$) δ 8.01 (d, J = 7.6 Hz, 1H), 7.68–7.62 (m, 2H), 7.56 (t, J = 7.5 Hz, 1H), 6.94 (d, J = 7.8 Hz, 2H), 6.65 (t, J = 7.6 Hz, 1H), 6.21 (d, J = 7.8 Hz, 1H), 5.56–5.51 (m, 1H), 5.17 (d, J = 17.5 Hz, 1H), 5.12 (d, J = 10.3 Hz, 1H), 4.86 (s, 1H), 4.65 (d, J =

17.2 Hz, 1H), 4.50 (d, *J* = 9.0 Hz, 1H), 4.20 (q, *J* = 6.7 Hz, 2H), 4.11 (dt, *J* = 17.2, 2.7 Hz, 1H), 3.84 (t, *J* = 8.5 Hz, 1H), 3.39–3.34 (m, 1H), 2.77 (ddd, *J* = 18.0, 8.1, 3.0 Hz, 1H), 2.64 (dd, *J* = 14.8, 5.8 Hz, 1H), 2.42 (dd, *J* = 14.8, 8.1 Hz, 1H), 2.29 (dt, *J* = 18.1, 4.1 Hz, 1H), 2.19 (dd, *J* = 12.1, 5.4 Hz, 1H), 2.04–1.99 (m, 1H), 1.29 (t, *J* = 7.2 Hz, 3H); ^{13}C NMR (125 MHz, $CDCl_3$): δ 165.0, 147.5, 136.2, 133.8, 133.6, 128.2, 127.2, 124.1, 123.4, 118.4, 118.3, 107.9, 105.4, 67.2, 60.7, 58.8, 53.8, 41.3, 40.4, 40.1, 26.4; HRMS–ESI (m/z) $[M + H]^+$ cald $C_{27}H_{30}N_3O_6S$, 540.1804, found 540.1803.

Tsuji-Trost Reaction with ester 69. Following the same produce as previous Tsuji-Trost Reaction condition, allyl indole **73** was isolated (428 mg, 90% yield). ^{1}H NMR (500 MHz, $CDCl_3$) δ 7.74 (d, *J* = 8.2 Hz, 2H), 7.32 (d, *J* = 8.4 Hz, 1H), 7.28 (d, *J* = 8.0 Hz, 3H), 7.22 (t, *J* = 8.2 Hz, 1H), 7.09 (dt, *J* = 8.1 Hz, 1H), 6.02–5.94 (m, 1H), 5.27 (s, 1H), 5.13 (d, *J* = 10.4 Hz, 1H), 4.94 (d, *J* = 18.4 Hz, 2H), 4.82 (d, *J* = 17.2 Hz, 1H), 4.80 (s, 1H), 4.72 (s, 1H), 4.16 (d, *J* = 6.0 Hz, 1H), 4.10 (d, *J* = 16.8 Hz, 1H), 3.88 (d, *J* = 16.4 Hz, 1H), 3.63 (s, 3H), 3.09–3.08 (m, 2H), 2.43 (s, 3H), 1.82 (d, *J* = 12.8 Hz, 1H), 1.72 (td, *J* = 1.1, 16.5 Hz, 1H); ^{13}C NMR (125 MHz, $CDCl_3$): δ 172.7, 143.4, 141.2, 138.0, 136.8, 133.7, 131.3, 129.7, 127.2, 125.5, 122.5, 119.7, 119.3, 113.4, 110.0, 109.4, 51.7, 46.5, 45.8, 45.1, 44.7, 39.0, 31.3, 21.5; HRMS–ESI (m/z) $[M + H]^+$ cald $C_{27}H_{29}N_2O_4S$, 477.1848, found 477.185

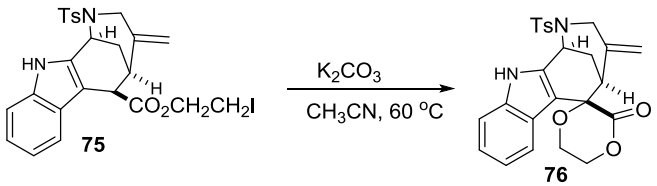

Ester 76. The ester **75** (57.6 mg, 0.1 mmol) was dissolved in 3 mL CH_3CN. To the solution was added K_2CO_3 (27.6 mg, 0.2 mmol, 2.0 equiv) and stirred at 60 °C until the starting material

was consumed (as determined by TLC). The reaction was concentrated in vacuo and the residue was purified through FCC to give a yellow foam (37.1 mg, 80% yield). ^{1}H NMR (500 MHz, $CDCl_3$) δ 7.93 (s, 1H), 7.74 (d, *J* = 8.4 Hz, 2H), 7.39 (d, *J* = 8.4 Hz, 1H), 7.32 (d, *J* = 8.3 Hz, 2H), 7.25–7.17 (m, 3H), 7.12 (dt, *J* = 1.0, 8.2 Hz, 1H), 5.04 (s, 1H), 4.98 (s, 1H), 4.90 (s, 1H), 4.77 (td, *J* = 3.5, 11.2 Hz, 1H), 4.62 (td, *J* = 3.4, 11.6 Hz, 1H), 4.08 (t, *J* = 4.4 Hz, 1H), 4.00 (d, *J* = 14.2 Hz, 1H), 3.67 (d, *J* = 14.2 Hz, 1H), 3.15 (t, *J* = 3.4 Hz, 1H), 2.60 (td, *J* = 2.4, 12.5 Hz, 1H), 2.46 (s, 3H), 1.94 (td, *J* = 3.1, 12.5 Hz, 1H); ^{13}C NMR (125 MHz, $CDCl_3$): δ 167.3, 143.7, 140.0, 137.7, 136.0, 131.6, 129.9, 127.1, 123.8, 123.3, 120.8, 118.5, 115.3, 112.8, 111.6, 78.5, 69.2, 60.3, 46.6, 45.7, 44.3, 29.7, 21.5; HRMS–ESI (m/z) $[M + H]^+$ cald $C_{25}H_{25}N_2O_5S$, 465.1484, found 465.1480.

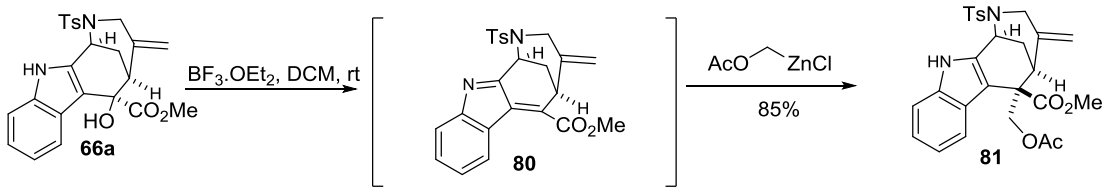

Indole ester 81. $BF_3.OEt_2$ (28.4 mg, 0.2 mmol, 2.0 equiv) was add dropwise to hydroxyester 66a (45 mg, 0.1 mmol) in 2 mL DCM at room time. The reaction mixture will turn deep red solution, indicating the formation of indole-quinonemethide intermediate **80**. Then, freshly prepared zinc reagent (2.0 equiv) was added in one pot (slow addition resulted in epimerization of starting material). The product **81** was formed immediately. The reaction was concentrated in vacuo and the residue was purified through FCC to give a yellow foam (42 mg, 80% yield). ^{1}H NMR (500 MHz, $CDCl_3$) δ 8.10 (s, 1H), 7.72 (d, *J* = 8.6 Hz, 2H), 7.47 (d, *J* = 8.6 Hz, 1H), 7.32 (d, *J* = 8.2 Hz, 2H), 7.25 (d, *J* = 8.2 Hz, 2H), 7.16 (t, *J* = 8.2 Hz, 1H), 7.05 (t, *J* = 8.1 Hz, 1H), 5.29 (s, 1H), 5.05 (t, *J* = 3.0 Hz, 1H), 4.87 (d, *J* = 18.5 Hz, 2H), 4.60 (d, *J* = 10.9 Hz, 1H), 4.44 (d, *J* = 10.8 Hz, 1H), 3.92 (d, *J* = 14.2 Hz, 1H), 3.59 (s, 1H), 2.82 (s, 1H), 2.45 (s, 3H), 2.34 (dt, *J* = 2.6, 12.8 Hz, 1H), 1.94 (dt, *J* = 3.1, 12.7 Hz, 1H); ^{13}C NMR (125 MHz, $CDCl_3$): δ

172.9, 170.5, 143.7, 140.9, 137.7, 136.0, 129.9, 129.5, 127.0, 126.2, 122.6, 121.6, 119.6, 114.7, 111.8, 111.1, 69.6, 60.4, 52.0, 51.9, 46.3, 45.8, 42.7, 31.5, 30.2, 21.5, 21.0; HRMS–ESI (m/z) $[M + H]^+$ cald $C_{27}H_{29}N_2O_6S$, 509.1746, found 509.1744.

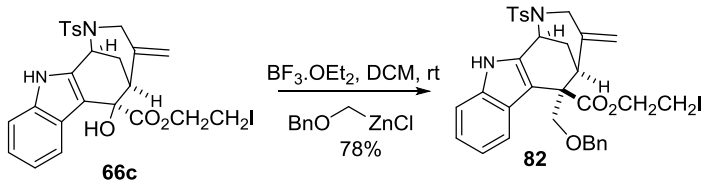

Compound **82** was formed following the same procedure. ^{1}H NMR (500 MHz, $CDCl_3$) δ 7.92 (s, 1H), 7.72 (d, *J* = 8.4 Hz, 2H), 7.46 (d, *J* = 8.2 Hz, 1H), 7.30 (d, *J* = 8.3 Hz, 2H), 7.24–7.20 (m, 4H), 7.16 (t, *J* = 8.1 Hz, 1H), 7.10 (dd, *J* = 1.2, 8.0 Hz, 1H), 6.97 (t, *J* = 8.1 Hz, 1H), 5.02 (t, *J* = 3.0 Hz, 1H), 4.89 (s, 2H), 4.44 (d, *J* = 12.0 Hz, 1H), 4.33 (d, *J* = 12.2 Hz, 1H), 4.25 (ddd, *J* = 6.0, 8.2, 11.5 Hz, 1H), 4.11 (d, *J* = 8.5 Hz, 1H), 3.94 (d, *J* = 14.2 Hz, 1H), 3.79 (d, *J* = 8.5 Hz, 1H), 3.61 (d, *J* = 14.2 Hz, 1H), 3.08 (ddd, *J* = 6.1, 8.0, 11.4 Hz, 1H), 2.91 (t, *J* = 3.2 Hz, 1H), 2.45 (s, 3H), 2.35 (td, *J* = 2.4, 12.7 Hz, 1H), 1.89 (td, *J* = 3.1, 12.7 Hz, 1H); ^{13}C NMR (125 MHz, $CDCl_3$): δ 172.2, 143.6, 141.4, 137.9, 137.8, 136.0, 129.9, 129.4, 128.1, 127.6, 127.4, 127.0, 126.2, 122.5, 122.3, 119.5, 114.8, 112.8, 110.9, 76.4, 73.6, 64.9, 53.2, 46.7, 45.9, 43.2, 30.6, 21.5; HRMS–ESI (m/z) $[M + H]^+$ cald $C_{33}H_{34}IN_2O_5S$, 697.1233, found 697.1230.

Section 2.16 References

(1) Henry, T. A. *J. Chem. Soc.* **1932**, 2759.

(2) For a review, see: Ramirez, A.; Garcia-Rubio, S.; *Curr. Med.Chem.* **2003**, *10*, 1891.

(3) Subramaniam, G.; Hiraku, O.; Hayashi, M.; Koyano, T.; Komiyama, K.; Kam, T. S.*; J. Nat. Prod.* **2007**, *70*, 1783.

(4) Shang, J. H.; Cai, X. H.; Feng, T.; Zhao, Y. L.; Wang, J. K.; Zhang, L. Y.; Yan, M.; Luo, X. D. *J. Ethnopharmacol.* **2010**, *129*, 174.

(5) Pousset, J. L.; Poisson, J.; Olivier, L. Man, J.; Janot, M. M.; *C. R. Hebd. Seances Acad. Sci.* **1965**, *261*, 5538.

(6) Lim, S. H.; Low, Y. Y.; Sinniah, S. K.; Yong, K. T.; Sim, K. S.; Kam, T. S. *Phytochemistry* **2014**, *98*, 204.

(7) Ahmad, Y.; Fatima, K.; Le Quesne, P. W.; Atta-Ur-Rahman, *Phytochemistry* **1983**, *22*, 1017.

(8) Ohashi, M.; Joule, J. A.; Djerassi, C. *Tetrahedron Lett.* **1964**, *5*, 3899.

(9) Naranjo, J.; Hesse, M.; Schmid, H. *Helv. Chim. Acta* **1970**, 53, 749.

(10) (a) A. F. Thomas, D. Phil. Thesis, Oxford, England, **1954**; (b) A. Z. Britten, G. F. Smith, *J. Chem. Soc.* **1963**, 3850.

(11) (a) Henry, T. A. *J. Chem. Soc.* 1932, 2759; (b) Olivier, L. J.; Lvy, J.; Men, L.; Janot, M. M.; Budzikiewicz, H.; Djerassi, C. *Bull. Soc. Chim. Fr*. **1965**, 868.

(12) Kiang, A. K.; Smith, G. F. *Proc. Chem. Soc.* **1962**, 298.

(13) J. Mokry´, L. Dfflbravkov, P. S *efc˘ovic˘, Experientia* **1962**, *18*, 564.

(14) Cai, X. H.; Tan, Q. G.; Liu, Y. P., Feng, T.; Du, Z. Z.; Li, W. Q.; Luo, X. D. *Org. Lett*. **2008**, *10*, 577.

(15) (a) Zu, L.; Boal, B. W.; Garg, N. K. *J. Am. Chem. Soc.* **2011**, *133*, 8877. (b) Ren, W.; Wang, Q.; Zhu, J. *Angew. Chem., Int. Ed.* **2014**, *53*, 1818. (c) Teng, M.; Zi, W.; Ma, D. *Angew. Chem., Int. Ed.* **2014**, *53*, 1814.

(16) Smith, J. M.; Moreno, J.; Boal, B. W.; Garg, N. K. *J. Am. Chem. Soc.* **2014**, *136*, 4504.

(17) Moreno, J.; Picazo, E.; Morrill, L. A.; Smith, J. M.; Garg, N. K. *J. Am. Chem. Soc.* **2016**, *138*, 1162.

(18) Ren, W.; Wang, Q.; Zhu, J. *Angew. Chem., Int. Ed.* **2016**, *55*, 1.

(19) Li, Y.; Zhu, S.; Li, J.; Li, A. *J. Am. Chem. Soc.* **2016**, *138*, 3982.

(20) Smith, J. M.; Moreno, J.; Boal, B. W.; Garg, N. K. *Angew. Chem., Int. Ed.* **2016**, *55*, 400.

(21) (a) Dolby, L.J.; Esfandiari, Z. J. *J. Org. Chem.* **1972**, *37*, 43; (b) Dolby, L. J.; Nelson, S. J. *J. Org. Chem.* **1973**, *38*, 2882.

(22) (a) Zhang, M.; Huang, X.; Shen, L.; Qin, Y. *J. Am. Chem. Soc*. **2009**, *131*, 6013. (b) Zhang, D.; Song, H.; Qin, Y. *Acc. Chem. Res*. **2011**, *44*, 447.(c) Zi, W.; Xie, W.; Ma, D. *J. Am. Chem. Soc.* **2012**, *134*, 9126 (d) Horning, B. D.; MacMillan, D. W. C. *J. Am. Chem. Soc.* **2013**, *135*, 6442.(e) Adams, G. L.; Carroll, P. J.; Smith, A. B., III. *J. Am. Chem. Soc.* **2012**, *134*, 4037 (f) Adams, G. L.; Carroll, P. J.; Smith, A. B., III. *J. Am. Chem. Soc.* **2013**, *135*, 519 (g) Smith, M. W.; Snyder, S. A. *J. Am. Chem. Soc.* **2013**, *135*, 12964.

(23) Jiang, S. Z.; Zeng, X. Y.; Liang, X.; Lei, T.; Wei, K.; Yang, Y. R. *Angew. Chem., Int. Ed.* **2016**, *55*, 4044.

(24) Nishiyama, D.; Ohara, A.; Chiba, H.; Kumagai, H.; Oishi, S.; Fujii, N.; Ohno, H. *Org. Lett*. **2016**, *18*, 1670.

(25) (a) Arbusow, B. A.; *Pure Appl. Chem*. **1964**, *9*, 307. (b) Staudinger, H.; Mayer, J. *Helv. Chim. Acta*, **1919**, *2* 635. (c) Appel, R. *Angew. Chem., Int. Ed.* **1975**, *14*, 801. (d) Wittig,

G.; Schollkopf, U. *Angew. Chem.*, **1954**, *9*, 1318. (e) Pommer, H. *Angew. Chem., Int. Ed.* **1977**, *16*, 423.

(26) *A Guide to Organophosphorus Chemistry*, ed. L. D. Quin, Wiley, New York, 2000.

(27) (a) Zhu, X. F.; Henry, C. E.; Kwon, O. *Tetrahedron* **2005**, *61*, 6276. (b) Andrews, I. P.; Kwon, O. *Org. Synth.* **2011**, *88*, 138. (c) Andrews, I. P.; Kwon, O. *Chem. Sci.* **2012**, *3*, 2510. For reports on Lu's original allene–imine [3 + 2] annulation, see: (d) Xu, Z.; Lu, X. *Tetrahedron Lett.* **1997**, *38*, 3461; (e) Xu, Z.; Lu, X. *J. Org. Chem.* **1998**, *63*, 503.

(28) Henry, C. E.; Xu, Q.; Fan, Y. C.; Martin, T. J.; Belding, L.; Dudding, T.; Kwon, O. *J. Am. Chem. Soc.* **2014**, *136*, 11890.

(29) Villa, R. A.; Xu, Q.; Kwon, O. *Org. Lett*. **2012**, *14*, 4634.

Chapter 3

Catalytic Asymmetric Staudinger–Aza-Wittig Reaction *via* Desymmetrization

Section 3.1 Introduction

Phosphorus-containing compounds play an important role in synthetic organic chemistry and biochemical sciences.[1] In 1906 Michaelis and Arbuzov first introduced the formation of phosphonate from trialkyl phosphite *via* a simple procedure.[2] Since then, phosphorus chemistry has entered a flourishing period. A lot of named reactions were developed such as Appel reaction,[3] Wittig reaction,[4] Staudinger reaction,[5] and Mitsunobu reaction.[6] All of these reactions are still widely used in laboratory and industrial processes. One significant moment was that, in 1979, George Wittig was awarded the Nobel Prize for "his development of the use of phosphorus-containing compounds into important reagents in organic synthesis." As well as phosphine-mediated stoichiometric reactions, phosphorus compounds were also found to be fundamentally important toward transition metal chemistry. Especially in recent years, fine tuning of the electronic and steric properties of the phosphorus ligands could result in efficient C–H activation that is chemoselective and enantioselective.[7] Half a century after the discovery of the Michaelis–Arbuzov reaction, phosphine(III) were applied as nucleophilic catalysts, which is another significant development of phosphorus compounds. The first example as nucleophilic catalyst could trace back to 1955 when Horner accidently discovered polymerization of acrylonitrile to form head-to-tail polymers catalyzed by triethylphosphine.[8] In 1963, Rauhut and Currier reported tributylphosphine-catalyzed dimerization of acrylates to form α-methylene succinates.[9] In the past two decades, phosphines(III) were extensively used to construct C–C and C–heteroatom bonds to form all different sized carbocycles and heterocycles.[10]

It has been over 100 years since the first Michaelis–Arbuzov reaction was discovered. All these phosphorus-mediated reactions (Appel reaction, Wittig reaction, Staudinger reaction, Mitsunobu reaction) are still extensively used to functionalize C–O and C=O bonds by organic chemists, ranking highly on the list of useful organic transformations. One severe issue associated

with these reactions was the generation of stoichiometric phosphine oxide as a byproduct, which often complicates efforts to isolate product and lead to waste disposal, hampering the efficiency of those transformations. Some creative strategies have been developed to alleviate purification issues, like polymeric phosphine reagent,[11] bipyridyl tagged phosphine reagent,[12] monolithic phosphines,[13] anthracene tagged reagents,[14] fluorous phosphines,[15] tetraaryl supported phosphines,[16] PEG based polymers[17] and post reaction polymerization.[18] Given the importance of these reactions in synthesis, as well as pursuing atom economic and environmentally friendly reactions, ideally, developing phosphine-catalyzed versions of those type of named reactions is highly desirable.

For converting these stoichiometric phosphine-mediated reactions to phosphine-catalyzed reactions, there is tremendous development towards this new area. In the last decade, there were two main strategies developed to address this challenge, which includes activation mode and reduction mode (Figure 3.1.1). (a) In the activation case, it involves the in situ activation of a phosphine oxide to halophosphonium(V) salt without affecting the phosphorus oxidation state, thereby avoiding the challenging reduction of strong phosphorus oxygen bonds, which could be considered a redox-neutral process. This strategy mainly applies to the reactions which form phosphonium(V) salt intermediates like the Appel reaction. (b) In reduction mode, phosphorus is shuttled between phosphorus(V) and phosphorus(III) throughout the catalytic cycle. The phosphine(V) oxide generated from the reaction is reduced back to phosphine(III) by a terminal reductant, which could also be considered a redox-driven process.[19]

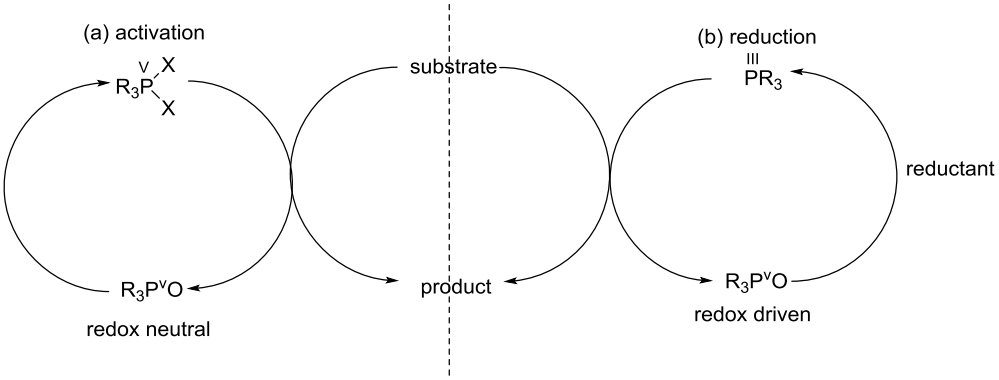

Figure 3.1.1 Approaches in Organophosphorus Catalysis

Section 3.2 Phosphorus-Mediated Reaction *via* Redox-Neutral Process

Section 3.2.1 McKeever-Abbas's Catalytic Aza-Wittig Reaction with Isocyanates

In 2008, McKeever-Abbas and coworkers reported a smart strategy to realize a catalytic aza-Wittig reaction with isocyanates.[20] The classical Aza-Wittig reaction starts with phosphine(III) and azides to form the key aza-ylide intermediate for further Wittig reaction, generating stoichiometric phosphine oxide by-product. The authors employed isocyanates as starting material instead of azides. Different from azides, which need activativation by phosphine(III), the isocyanates could directly react with phosphine(V) oxide to generate aza-ylide intermediate, releasing one equivalent of carbon dioxide, which avoided regenerating the reactive phosphine(III) species. During the reaction process, the phosphorus was kept at P(V) oxidation state. By employing this strategy, a variety of heterocycles were synthesized.

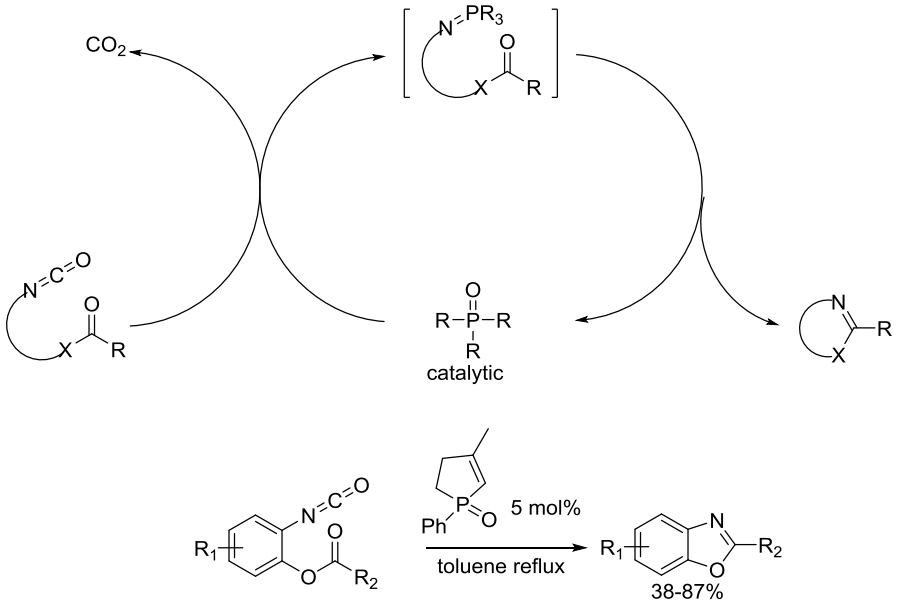

Scheme 3.2.1 McKeever-Abbas's Catalytic Aza-Wittig Reaction with Isocyanates

Section 3.2.2 Denton's Phosphorus(V)-Catalyzed Dichlorination of Epoxides

In 2010, Denton and co-workers developed a stereospecific triphenylphosphine oxide-catalyzed 1,2-dichlorination reaction of epoxides.[21] The reaction was effective for a range of terminal and internal epoxides. Catalytic amounts of triphenylphosphine oxide was used, which was converted to chlorophosphonium salt by oxalyl chloride.

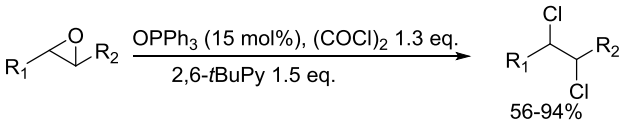

Scheme 3.2.2 Denton's Phosphorus(V)-Catalyzed Dichlorination of Epoxides

Section 3.2.3 Denton's Phosphorus(V)-Catalyzed Appel Reaction

In the same year, the same group reported a triphenylphosphine oxide-catalyzed Appel reaction.[22] The reaction was effective for acyclic primary and secondary alcohols. However, one drawback associated with this strategy compared with a redox strategy was background reactions between the substrates with oxalyl chloride.

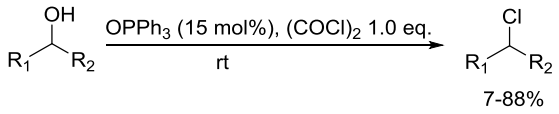

Scheme 3.2.3 Denton's Phosphorus(V)-Catalyzed Appel Reaction

Section 3.2.4 Denton's Phosphorus(V)-Catalyzed Synthesis of Nitriles from Oximes

In 2012, Denton' group reported triphenylphosphine oxide-catalyzed nitrile formation from aromatic and aliphatic aldoximes at room temperature in the presence of oxalylchloride with the same strategy.[23]

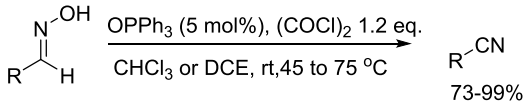

Scheme 3.2.4 Denton's Phosphorus(V)-Catalyzed Synthesis of Nitriles from Oximes

Section 3.2.5 Denton's Phosphorus(V)-Catalyzed Deoxydichlorination Reaction

In 2013, the same group adopted the same strategy using triphenylphosphine oxide to catalyze a deoxydichlorination reaction of aldehyde to form 1,1-dichloride.[24]

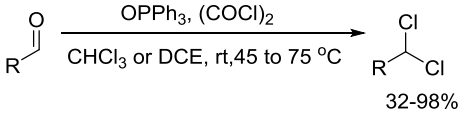

Scheme 3.2.5 Denton's Phosphorus(V)-catalyzed Deoxydichlorination Reaction

Section 3.3 Phosphorus-Mediated Reaction *via* Redox-Driven Process

Section 3.3.1 O'Brien's Catalytic Wittig Reaction

In 2009, O'Brien and co-workers reported the first catalytic Wittig reaction.[25] In this paper, they found silane could chemoselectively reduce phosphine oxide back to phosphine in the presence of a ketone or aldehyde. Through computational studies, they found that 3-methyl-1-phenylphospholane-1-oxide was easier to reduce than triphenylphosphine oxide. Under the

standard reaction conditions: diphenylsilane, Na_2CO_3, toluene at 100 °C, a variety of heteroaryl, aryl and alkyl aldehyde could be efficiently converted to the corresponding alkenes in moderate to high yield.

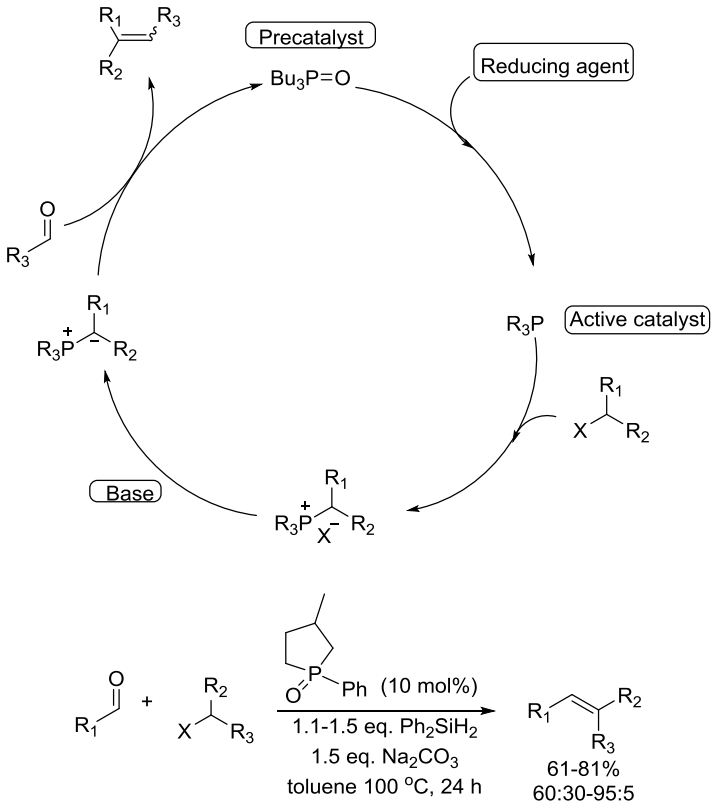

Scheme 3.3.1 O' Brien's First Catalytic Wittig Reaction and Proposal

In 2013, the same group reported a catalytic Witting reaction at room temperature.[26] For the catalytic Wittig reaction, the reduction cycle is the rate-limiting step. In order to improve the efficiency of the reduction, usually elevated temperature was required. In this paper, O'Brien developed a condition which could realize the reduction cycle at room temperature by using a combination of 4-nitrobenzoic acid and diisopropylethyl amine to accelerate the reduction rate.

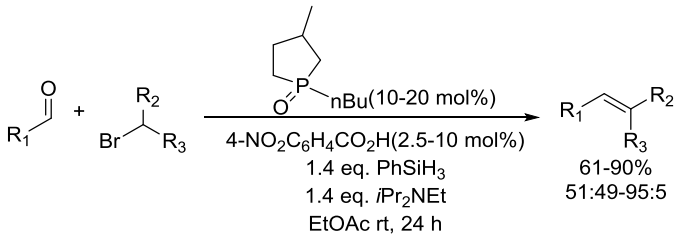

Scheme 3.3.2 O' Brien's Room Temperature Catalytic Wittig Reaction

Section 3.3.2 Delft's Catalytic Appel Reaction *via* In Situ Phosphine Oxide Reduction

In 2011, Delft's group reported a catalytic Appel reaction *via* in situ phosphine oxide reduction cycle.[27] Different from Denton's phosphorus(V)-catalyzed Appel reaction, which adopted an activation strategy, they used a redox-driven strategy. The challenge associated with this strategy was the compatibility between reductant, silanes and electrophilic halogen. After extensive screening, they found diethyl bromomalonate or diethyl chloromalonate were good choices for this reaction. Under optimized conditions, alcohols were effectively transformed to bromides or chlorides. In this paper, they tested the effect of ring size on the rate of reduction by silanes, as well as the degree of saturation of seven-membered rings. After the study, they found that five-membered ring phosphine oxides were more efficient than other sized ring phosphine oxides. These results indicated a correlation between relief of ring strain and susceptibility to reduction by silanes. They further compared the reduction efficiency between five-membered phosphine oxides and aromatic phospholes, which might be a good candidate due to the increased ring strain and recovery of aromaticity after reduction. However, the results showed there was only a small difference between phospholanes and phospholes with respect to the rate of reduction. Reduction of dibenzophosphole was approximately 1.5 times slower than that of the five-membered phosphine oxide.

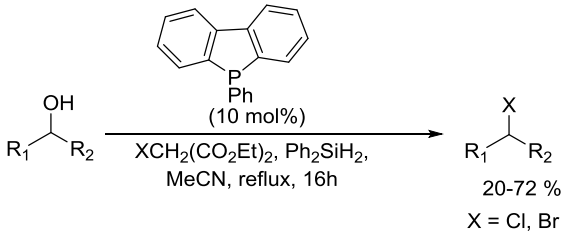

Scheme 3.3.3 Delft's Catalytic Appel Reaction

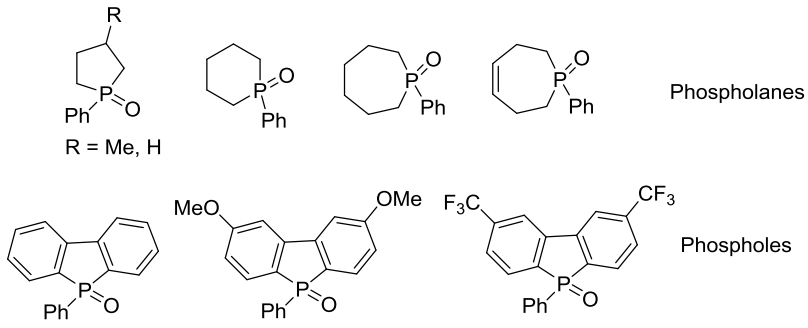

Scheme 3.3.4 Delft's Phosphine Oxide for Reduction Test

Section 3.3.3 Delft's Phosphine-Catalyzed Staudinger Reaction

In 2012, Delft and co-workers first reported the phosphine-catalyzed Staudinger reduction.[28] They utilized dibenzophosphole as a catalyst and phenylsilane as a reducing reagent in refluxing dixoane to facilitate this process. It is interesting that they claimed the Staudinger reduction for their system involved in situ P=N bond reduction rather than direct formation of the amine from hydrolyzing P=N bond by water. They also used NMR studies to further confirm their proposal, where they could trap the aza-ylide intermediate with silane by formation of aminosiliane.

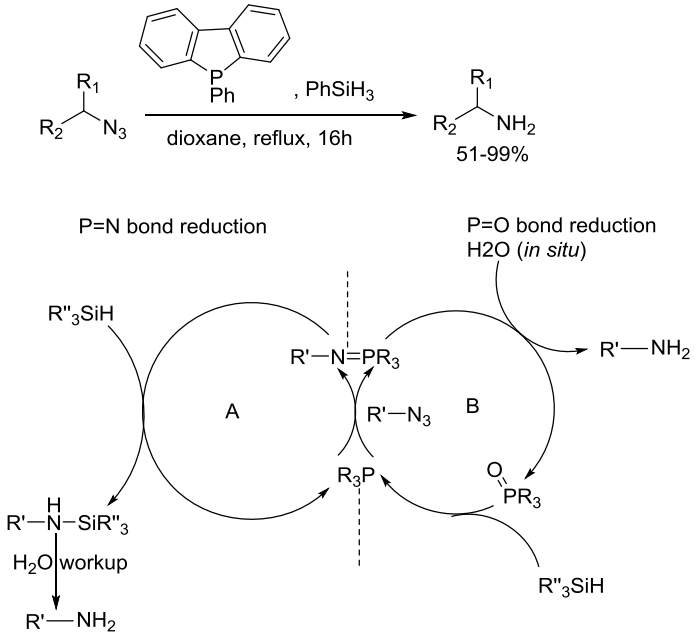

Scheme 3.3.5 Delft's Phosphine-Catalyzed Staudinger Reaction

Section 3.3.4 Ashfeld's Phosphine-Catalyzed Staudinger Ligation Reaction

In 2012, the Ashfeld group reported phosphine-catalyzed Staudinger Ligation for the chemoselective, direct conversion of carboxylic acid to amide, which formed the amide C–N bond *via* aza-ylide intermediate.[29] Traditionally, this type of reaction would produce stoichiometric phosphine oxide byproduct. After screening various silane reducing reagents, they found phenylsilane could drive the P^{III}/P^{V}-redox cycle to reduce the phosphine required to a catalytic amount. Due to low reactivity of phenylsiliane, the reaction was performed at elevated temperature. It is worthwhile to mention, they used PPh_3, which proved inferior during the reduction cycle, to facilicate this reaction.

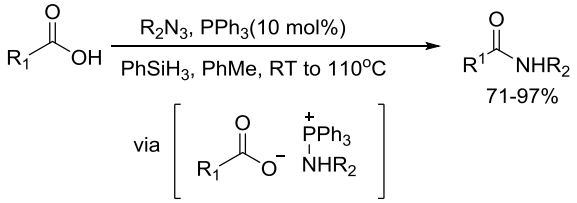

Scheme 3.3.6 Ashfeld's Phosphine-Catalyzed Staudinger Ligation reaction

Section 3.3.5 Ding's Phosphine-Catalyzed Aza-Wittig Reaction

In 2014, Ding and co-workers reported a catalytic intramolecular Aza-Wittig reaction based on the phosphine/phosphine oxide catalytic cycle strategy to synthesize 4(3*H*)-quinazolinones efficiently.[30] In their system, they used a combination of tetramethyldisiloxane and titanium tetraisopropoxide as a terminal reducing system to recycle phosphine oxide in refluxing toluene. They also applied their methodology to synthesize (*S*)-vasicinone in an efficient way.

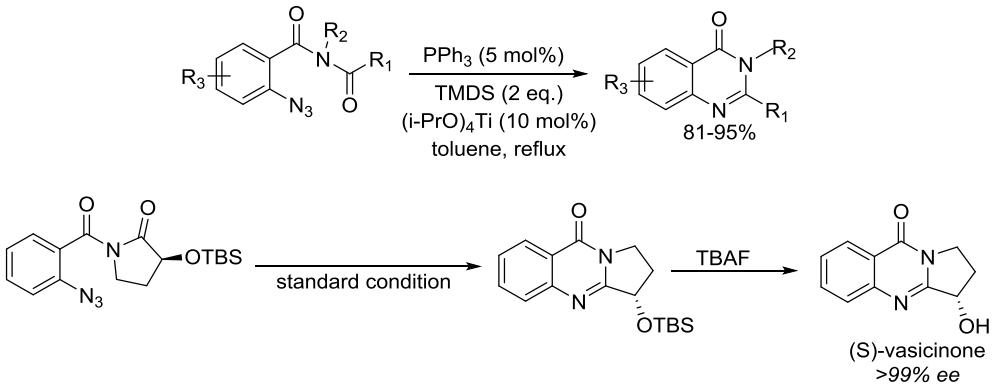

Scheme 3.3.7 Ding's Phosphine-Catalyzed Aza-Wittig Reaction and Vasicinone Synthesis

Section 3.3.6 Voiturez's Cyclization Reaction of Huisgen Zwitterion with α-Ketoesters

In 2015, Voiturez's group presented the first catalytic cyclization reaction between the Huisgen zwitterion and carbonyl substrates by in *situ* recycling of phosphine oxide.[31] In their reduction system, they used a combination of silane/phosphoric acid/amine, which was inspired by the work of Beller. From the perspective of the mechanism, they believed the phosphonate-amine salt first reacted with silane to generate phosphasilane, which was the key intermediate for the efficiency of the reduction cycle, activating both the silane and phosphine oxide to accelerate the phosphine oxide reduction.

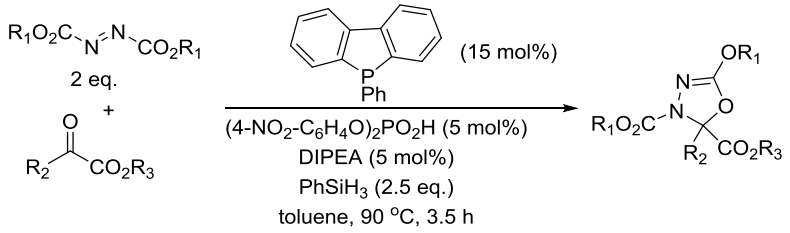

Scheme 3.3.8 Voiturez's Cyclization Reaction of Huisgen Zwitterion with α-Ketoesters

Section 3.3.7 Aldrich's Phosphine-Catalyzed Mitsunobu Reaction

In 2015, Aldrich's group reported the first fully catalytic Mitsunobu reaction, employing both catalytic amounts of phosphine and azocarboxylate.[32] The idea was inspired by both O'Brien and Taniguchi's catalyst system. O'Brien and co-workers discovered the first example of a Mitsunobo reaction, which was catalytic with phosphine. Taniguchi and co-workers disclosed an iron(III) phthalocyanine catalytic system employing oxygen as a terminal oxidant to recycle azodicarboxylate. It is interesting that both the reductive cycle and oxidative cycle were compatible under the reaction conditions they developed.

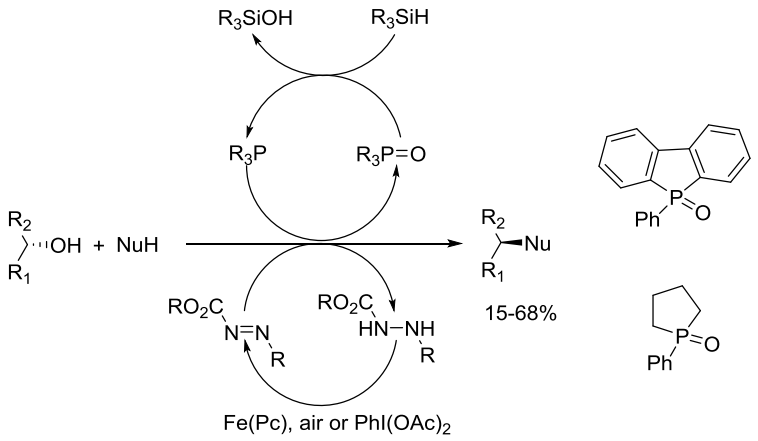

Scheme 3.3.9 Aldrich's Catalytic Misunobu Reaction

Section 3.3.8 Werner's First Microwave-Assisted Catalytic Wittig Reaction

In 2014, Werner and co-workers reported a catalytic Wittig reaction using tributylphosphine oxide as a pre-catalyst which was reduced by phenylsilane.[33] The reaction

performed under microwave irradiation at 150 °C to furnish the desired product with up to 75% yield and medium-to-good selectivity. The base in this reaction was actually generated by ring opening of the oxirane by the bromide anion. Typical inorganic base was proven unsuitable for this reaction. They also applied this methodology to catalytic asymmetric Wittig reactions. As shown below, by employing (*S, S*)-Me-Duphos as a chiral phosphine, they could obtain the desired product in 39% yield and medium enantioselectivity.

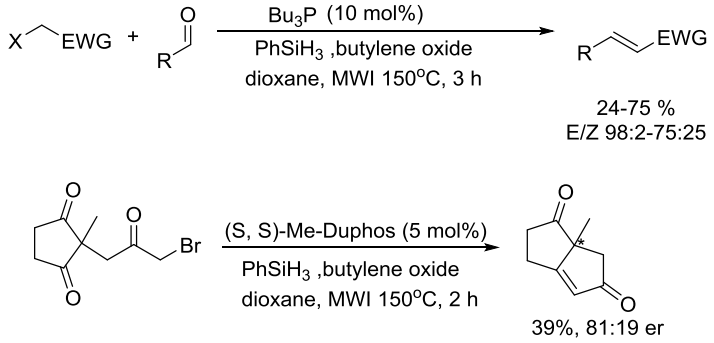

Scheme 3.3.10 Microwave-Assisted Catalytic Wittig Reaction and Asymmetric Wittig Reaction

Section 3.3.9 Werner's First Base-Free Catalytic Wittig Reaction

In 2015, the same group published the first base-free catalytic Wittig reaction between maleate and aldehyde.[34] The classical Wittig reaction needs stoichiometric phosphine and base to be promoted. In this case, the authors chose maleate as the Michael acceptor. First, tributylphosphine underwent nucleophilic addition to maleate, followed by a [1,2]-H-shift to generate the corresponding ylide without any base. Subsequently, the resulting ylide reacted with the aldehyde to generate alkene and phosphine oxide, which was reduced back to phosphine by silane to close the catalytic cycle.

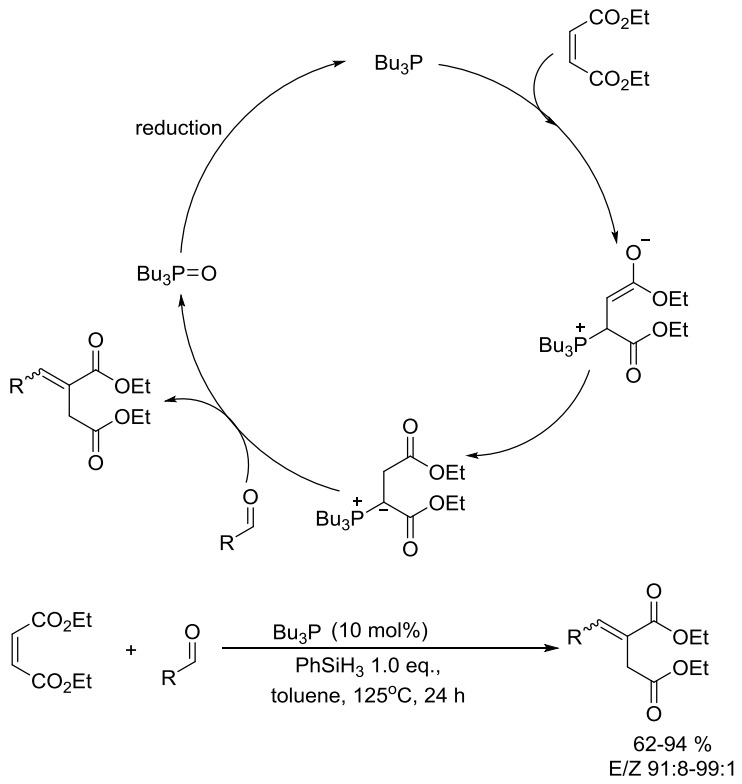

Scheme 3.3.11 Werner's First Base-Free Catalytic Wittig Reaction

Section 3.4 Reduction of Phosphine Oxide to Phosphine

As we all know, the driving force for these phosphorus-mediated named reactions is highly dependent on the formation of the thermodynamically favorable phosphine oxide bond (128 Kcal/mol). This high entropy gain allows the formation of products that are substantially higher in energy than the reactants. However, due to the strength of the phosphorus-oxygen double bond, reduction to phosphine typically requires significant activation. The methods developed for this type of reduction could fall into four categories: (1) activation of phosphine oxide to more reactive halophosphorus salt which has weaker bond than phosphorus-oxygen bond, then reduction of this activated species could be easier; (2) reduction with metal hydride; (3) direct reduction with silanes; (4) catalyst-mediated reduction with silanes, typically, titanium species can catalyze this process.[35]

Section 3.4 1 Reduction via Activation Model

In 1996, Siegel filed a patent which described a combination of phosgene and aluminum to reduce phosphine oxide.[36] They first converted phosphine oxide to the chlorophosphium salt, which could be reduced to phosphine by aluminum. Later on, Kakeya employed a combination of chlorine and carbon monoxide gas under high pressure to convert phosphine oxide to the chlorophosphium salt, which could be reduced further by hydrogen under high temperature.[37] In 2011, Tanaka and co-workers used electrochemsitry to reduce phosphine oxide.[38] They first converted phosphine oxide to chlorophosphium salt. Then under electrochemisty, the desired phosphine could be formed. They could also apply silylation of phosphine oxide followed by reduction *via* electrochemistry. Methylation of phosphine oxide resulted in low yield. Gilheany's group demonstrated chlorophosphium could be reduced by LAH at low temperature.[39]

Table 3.4.1 Phosphine Oxide Reduction via Activation Model

Entry	Phosphorus(V)	Reagent	Conditions	Yield (%)
1	Ph_3PO	$COCl_2$/Al	100 ^oC ($COCl_2$) 130 ^oC, 1.5 h (Al)	96
2	Ph_3PO	$Cl_2/CO/H_2$	59 bar, 25 ^oC (Cl_2/CO) 98 bar, 160 ^oC (H_2)	86
3	Ph_3PO	$Bi/TiO_2 + H_2$	500 ^oC	73
4	Ph_3PO	($COCl_2$) electrochem	$AlBr_3$, (Al-Pt), 50 mA	72
5	Ph_3PO	TMSCl electrochem	Bu_4NBr, (Zn-Cu), 100 mA	89
6	Ph_3PO	TMSOTf electrochem	(Al-Pt), 50 mA	66
7		MeOTf electrochem	(Al-Pt), 50 mA	11
8	Ph_3PO	($COCl_2$) + LAH	25 ^oC, 20 min ($COCl_2$) -78 ^oC, instant (LAH)	86

Section 3.4 2 Reduction *via* Metal Hydride

Metal hydrides, such as LAH, have also been employed for the direct reduction of

phosphine oxide, albeit in low yield, which could have been drastically improved by adding a Lewis acid like $CeCl_3$. One disadvantage associated with this methodology is that enantiopure phosphine oxide yields racemic phosphine. Dibal-H could also reduce phosphine oxide to phosphine, sacrificing one equivalent of tricyclohexyl phosphine.

Table 3.4.2 Reduction via Metal Hydride

Entry	Phosphorus(V)	Reagent	Conditions	Yield (%)
1	Ph_3PO	$NaBH_4$		
2	Ph_3PO	LAH	80 ^oC, 4 h	54
3	Ph_3PO	LAH + $CeCl_3$	40 ^oC, 30 min	95
4	Ph_3PO	DIBAL + Cy_3PO	72 ^oC, 16 h	91

Section 3.4 3 Reduction via Silanes

Comparing the two methods above, silane reduction showed broad functional group compatibility. In 1964, Korte and co-workers first reported reduction of phosphine oxide to phosphine by PMHS.[40] As indicated below, direct reduction by silanes usually requires high temperature. Phenylsilane showed higher reactivity than PMHS, which could proceed with the reduction at 120 ^oC. More reactive silane, trichlorosilane could reduce the phosphine oxide more efficiently. The combination of trichlorosilane and triethylamine worked equally as well, however, it could invert the stereocenter of phosphorus.

Table 3.4.3 Reduction via Silanes

Entry	Phosphorus(V)	Reagent	Conditions	Yield (%)
1	Ph_3PO	PMHS	280-300^oC, 2 h, neat	86
2	Ph_3PO	PMHS	218 ^oC, 2 h, solution	65
3	Ph_3PO	$PhSiH_3$	120 ^oC, 2 h, neat	82
4	Ph_3PO	Ph_2SiH_2	120 ^oC, 2 h, neat	90
5	Ph_3PO	$HSiCl_3$	80 ^oC, 2 h	98
6	Ph_3PO	$HSiCl_3$ + Et_3N	80 ^oC, 2 h	85

Section 3.4 4 Reduction *via* Combination of Metal Catalyst and Silanes

In 1994, Lawrence and co-workers reported the titanium-catalyzed phosphine oxide

reduction to phosphine in the presence triethyoxysilane which showed a lower reaction temperature and shorter reaction time.[41] Later, they identified tetramethyldisiloxane (TMDS) worked more efficiently. The mechanism of titanium-catalyzed reduction originally was believed to involve formation of a titanium hydride species. Later, electron paramagnetic resonance (EPR) and UV spectroscopy showed generation of titanium(III) which produced silyl radical was more likely. Other Lewis acids like copper triflate and iridium bromide worked as well. The combination of phosphate diester and diethyxomethylsilane could also promote the reduction.

Table 3.4.4 Reduction via Combination of Metal Catalyst and Silanes

Entry	Phosphorus(V)	Reagent	Conditions	Yield (%)
1	Ph_3PO	$Ti(OiPr)_4$ (0.1eq.)/$(EtO)_3SiH$	67 ^oC, 1 h	86
2	Ph_3PO	$Ti(OiPr)_4$ (0.1eq.)/TMDS	100 ^oC	100
3	Ph_3PO	$IrBr_3$ (0.01 eq.)/TMDS	100 ^oC	84
4	Ph_3PO	$Cu(OTf)_2$ (0.1 eq.)/TMDS	100 ^oC, 10-24 h	96
5	Ph_3PO	$Cu(OTf)_2$ (0.1 eq.)/PMHS	100 ^oC, 10-24 h	88
6	Ph_3PO	$(4\text{-}NO_2C_6H_4O)_2PO_2H$(0.15)/ $(EtO)_2SiMeH$	110 ^oC, 24 h	99

Section 3.5 First Asymmetric Aza-Wittig reaction

In 2006, Marsden and co-workers reported the first asymmetric aza-Wittig reaction to form polysubstituted nitrogen-containing heterocycles, which were prevalent in pharmaceutical and biologically important natural product targets *via* desymmetrization of 1,3-diketones.[42] The chiral phosphorus(III) reagents they used were prepared from the known and readily available proline-derived diazaphospholidine and oxazaphospholidine and the cyclohexyldiamine-derived diazaphospholidine which were less reactive than triaryl or trialkylphosphine with respect to Staudinger reaction. The initial study showed the reaction could be finished within 56 hours at room temperature when using proline-derived diazaphospholidine. However, they found the results were not reproducible under identical experimental conditions. They suspected trace

amounts of water in the reaction system could hydrolyze the imine to the achiral aminodiketone, which was confirmed by exposing the enantiomerically enriched sample to atmospheric moisture, the enantiomeric purity dropped to 0% over a period of three days. After further optimization, they trapped the initially formed keto imine to *N*-acyl enamine, which could block racemization. Under the optimized condition, four different substrates were developed, giving low to medium enantioselectivity. The maximum levels of asymmetric induction were around 60% ee.

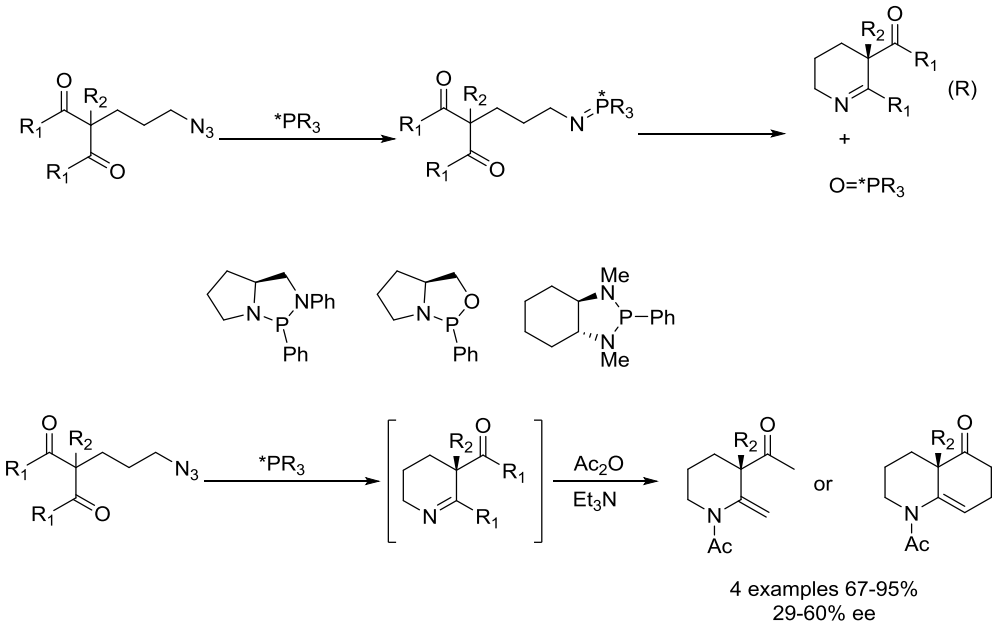

Scheme 3.5.1 Chiral Phosphorus(III) Catalysts and First Asymmetric Aza-Wittig Reaction

Section 3.6 Reaction Design

In 2014, our group developed new chiral [2.2.1]bicyclic phosphines, which were derived from commercially available *L*-hydroxyproline in six chemical operations.[10d] The synthesis of the chiral phosphine is straightforward. Hydroxyproline could be converted to the tritosylate in 82% yield over three steps. Bisalkylation of dilithium phenylphosphide with the tritosylate could furnish a 1:0.96 mixture of the *exo*- and *endo*-P-phenylphosphine oxide after oxidative workup. Trichlorosilane reduction could afford the chiral phosphine in high yield (Scheme 3.6.1). With the

chiral phosphine in hand, we explored its application in the enantioselective synthesis of pyrrolines from allenoates and imines. The *exo*- and *endo*-P-phosphines worked as pseudoenantiomers, providing opposite enantiomerically pure pyrrolines (Scheme 3.6.2).

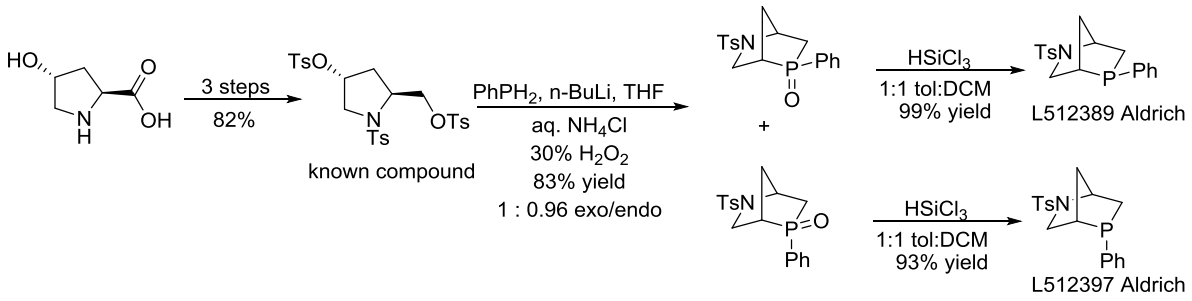

Scheme 3.6.1 Synthesis of Hydroxyproline-Derived Chiral Phosphine

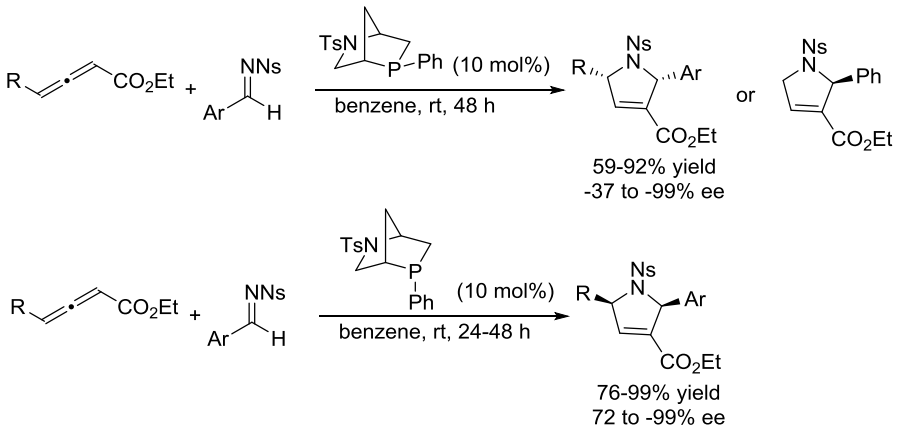

Scheme 3.6.2 Chiral Phosphine-Catalyzed Enantioselective Allene–Imine [3 + 2] Annulations

This new rigid [2.2.1]bicyclic ring system in the chiral phosphine reminded us of the efficiency of reduction cycles from phosphine oxide to phosphine with five-membered rings. A P NMR study of our chiral phosphine oxide showed higher efficiencies in the reduction cycle than the known phosphine oxide by using silane as reductant, which was consistant with computational studies.[43] The activation free energies for O'Brien's five-membered phosphine and our chiral phosphine were 25.9 and 25.5 kcal/mol, respectively, indicating 0.4 kcal/mol lower energy with our chiral phosphine due to rigidity of our chiral phosphine. Given the efficiency in the reduction of our chiral phosphine, we considered applying our chiral phosphine to catalytic asymmetric

reactions, which traditionally needed stoichiometric phosphine. The first idea that came to our mind was the Staudinger–aza-Wittig reaction. Marsden and co-workers reported the first Staudinger–aza-Wittig reaction. Stoichiometric chiral phosphine was applied which made this reaction synthetically less useful, and the substrates scope was limited. In order to achieve the first catalytic asymmetric Stuadinger–aza-Wittig reaction, there were some challenges that needed to be addressed:

(1) High reduction cycle turnover to avoid high temperatures. Typically, the reduction cycle from phosphine oxide to phosphine needs high temperatures. Although O'Brien showed a combination of acid and amine base could promote the reduction cycle at room temperature, this condition would invert the phosphorus stereocenter, which would complicate the asymmetric reaction catalyzed by *P*-chiral phosphine. We were concerned about the functional group compatibility when applying organometallic or Lewis acid to accelerate reduction cycle.

(2) Racemization of product. Trace amounts of water in the reaction could hydrolyze imine to aminoketone, which cyclizes with ketone to deliver racemic product.

(3) Developing conditions which could be compatible with substrates, intermediates, and products. Although silane reduction is compatible with aldehydes and ketones, Delft's results showed direct reduction of iminophosphranes was possible. If the reduction of iminophosphrans was faster than the aza-Wittig reaction, that would deliver racemic product.

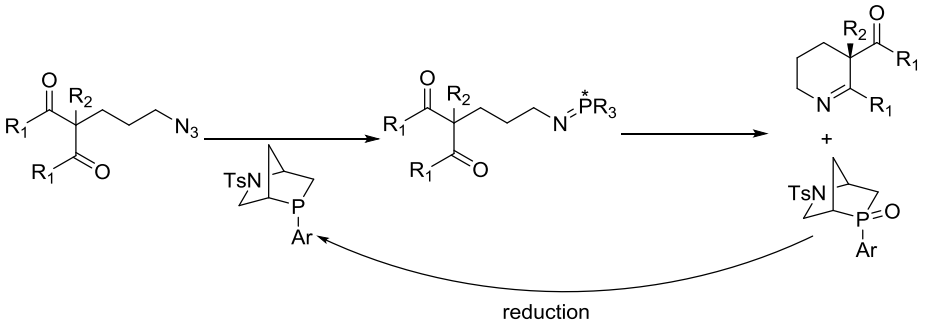

Scheme 3.6.3 Our Proposal for Asymmetric Staudinger–Aza-Wittig Reaction

Section 3.7 Results

Table 3.7.1 Optimization of Staudinger Aza-Wittig Reaction[a]

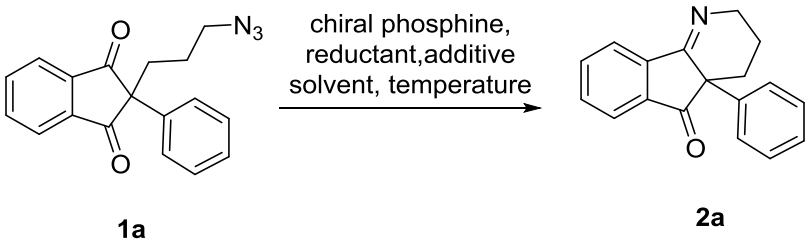

1a **2a**

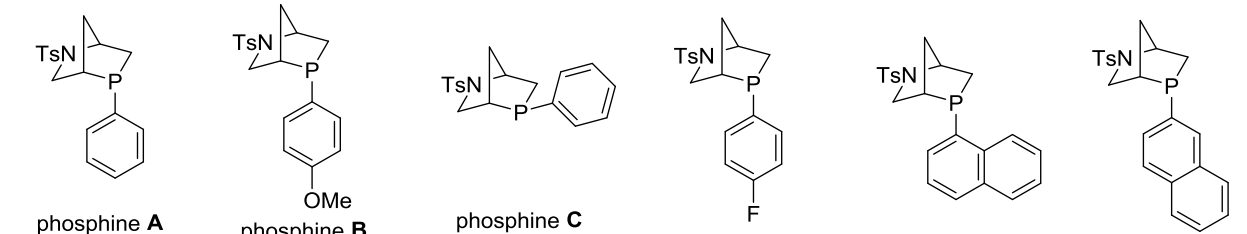

phosphine **A** Aldrich # L512398; phosphine **B** Aldrich # L512478; phosphine **C** Aldrich # L512389; phosphine **D** Aldrich # L512451; phosphine **E** Aldrich # L512486; phosphine **F** Aldrich # L512494

entry	cat.	amount (%)	solvent	temp	reductant	additive	time (h)	yield (%)[b]	ee (%)[c]
1	**A**	100	toluene	rt			12	99	79
2	**C**	100	toluene	rt			12	99	11
3	**A**	20	toluene	80 °C	$PhSiH_3$		48	95	70.2
4	**A**	20	toluene	100 °C	$PhSiH_3$		24	96	65
5	**A**	20	toluene	30 °C	$PhSiH_3$	benzoic acid	24	99	54
6	**A**	20	toluene	30 °C	$PhSiH_3$	2-nitro-4-trifluoromethylbenzoic acid	24	99	70
7	**A**	20	toluene	30 °C	$PhSiH_3$	4-trifluomethylbenzoic acid	24	99	60
8	**A**	20	toluene	30 °C	$PhSiH_3$	2,4-dinitrobenzoic acid	24	99	60
9	**A**	20	toluene	30 °C	$PhSiH_3$	4-nitrobenzoic acid	24	99	75

10	**A**	20	toluene	30 °C	$PhSiH_3$	*r*-Binol	24	53	76
11	**A**	20	toluene	30 °C	$PhSiH_3$	*s*-Binol	24	55	74
12	**A**	20	toluene	30 °C	$PhSiH_3$	2-thiophenecarboxylic acid	24	97	59
13	**A**	20	toluene	30 °C	$PhSiH_3$	*s*-1,1'-binaphthyl-2,2'-dicarboxylic acid	24	NR	
14	**A**	20	toluene	30 °C	$PhSiH_3$	*r*-1,1'-binaphthyl-2,2'-dicarboxylic acid	24	NR	
15	**A**	20	Toluene/THF 1:9	30 °C	$PhSiH_3$	*s*-1,1'-binaphthyl-2,2'-dicarboxylic acid	24	88	66
16	**A**	20	Toluene/THF 1:9	30 °C	$PhSiH_3$	*r*-1,1'-binaphthyl-2,2'-dicarboxylic acid	24	76	74
17	**A**	20	toluene	rt	$PhSiH_3$	2-nitrobenzoic acid	48	99	86
18	**A**	20	CH_3CN	rt	$PhSiH_3$	2-nitrobenzoic acid	96	90	60
19	**A**	20	benzene	rt	$PhSiH_3$	2-nitrobenzoic acid	72	90	84
20	**A**	20	THF	rt	$PhSiH_3$	2-nitrobenzoic acid	72	99	79
21	**A**	20	dioxane	rt	$PhSiH_3$	2-nitrobenzoic acid	Reaction not finshied		
22	**A**	20	$CHCl_3$	rt	$PhSiH_3$	2-nitrobenzoic acid	Reaction not finshied		
23	**A**	20	oxylene	rt	$PhSiH_3$	2-nitrobenzoic acid	Reaction not finshied		
24	**A**	20	toluene	rt	$PhSiH_3$	2-nitrobenzoic acid(50%)	30	99	75
25	**A**	20	toluene	rt	$PhSiH_3$	2-nitrobenzoic acid(100%)	30	99	68
26	**B**	20	toluene	rt	$PhSiH_3$	2-nitrobenzoic acid	48	99	84
27	**D**	20	toluene	rt	$PhSiH_3$	2-nitrobenzoic acid	48	99	84
28	**E**	20	toluene	rt	$PhSiH_3$	2-nitrobenzoic acid	48	99	66
29	**F**	20	toluene	rt	$PhSiH_3$	2-nitrobenzoic acid	48	99	84
30	**A**	20	toluene	rt	$PhSiH_3$	2-nitrobenzoic acid/molecular sieve	48	99	88

[a] Unless otherwise noted, reactions were conducted using 0.05 mmol of azide, 20% mmol of chiral phosphine, 20 mol% additive, 0.1 mmol of $PhSiH_3$. [b] Isolated yield after silica gel flash column chromatography. [c]determined by HPLC.

To test our hypothesis, we used diketone azide **1a** as our starting material. First, we applied stoichiometric PPh_3 to promote the Staudinger–aza-Wittig reaction. The desired imineketone formed after a few hours. By using stoichiometric chiral phosphine **A** and **C** at room temperature, the reaction could be finished within 12 h with 79% and 11% ee respectively (Table 3.7.1 entries 1 and 2). When using 20 mol% catalyst **A** with phenyl silane as the reducing reagent, we screened the reaction under 80 °C and 100 °C, resulting in 70% and 65% ee respectively (Table 3.7.1 entries 3 and 4). In order to achieve higher enantioselectivity, we attempted to lower the reaction

temperature through adding Brønsted acid.[26] After screening various of Brønsted acids, we found 2-nitrobenzoic acid gave us the best result, which could promote the reaction at room temperature with 86% ee and 99% yield (Table 3.7.1 entries 5–17). By applying 2-nitrobenzoic acid as an additive, we then screened different solvents and chiral phosphines. Toluene and chiral phosphine **A** was the best combination for this reaction (Table 3.7.1 entries 17–29). Increasing the 2-nitrobenzoic acid loading up to 100 mol%, the enantioselectivity dropped to 65%. Considering the racemization challenging Marsden's system where trace amount of water in the reaction system could hydrolyze the imine to the achiral aminodiketone, we added molecular sieves as a water scavenger. We could thus further improve the enantioselectivity up to 88% with 99% yield (Table 3.7.1 entry 30). The optimized condition for our reaction was: 1.0 equiv of diketonamine, 20 mol % chiral phosphine **A**, 20 mol % 2-nitrobenzoic acid, 2.0 equiv phenylsilane, and molecular sieve in 1.0 mL toluene at room temperature.

Table 3.7.2 Substrates for Aza-Wittig Staudinger Reaction[a]

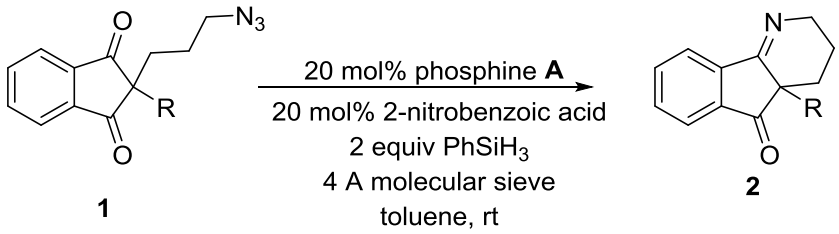

entry	Ar	time (h)	yield (%)[b]	ee (%)[c]
1	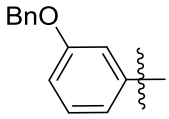	48	99	90
2	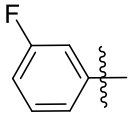	48	99	86

3	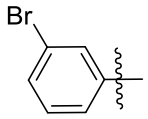	48	99	91
4	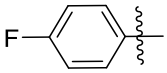	48	99	86
5	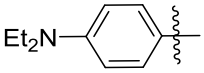	48	99	85
6	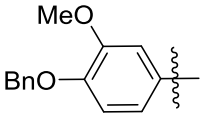	48	99	87
7	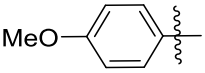	48	99	86
8	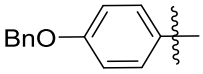	48	99	86
9	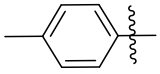	48	99	91
10	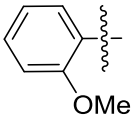	96	95	84
11	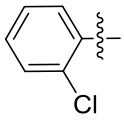	96	88	70
11	Methyl	48	96	90
12	Ethyl	72	97	91
13	Cyclohexyl	36	99	94

[a] Unless otherwise noted, reactions were conducted using 0.05 mmol of azide, 20% mmol of chiral phosphine, 20 mol% additive, 0.1 mmol of $PhSiH_3$. [b] Isolated yield after silica gel flash column chromatography. [c] determined by HPLC.

With optimized conditions in hand, we tested the reaction with other substrates. First, we changed the phenyl group to other substituted aryl groups. Electronic differences did not affect the

enantioselectivity too much, which varied from 85% to 91% (Table 3.7.2 entries 1–9). Sterically, *ortho*-substituted aryl groups gave lower enantioselectivity with longer reaction time, resulting in 84% ee and 70% ee for chloro and methoxy group respectively (Table 3.7.2 entries 10 and 11). Then we switched the aryl group to an aliphatic group. Methyl group gave 96% yield and 90% ee. Ethyl group gave 97% yield and 91% ee. Cyclohexyl could further improve the yield and enantioselectivity up to 99% and 94%, respectively.

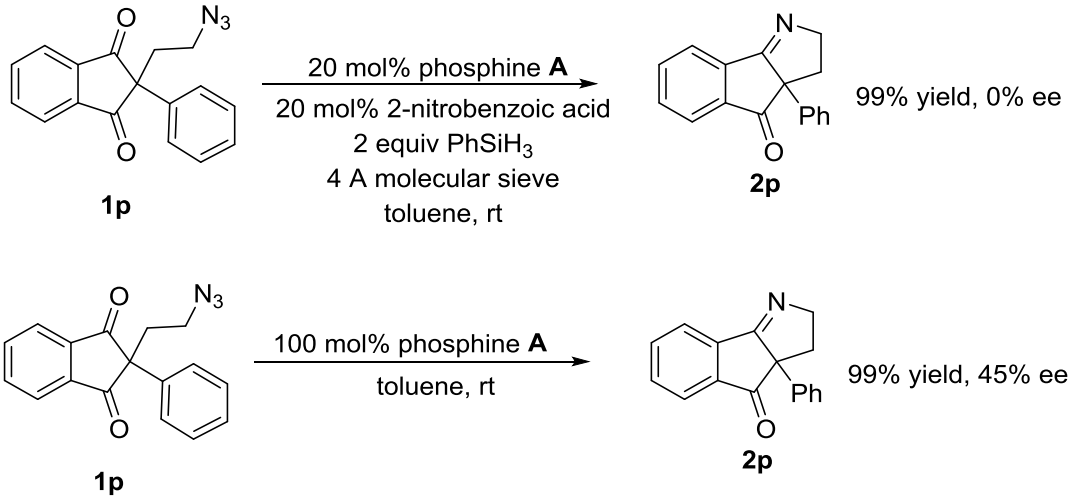

Scheme 3.7.1 Catalytic Asymmetric Staudinger–Aza-Wittig Reaction for Five-Member Ring Formation

Later, we applied our methodology to five membered ring formation. The reaction could be finished within two days, resulting in 99% yield and 0% ee. We assumed the low enantioselectivity could arise from the rapid racemization of the ketone imine product. The high reactivity of ketone imine product could be attributed to ring strain from a 5,5 fused ring system. In order to test our hypothesis, we used stoichiometric chiral phosphine **A** for the reaction. The reaction could be finished in a few hours. After a quick column, we found the enantioselectivity was 45%, which dropped to 0% within half hour (scheme 3.7.1).

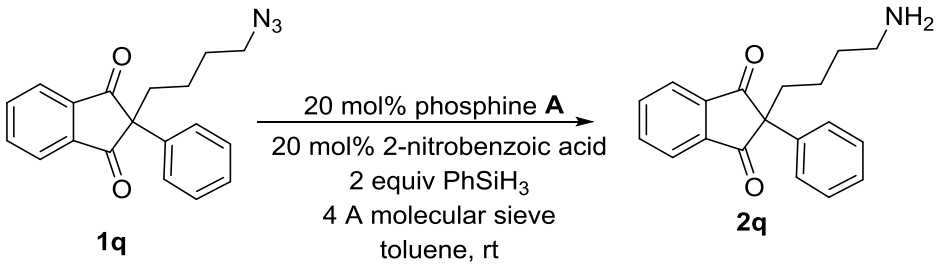

Scheme 3.7.2 Attempted Seven-Membered Ring Formation

Then, we subjected **1q** under our standard conditions for seven-membered ring formation. The compound isolated was the Staudinger reaction product. The non-reactivity toward the aza-Wittig reaction is probably due to the less favorable kinetic process associated with seven-membered ring formation.

Section 3.8 Conclusion

In conclusion, we have successfully developed a catalytic asymmetric Staudinger–aza-Wittig reaction. Historically, both Staudinger and Wittig reactions need stoichiometric amounts of phosphine, which prohibit the development of catalytic asymmetric version for these type of reactions. Marsden and co-workers, in 2006, developed the first asymmetric Staudinger–aza-Wittig reaction with stoichiometric chiral phosphine, which was less economically and environmentally friendly. Based on our previous studies about phosphine design, we found that bridged [2.2.1] bicyclic phosphine oxides had a more efficient reduction cycle with silane than known phosphine oxides at high temperatures. In this project, after screening a variety of Brønsted acids, we could realize the catalytic asymmetric Staudinger-aza-Wittig reaction at lower temperature, resulting in 85–94 % ee.

Section 3.9 Experimental procedures

General Information

All reactions were performed in dry solvents under an Ar atmosphere and anhydrous conditions. DCM, THF, and MeCN were freshly distilled over CaH_2 prior to use. All other reagents were used as received from commercial sources. Reactions were monitored through thin layer chromatography (TLC) on 0.25-mm SiliCycle silica gel plates and visualized under UV light. Flash column chromatography (FCC) was performed using SiliCycle Silica-P Flash silica gel (60-Å pore size, 40–63 μm) NMR spectra were recorded using Bruker Avance-500 instruments, calibrated to $CD(H)Cl_3$ as the internal reference (7.26 and 77.0 ppm for ^1H and ^{13}C NMR spectra, respectively) unless otherwise noted. ^1H NMR spectral data are reported in terms of chemical shift (δ, ppm), multiplicity, coupling constant (Hz), and integration. ^{13}C NMR spectral data are reported in terms of chemical shift (δ, ppm). The following abbreviations indicate the multiplicities: s, singlet; d, doublet; t, triplet; q, quartet; m, multiplet. High resolution mass spectra were recorded using a Waters LCT Premier XE time-of-flight instrument controlled by MassLynx 4.1 software. Samples were infused using direct loop injection from a Waters Acquity UPLC into the multi-mode ionization source. The lock mass standard for accurate mass determination was leucine enkephalin (Sigma L9133). Enantiomeric excess was measured through chiral HPLC using a Shimadzu CBM Lite system and a REGIS (*R, R*)-DACH DNB analytical (diameter: 4.5 mm) chiral column, with CH_2Cl_2/hexanes as the eluent and CHIRALCEL AD-H analytical (diameter: 4.6 mm) chiral column, with *i*PrOH/hexanes as the eluent.

General procedure for Aza-Wittig Staudinger Reaction

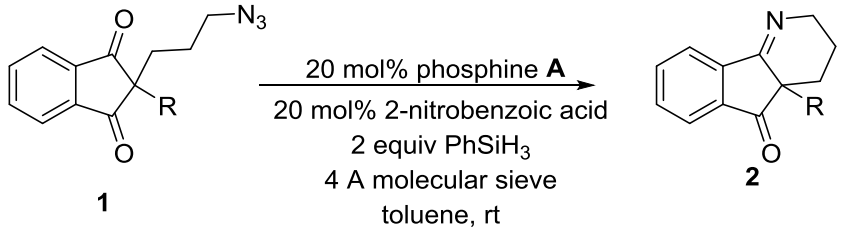

A flame-dried 5 mL vial was charged with diketone azide (0.05 mmol), 2-nitrobenzoic acid (1.68 mg, 0.01 mmol, 0.2 equiv) and chiral phosphine **A** (3.45 mg, 0.01 mmol, 0.2 equiv). Then freshly activated molecular sieve (10 mg) was added to the mixture inside the desicator. 1 mL fresh dry toluene was added to the mixture under argon protection. Then phenylsilane (12.3 μL, 0.1 mmol, 2 equiv) was added to the mixture. The mixture was stirred at room temperature until the diketone azide was consumed (determined by TLC). The crude reaction product was loaded directly onto a column of SiO_2 and purified through flash column chromatography (30% EA/Hexanes) to yield ketone amine.

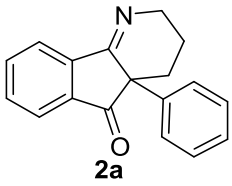

2a

(13.05 mg, 99% yield) ^{1}H NMR (500 MHz, $CDCl_3$) δ 8.05 (d, *J* = 7.7 Hz, 1H), 7.66 (d, *J* = 7.6 Hz, 1H), 7.72 (t, *J* = 8.3 Hz, 1H), 7.56 (t, *J* = 7.3 Hz, 1H), 7.35 (d, *J* = 8.3 Hz, 2H), 7.28–7.25 (m, 2H), 7.22 (d, *J* = 8.0 Hz, 1H), 3.93 (td, *J* = 8.3, 19.1 Hz, 1H), 3.85 (ddd, *J* = 3.0, 7.6, 19.1 Hz, 1H), 2.57 (td, *J* = 4.0, 13.6 Hz, 1H), 1.84 (dt, *J* = 4.8, 12.7 Hz, 1H), 1.69–1.66 (m, 1H), 1.56–1.48 (m, 1H); ^{13}C NMR (125 MHz, $CDCl_3$): δ 201.1, 169.2, 146.4, 137.7, 137.0, 135.5, 132.0, 128.8, 127.5, 127.3, 124.0, 121.8, 55.4, 49.4, 27.4, 17.9; HRMS–ESI (m/z) $[M + H]^+$ calcd $C_{18}H_{16}NO$, 262.1232, found 262.1234.

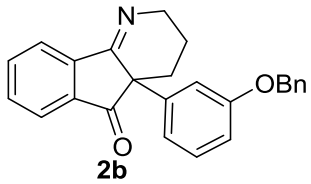

2b

(18.35 mg, 99% yield) ^{1}H NMR (500 MHz, $CDCl_3$) δ 8.04 (d, *J* = 7.9 Hz, 1H), 7.77 (d, *J* = 8.2 Hz, 1H), 7.72 (t, *J* = 8.1 Hz, 1H), 7.56 (t, *J* = 7.4 Hz, 1H), 7.39–7.30 (m, 5H), 7.18 (t, *J* = 8.0 Hz, 1H), 6.98 (s, 1H), 6.94 (d, *J* = 7.6 Hz, 1H), 6.68 (dd, *J* = 1.9, 8.0 Hz, 1H), 4.99 (s, 2H), 3.93 (td, *J* = 8.2, 18.8 Hz, 1H), 3.84 (ddd, *J* = 3.0, 8.1, 18.4 Hz, 1H), 2.54 (td, *J* = 3.8, 14.1 Hz, 1H), 1.81 (dt, *J* = 4.4, 13.1 Hz, 1H), 1.70–1.63 (m, 1H), 1.57–1.49 (m, 1H); ^{13}C NMR (125 MHz, $CDCl_3$): δ 200.9, 169.0, 159.0, 146.4, 139.2, 137.0, 136.6, 135.5, 132.0, 129.7, 128.5, 128.0, 127.6, 124.0, 121.9, 120.0, 114.3, 113.7, 70.0, 55.3, 49.4, 27.4, 18.0. HRMS–ESI (m/z) $[M + H]^+$ calcd $C_{25}H_{22}NO_2$, 368.1651, found 368.1650.

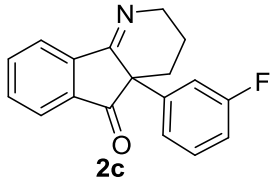

2c

(13.95 mg, 99% yield) ^{1}H NMR (500 MHz, $CDCl_3$) δ 8.06 (d, *J* = 7.7 Hz, 1H), 7.76 (t, *J* = 7.4 Hz, 2H), 7.58 (t, *J* = 7.9 Hz, 1H), 7.22 (d, *J* = 6.6 Hz, 1H), 7.21 (d, *J* = 7.9 Hz, 1H), 6.91 (dt, *J* = 2.2, 8.1 Hz, 1H), 3.93 (td, *J* = 7.7, 18.8 Hz, 1H), 3.85 (ddd, *J* = 3.1, 7.9, 18.6 Hz, 1H), 2.54 (td, *J* = 3.8, 14.1 Hz, 1H), 1.84 (dt, *J* = 4.4, 13.1 Hz, 1H), 1.72–1.68 (m, 1H), 1.54–1.48 (m, 1H); ^{13}C NMR (125 MHz, $CDCl_3$): δ 200.4, 168.7, 146.2, 140.2, 140.1, 136.8, 136.3, 135.7, 132.2, 130.3, 130.2, 124.1, 123.0, 122.1, 114.7, 114.5, 55.1, 49.2, 27.4, 17.9. HRMS–ESI (m/z) $[M + H]^+$ calcd $C_{18}H_{15}FNO$, 280.1138, found 280.1133.

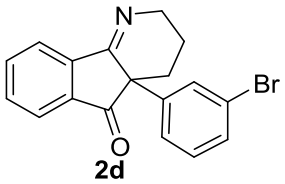

2d

(16.95 mg, 99% yield) ^{1}H NMR (500 MHz, $CDCl_3$) δ 8.06 (d, *J* = 7.6 Hz, 1H), 7.78–7.73 (m, 2H), 7.58 (t, *J* = 7.4 Hz, 1H), 7.49 (t, *J* = 2.0 Hz, 1H), 7.35 (td, *J* = 2.0, 8.0 Hz, 1H), 7.27 (td, *J* = 1.9, 8.0 Hz, 1H), 7.22 (t, *J* = 8.2 Hz, 1H), 3.94 (ddd, *J* = 7.0, 8.8, 18.6 Hz, 1H), 3.87 (ddd, *J* = 3.2, 8.6, 18.4 Hz, 1H), 2.54 (ddd, *J* = 3.0, 4.8, 14.1 Hz, 1H), 1.84 (dt, *J* = 4.6, 12.1 Hz, 1H), 1.72–1.67 (m, 1H), 1.54–1.48 (m, 1H); ^{13}C NMR (125 MHz, $CDCl_3$): δ 200.4, 168.4, 146.3, 140.0, 136.8, 135.8, 132.2, 130.8, 130.38, 130.33, 126.0, 124.1, 123.0, 122.0, 54.9, 49.4, 27.5, 17.9. HRMS–ESI (m/z) $[M + H]^+$ calcd $C_{18}H_{15}BrNO$, 340.0337, found 340.0335.

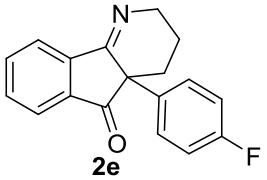

2e

(16.95 mg, 99% yield) δ 8.05 (d, *J* = 7.7 Hz, 1H), 7.76 (t, *J* = 7.4 Hz, 1H), 7.73 (t, *J* = 7.4 Hz, 1H), 7.58 (t, *J* = 7.6 Hz, 1H), 7.32 (d, *J* = 7.4 Hz, 1H), 7.30 (d, *J* = 7.2 Hz, 1H), 6.96 (t, *J* = 8.1 Hz, 2H), 3.95 (td, *J* = 7.6, 18.9 Hz, 1H), 3.85 (ddd, *J* = 3.2, 8.1, 18.6 Hz, 1H), 2.53 (td, *J* = 3.6, 14.5 Hz, 1H), 1.83 (dt, *J* = 4.3, 14.0 Hz, 1H), 1.72–1.66 (m, 1H), 1.53–1.46 (m, 1H); ^{13}C NMR (125 MHz, $CDCl_3$): δ 200.8, 169.1, 146.2, 136.8, 136.2, 135.6, 133.4, 132.2, 129.1, 129.0, 124.0, 123.8, 122.0, 115.9, 115.7, 54.6, 49.2, 27.4, 17.8; HRMS–ESI (m/z) $[M + H]^+$ calcd $C_{18}H_{15}FNO$, 280.1138, found 280.1136.

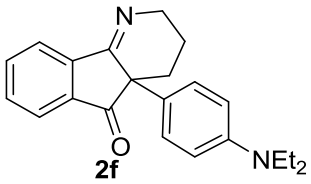

2f

(16.60 mg, 99% yield) ^{1}H NMR (500 MHz, $CDCl_3$) δ 8.02 (d, *J* = 7.3 Hz, 1H), 7.75 (d, *J* = 7.4 Hz, 1H), 7.69 (dt, *J* = 1.2, 7.6 Hz, 1H), 7.53 (dt, *J* = 1.1, 7.5 Hz, 1H), 7.13 (d, *J* = 8.1 Hz, 2H), 6.53 (d, *J* = 8.0 Hz, 2H), 3.91–3.88 (m, 2H), 3.26 (q, *J* = 7.2 Hz, 4H), 2.49 (td, *J* = 3.8, 13.4 Hz, 1H), 1.80 (dt, *J* = 4.3, 13.1 Hz, 1H), 1.68–1.58 (m, 2H), 1.09 (t, *J* = 7.0 Hz, 6H); ^{13}C NMR (125 MHz, $CDCl_3$): δ 201.4, 169.7, 146.9, 146.4, 137.3, 135.1, 131.7, 128.3, 124.0, 123.5, 121.6, 111.6, 54.4, 49.5, 44.1, 26.9, 18.0, 12.5; HRMS–ESI (m/z) $[M + H]^+$ calcd $C_{22}H_{25}N_2O$, 333.1967, found 333.1970.

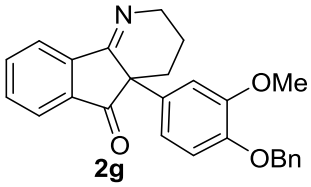

2g

(19.85 mg, 99% yield) ^{1}H NMR (500 MHz, $CDCl_3$) δ 8.02 (d, *J* = 7.5 Hz, 1H), 7.76 (d, *J* = 7.4 Hz, 1H), 7.71 (t, *J* = 8.3 Hz, 1H), 7.55 (t, *J* = 7.2 Hz, 1H), 7.36 (d, *J* = 8.1 Hz, 2H), 7.32 (t, *J* = 8.2 Hz, 2H), 7.26 (d, *J* = 8.2 Hz, 1H), 6.99 (s 1H), 6.71 (d, *J* = 8.5 Hz, 1H), 6.68 (dd, *J* = 1.9, 8.3 Hz, 1H), 5.06 (s, 2H), 3.92–3.88 (m, 2H), 3.85 (s, 3H), 2.51 (td, *J* = 3.90, 13.8 Hz, 1H), 1.81 (dt, *J* = 4.6, 12.8 Hz, 1H), 1.70–1.65 (m, 1H), 1.57–1.52 (m, 1H); ^{13}C NMR (125 MHz, $CDCl_3$): δ 201.2, 169.1, 149.8, 147.7, 146.4, 136.99, 136.98, 135.4, 132.0, 130.5, 128.5, 127.8, 127.1, 124.0, 121.8, 120.0, 113.4, 110.6, 70.8, 56.0, 54.8, 49.5, 27.4, 17.9; HRMS–ESI (m/z) $[M + H]^+$ calcd $C_{26}H_{24}N_2O$, 380.1889, found 380.1890.

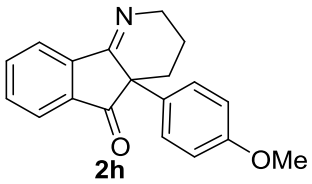

2h

(14.55 mg, 99% yield) ^{1}H NMR (500 MHz, $CDCl_3$) δ 8.04 (d, *J* = 7.4 Hz, 1H), 7.75 (d, *J* = 7.3 Hz, 1H), 7.71 (t, *J* = 7.8 Hz, 1H), 7.55 (t, *J* = 7.2 Hz, 1H), 7.25 (d, *J* = 7.6 Hz, 2H), 6.80 (d, *J* = 7.9 Hz, 1H), 3.93 (td, *J* = 8.1, 18.2 Hz, 1H), 3.86 (ddd, *J* = 3.0, 7.6, 18.4 Hz, 1H), 3.73 (s, 3H), 2.52 (td, *J* = 3.8, 14.0 Hz, 1H), 1.82 (dt, *J* = 4.2, 13.1 Hz, 1H), 1.71–1.65 (m, 1H), 1.58–1.49 (m, 1H); ^{13}C NMR (125 MHz, $CDCl_3$): δ 201.1, 169.4, 158.9, 146.2, 137.0, 135.4, 132.0, 129.6, 128.5, 124.0, 121.9, 114.2, 55.2, 54.6, 49.3, 27.2, 17.9; HRMS–ESI (m/z) $[M + H]^+$ calcd $C_{19}H_{18}NO_2$, 292.1338, found 292.1335.

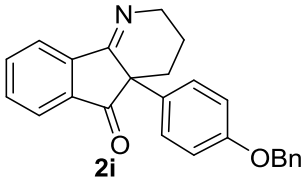

2i

(18.35 mg, 99% yield) ^{1}H NMR (500 MHz, $CDCl_3$) δ 8.04 (d, *J* = 7.7 Hz, 1H), 7.76 (d, *J* = 7.4 Hz, 1H), 7.72 (t, *J* = 8.0 Hz, 1H), 7.56 (t, *J* = 7.8 Hz, 1H), 7.37–7.28 (m, 5H), 7.26–7.24 (m, 3H), 6.87 (d, *J* = 8.0 Hz, 2H), 4.98 (s, 2H), 3.93 (td, *J* = 8.1, 18.16 Hz, 1H), 3.86 (ddd, *J* = 2.8, 7.7, 18.9 Hz, 1H), 2.52 (td, *J* = 3.9, 14.1 Hz, 1H), 1.81 (dt, *J* = 4.5, 13.1 Hz, 1H), 1.69–1.66 (m, 1H), 1.57–1.52 (m, 1H); ^{13}C NMR (125 MHz, $CDCl_3$): δ 201.2, 169.3, 158.2, 146.3, 137.0, 136.7, 135.4, 132.0, 129.9, 128.6, 128.5, 128.0, 127.4, 124.0, 121.8, 115.1, 69.9, 54.6, 49.4, 30.9, 27.2, 17.9; HRMS–ESI (m/z) $[M + H]^+$ calcd $C_{25}H_{22}NO_2$, 368.1651, found 368.1547.

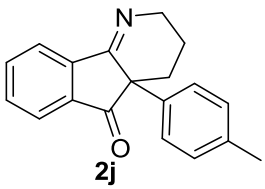

2j

(13.75 mg, 99% yield) ^{1}H NMR (500 MHz, $CDCl_3$) δ 8.04 (d, *J* = 7.8 Hz, 1H), 7.75 (d, *J* = 7.8 Hz, 1H), 7.71 (dt, *J* = 1.0, 7.6 Hz, 1H), 7.55 (dt, *J* = 1.0, 7.4 Hz, 1H), 7.22 (d, *J* = 8.4 Hz, 2H), 7.07 (d, *J* = 8.4 Hz, 2H), 3.93 (ddd, *J* = 7.0, 8.8, 18.6 Hz, 1H), 3.84 (ddd, *J* = 3.3, 8.6, 19.0 Hz, 1H), 2.55 (ddd, *J* = 3.1, 4.6, 12.6 Hz, 1H), 2.26 (s, 1H), 1.82 (dt, *J* = 4.4, 12.1 Hz, 1H), 1.70–1.64 (m, 1H), 1.61–1.51 (m, 1H); ^{13}C NMR (125 MHz, $CDCl_3$): δ 201.2, 169.3, 146.4, 137.3, 137.0, 135.4, 134.7, 132.0, 129.5, 127.2, 124.0, 121.8, 55.0, 49.4, 27.4, 20.9, 17.9; HRMS–ESI (m/z) $[M + H]^+$ calcd $C_{19}H_{18}NO$, 276.1388, found 276.1390.

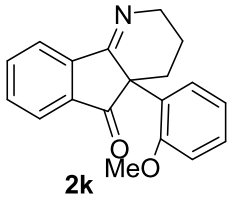

2k

(13.82 mg, 95% yield) ^{1}H NMR (500 MHz, $CDCl_3$) δ 8.05 (d, *J* = 7.6 Hz, 1H), 7.79 (d, *J* = 7.5 Hz, 1H), 7.74 (t, *J* = 7.6 Hz, 1H), 7.58 (t, *J* = 7.2 Hz, 1H), 7.49 (d, *J* = 7.6 Hz, 1H), 7.21 (d, *J* = 7.4 Hz, 1H), 6.97 (t, *J* = 7.4 Hz, 1H), 6.73 (d, *J* = 7.4 Hz, 1H), 3.91 (td, *J* = 7.9, 18.8 Hz, 1H), 3.42 (s, 3H), 3.37 (q, *J* = 7.8 Hz, 1H), 2.86 (td, *J* = 3.8, 14.0 Hz, 1H), 1.84–1.79 (m, 2H), 1.61–1.55 (m, 1H); ^{13}C NMR (125 MHz, $CDCl_3$): δ 201.9, 173.5, 157.6, 146.2, 137.0, 135.3, 131.5, 129.4, 129.0, 123.6, 121.4, 111.9, 55.2, 53.1, 47.5, 25.6, 19.0; HRMS–ESI (m/z) $[M + H]^+$ calcd $C_{19}H_{18}NO_2$, 292.1338, found 292.1338.

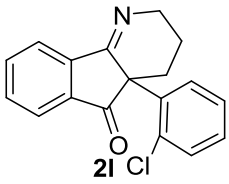

2l

(12.98 mg, 88% yield) ^{1}H NMR (500 MHz, $CDCl_3$) δ 8.06 (d, *J* = 7.6 Hz, 1H), 7.79 (d, *J* = 7.6 Hz, 1H), 7.76 (t, *J* = 7.8 Hz, 1H), 7.58 (t, *J* = 7.4 Hz, 1H), 7.55 (d, *J* = 7.6 Hz, 1H), 7.27–7.25 (m, 1H), 7.17 (d, *J* = 8.0 Hz, 1H), 3.99 (td, *J* = 7.4, 18.8 Hz, 1H), 3.50 (td, *J* = 7.1, 16.7 Hz, 1H), 3.04–2.98

(m, 1H), 1.82–1.78 (m, 1H), 1.71–1.62 (m, 2H); ^{13}C NMR (125 MHz, $CDCl_3$): δ 199.8, 171.3, 146.4, 137.0, 135.7, 133.7, 133.6, 131.9, 131.8, 130.9, 129.0, 127.3, 123.9, 122.0, 55.6, 48.4, 27.0, 18.8; HRMS–ESI (m/z) $[M + H]^+$ calcd $C_{18}H_{15}ClNO$, 296.0842, found 296.0840.

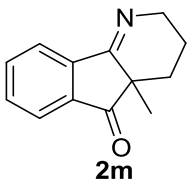

2m

(9.55 mg, 96% yield) ^{1}H NMR (500 MHz, $CDCl_3$) δ 7.94 (d, *J* = 8.0 Hz, 1H), 7.85 (td, *J* = 1.0, 8.2 Hz, 1H), 7.73 (dt, *J* = 1.1, 7.5 Hz, 1H), 7.60 (dt, *J* = 1.0, 7.6 Hz, 1H), 3.91 (d, *J* = 7.1 Hz, 1H), 3.90 (d, *J* = 7.6 Hz, 1H), 2.04 (ddd, *J* = 4.0, 6.1, 12.8 Hz, 1H), 2.00–1.94 (m, 1H), 1.78–1.72 (m, 1H), 1.66 (ddd, *J* = 6.4, 11.0, 16.8 Hz, 1H), 1.30 (s, 3H); ^{13}C NMR (125 MHz, $CDCl_3$): δ 205.0, 171.4, 145.5, 136.6, 135.4, 131.8, 123.7, 122.2, 48.7, 45.9, 24.9, 22.0, 18.4; HRMS–ESI (m/z) $[M + H]^+$ calcd $C_{13}H_{14}NO$, 200.1075, found 200.1076.

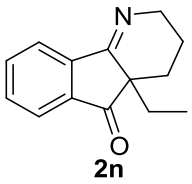

2n

(10.33 mg, 97% yield) ^{1}H NMR (500 MHz, $CDCl_3$) δ 7.97 (d, *J* = 8.0 Hz, 1H), 7.87 (d, *J* = 7.7 Hz, 1H), 7.75 (dt, *J* = 1.2, 7.8 Hz, 1H), 7.63 (dt, *J* = 1.1, 7.6 Hz, 1H), 4.00 (td, *J* = 6.5, 17.4 Hz, 1H), 3.87 (ddd, *J* = 4.9, 6.9, 17.6 Hz, 1H), 2.17 (ddd, *J* = 3.8, 6.2, 12.7 Hz, 1H), 2.04–1.59 (m, 5H), 0.81 (t, *J* = 7.6 Hz, 3H); ^{13}C NMR (125 MHz, $CDCl_3$): δ 204.8, 171.7, 146.1, 137.7, 135.3, 131.8, 123.1, 121.7, 49.9, 48.4, 28.1, 23.0, 18.4, 9.1; HRMS–ESI (m/z) $[M + H]^+$ calcd $C_{14}H_{16}NO$, 214.1232, found 214.1233.

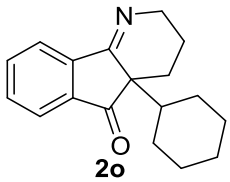

2o

(13.35 mg, 99% yield) ^{1}H NMR (500 MHz, $CDCl_3$) δ 7.91 (d, *J* = 7.8 Hz, 1H), 7.80 (td, *J* = 1.0, 8.2 Hz, 1H), 7.70 (dt, *J* = 1.1, 7.6 Hz, 1H), 7.57 (dt, *J* = 1.1, 7.5 Hz, 1H), 4.00 (ddd, *J* = 6.0, 7.1, 18.2 Hz, 1H), 3.82 (ddd, *J* = 5.9, 7.2, 18.1 Hz, 1H), 2.29 (ddd, *J* = 4.6, 6.4, 13.6 Hz, 1H), 1.94–1.86 (m, 2H), 1.78 (tt, *J* = 2.9, 12.8 Hz, 2H), 1.70–1.64 (m, 1H), 1.59–1.49 (m, 3H), 1.37–1.24 (m, 2H), 1.78 (tq, *J* = 3.1, 12.9 Hz, 1H), 1.06–0.97 (m, 1H); ^{13}C NMR (125 MHz, $CDCl_3$): δ 204.5, 172.4, 146.7, 138.3, 135.3, 131.7, 122.7, 121.1, 53.4, 48.0, 41.7, 30.2, 26.9, 26.7, 26.6, 25.9, 22.1, 18.5; HRMS–ESI (m/z) $[M + H]^+$ calcd $C_{18}H_{22}NO$, 268.1701, found 268.1700.

Section 3.10 References

(1) *A Guide to Organophosphorus Chemistry*, ed. L. D. Quin, Wiley, New York, **2000**.

(2) (a) Michaelis, A.; Kaehne, R. *Berichte*. **1898**, *31*, 1048. (b) Arbuzov, A. E. *J. Russ. Phys. Chem. Soc*. **1906**, *38*, 687. (c) Arbuzov, A. E. *Chem. Zentr* **1906**, 1639.

(3) Appel, R. *Angew. Chem., Int. Ed.* **1975**, *14*, 801.

(4) Wittig, G.; Schollkopf, U. *Angew. Chem.*, **1954**, *9*, 1318.

(5) Staudinger, H.; Mayer, J. *Helv. Chim. Acta*, **1919**, *2* 635.

(6) Mitsunobu, O.; Yamada, Y. *Bulletin of the Chem. Soc. of Japan* **1967**, *40*, 2380.

(7) (a) Hartwig, J. F. *Organotransition Metal Chemistry, from Bonding to Catalysis;* University Science Books: New York, **2010**. (b) Mcauliffe, C. A. *Transition Metal Complexes of Phosphorus, Arsenic, and Antimony Ligands*, J. Wiley, **1973**.

(8) Horner, L.; Jurgeleit, W.; Klupfel, K. *Liebigs Ann. Chem.* 1966, 591, 108.

(9) (a) Rauhut, M. M.; Currier, H. U. S. Patent 3074999, 1963; *Chem. Abstr.* **1963**, *58*, 66109. (b) Moria, K. Suzuki, Z.; Hirose, H. *Bull. Chem. Soc. Jpn.* **1968**, *41*, 2815.

(10) (a) Zhu, X. F.; Henry, C. E.; Kwon, O. *Tetrahedron* **2005**, *61*, 6276. (b) Andrews, I. P.; Kwon, O. *Org. Synth.* **2011**, *88*, 138. (c) Andrews, I. P.; Kwon, O. *Chem. Sci.* **2012**, *3*, 2510. (d) Henry, C. E.; Xu, Q.; Fan, Y. C.; Martin, T. J.; Belding, L.; Dudding, T.; Kwon, O. *J. Am. Chem. Soc.* **2014**, *136*, 11890. For reports on Lu's original allene–imine [3 + 2] annulation, see: (e) Xu, Z.; Lu, X. *Tetrahedron Lett.* **1997**, *38*, 3461; (f) Xu, Z.; Lu, X. *J. Org. Chem.* **1998**, *63*, 503.

(11) Ley, S. V.; Baxendale, I. R.; Bream, R. N.; Jackson, P. S.; Leach, A. G.; Longbottom, D. A.; Nesi, M.; Scott, J. S.; Storer, R. I. S. J. *J. Chem. Soc., Perkin Trans. 1* **2000**, 3815.

(12) Harrison, C. R.; Hodge, P.; Hunt, B. J.; Khoshdel, E.; Richardson, G. *J. Org. Chem.* **1983**, *48*, 3721.

(13) Smith, C. D.; Baxendal, I. R.; Tranmer, G. K.; Bauman, M.; Smith, S. C.; Lewthwaite, R. A.; Ley, S. V. *Org. Biomol. Chem*. **2007**, *5*, 1562.

(14) Lan, P.; Porco, J. A. Jr.; South, M. S.; Parlow, J. J. *J. Comb. Chem.* **2003**, *5*, 660.

(15) Dandapani, S.; Curran, D. P. *Tetrahedron* **2002**, *58*, 3855.

(16) Poupon, J. C.; Boezio, A. A.; Charette, A. B. *Angew. Chem. Int. Ed.* **2006**, *45*, 1415.

(17) Sieber, F.; Wentworth, P. W. Jr.; Toker, J. D.' Wentworth, A. D.; Metz, W. A.; Reed, N. N.; Janda, K. D. *J. Org. Chem.* **1999**, *64*, 5188.

(18) Barrett, A. G. M.; Roberts, R. S.; Schroder, J. *Org. Lett.* **2000**, *2*, 2999.

(19) (a) Kalkeren, H. A.; Lddnders, S. H. A. M.; Hommersom, R. A.; Rutjes, F. P. J. T.; Delft, F. L. *Chem. Eur. J.* **2011**, *17*, 11290. (b) Marsden, S. P. *Nat. Chem*. **2009**, *1*, 685. (c) Fairlamb, I. J. S. *ChemSusChem* **2009**, *2*, 1021.

(20) Marsden, S.; McGonagle, A. E.; McKeever-Abbas, B. *Org. Lett.* **2008**, 1*0*, 2589.

(21) Denton, R. M.; Tang, X. P.; Przeslak, A. *Org. Lett.* **2010**, 1*2*, 4678.

(22) Denton, R. M.; An, J.; Adeniran, B. *Chem. Commun*. **2010**, *46*, 3025.

(23) Denton, R. M.; An, J.; Lindovska, P.; Lewis, W. *Tetrahedron* **2012**, *68*, 2899.

(24) An, J.; Tang, X. P.; Moore, J.; Lewis, W.; Denton, R. M. *Tetrahedron*, **2013**, *69*, 8769.

(25) O'Brien, C. J.; Tellez, J. L.; Nixon, Z. S.; Kang, L. J.; Carter, A. L.; Kunkel, S. R.; Przeworski, K. C.; Chass, G. A. *Angew. Chem. Int. Ed.* **2009**, *48*, 6836.

(26) O'Brien, C. J.; Lavigne, F.; Coyle, E. E.; Holohan, A. J.; Doonan, B. J. *Chem. Eur. J.* **2013**, *19*, 5854.

(27) van Kalkeren, H. A.; Leenders, S. H. A. M.; Hommersom, C. R. A.; Rutjes, F. P. J. T.; van Delft, F. L. *Chem. Eur. J.* **2011**, *17*, 11290.

(28) van Kalkeren, H. A.; Bruins, J. J.; Rutjes, F. P. J. T.; van Delft, F. L. *Adv. Synth. Catal.* **2012**, *354*, 1417.

(29) Kosal, A. D.; Wilson, E. E.; Ashfeld, B. L. *Angew. Chem. Int. Ed.* **2012**, *51*, 12036.

(30) Wang, L.; Wang, Y.; Chen, M.; Ding, M.-W. *Adv. Synth. Catal.* **2014**, *356*, 1098.

(31) Zhao, W.; Yan, P. K.; Radosevich, A. T. *J. Am. Chem. Soc.* **2015**, *137*, 616. (o) Fourmy, K.; Voituriez, A. *Org. Lett.* **2015**, *17*, 1537.

(32) Buonomo, J. A.; Aldrich, C. C. *Angew. Chem. Int. Ed.* **2015**, *54*, 13041.

(33) Werner, T.; Hoffmann, M.; Deshmukh, S. *Eur. J. Org. Chem.* **2014**, 6873.

(34) Schirmer, M.; Adomeit, S.; Werner, T. *Org. Lett.* **2015**, *17*, 3078.

(35) van Kalkeren, H. A.; van Delft, F. L.; Rutjes, F. P. J. T. *ChemSusChem* **2013**, *6*, 1615.

(36) (a) Hermeling, P.; Bassler, P.; Hammes, P.; Hugo, R.; Lechtken, P.; Siegel, H. U. S. Patent 5527966, **1996**. (b) Pommer, H.; Nurrenbach, A.; *Pure Appl. Chem.* **1975**, *43*, 527.

(37) Masaki, M.; Kakeya, N. *Angew. Chem. Int. Ed.* **1977**, *16*, 552.

(38) Kuroboshi, M.; Yano, T.; Kamenoue, S.; Kawakubo, H.; Tanaka, H. *Tetrahedron* **2011**, *67*, 5825.

(39) Byrne, P. A.; Rajendran, K. V.; Muldoon, J.; Gilheany, D. G. *Org. Biomol. Chem.* **2012**, *10*, 3531.

(40) Fritzsche, H.; Korte, F.; Uasserodt, U. *Chem. Ber*. **1964**, *97*, 1988.

(41) Coumbe, T.; Lawrence, N. J.; Muhammad, F. *Tetrahedron Lett.* **1994**, *35*, 625.

(42) Lertpibulpanya, D.; Marsden, S. P.; Rodriguez-Garcia, I.; Kilner, C. A. *Angew. Chem. Int. Ed.* **2006**, *45*, 5000.

(43) Zhang, K.; Cai, L.; Yang, Z.; Houk, K. N.; Kwon, O. *J. Am. Chem. Soc*, submitted.